



[Home](#) ▶ [All Journals](#) ▶ [Therapeutic Delivery](#) ▶ [List of Issues](#) ▶ [Volume 10, Issue 12](#) ▶ [Marine Bioadhesives: Opportunities and C ...](#)

Therapeutic Delivery >

Volume 10, 2019 - Issue 12

✓ Free access

1,339 0

Views

CrossRef citations to date

0

Altmetric



Editorial

Marine Bioadhesives: Opportunities and Challenges

[Kamla Pathak](#)  

Pages 749-751 | Received 12 Sep 2019, Accepted 02 Oct 2019, Published online: 24 Oct 2019

 Cite this article <https://doi.org/10.4155/tde-2019-0070>



 Full Article

 Figures & data

 References

 Citations

 Metrics

 Reprints & Permissions

 View PDF

 View EPUB

Q Keywords: [alginate](#) [chitosan](#) [chitosan derivatives](#) [composite bioadhesives](#) [exopolysaccharides](#) [marine bioadhesives](#) [polysaccharides](#)
[proteins](#)

[< Previous article](#)

[View issue table of contents](#)

[Next article >](#)

Marine invertebrates produce adhesives that retain adhesion even in harsh conditions of sea water. Mussel adhesive proteins, polysaccharides and exopolysaccharides are distinct categories of bioadhesives obtained from sea. Of these, the former two have been extensively explored for developing a variety of drug-delivery systems, including nanoformulations. Combination of adhesives and development of composite bioadhesives are newer approaches to overcome issues related to use of solitary adhesive in formulations.

The ability of marine invertebrates to produce adhesives that retain adhesion, in the presence of harsh sea water conditions, has garnered considerable attention of pharmaceutical researchers. Mussel adhesive proteins, polysaccharides and exopolysaccharides are distinct groups of bioadhesives obtained from the sea [1]. Many therapeutic agents can be delivered via the drug-delivery systems containing these bioadhesives, including anti-inflammatory agents, antihypertensive agents, peptides and low molecular weight proteins, etc. The bioadhesives can be utilized for local drug delivery (topical) and requirements for successful bioadhesive devices for sustained topical delivery of active ingredients include: establishing and maintaining intimate contact with the site of application; ensuring sustained/controlled delivery of the drug in pathological skin conditions; be sufficiently adhesive and cohesive; be nontoxic and nonirritating; and allowing easy termination of therapy [2].

Marine polysaccharides

Research efforts on algal bioadhesives have led to the isolation of polysaccharides that are promising biomaterials, especially as adhesives in ophthalmic therapies. For the purpose of drug delivery, many polysaccharides, including chitin, chitosan, agar, alginate and carrageenans, have been investigated. Chitosan, a biopolymer derived from chitin, has wide pharmaceutical applications, ranging from capability to form gels, films, micro/nanoparticles and beads, as wound dressing and as a carrier for drug/gene delivery [3]. It has been utilized for designing mucoadhesive dosage forms but suffers from its limited mucoadhesive strength and limited water solubility at neutral and basic pH. These

issues have been tackled by designing chitosan derivatives such as carboxymethyl chitosan, chitosan-EDTA, glycol chitosan, chitosan-catechol and cyclodextrin-chitosan [4]. The derivatization of chitosan to improve its mucoadhesive properties has been explained in several publications. Few of them have demonstrated potential in transmucosal delivery, for example ChiSys[®] as a platform for nasal vaccination [5] and Lacimera[®] eye drops [6].

Alginates are linear polysaccharides obtained from seaweeds and marine algae, utilized in drug delivery, tissue engineering applications and immobilization of cells and enzymes owing to their ability to crosslink through bivalent cations. Alginates instantaneously form gel-spheres with divalent ions at pH >6 and are widely utilized for the microencapsulation of drugs. However, high viscosity gels are formed when the alginates are subjected to low pH values [7]. The ability of alginates to form pH-triggered gels has been widely used to develop ophthalmic drug-delivery systems. Furthermore, the ability of alginates to form microcapsules on cross-linking has been specifically explored for the oral delivery of low molecular weight proteins [8].

Alginates can be combined with other bioadhesives to develop novel efficacious drug-delivery systems and the concept has garnered considerable interest among pharmaceutical formulation researchers. For example, the chitosan-alginate microbeads for sustained vaginal delivery of chlorhexidine digluconate, jackfruit seed starch-alginate microspheres of metformin HCl [9], tamarind seed polysachharide-alginate beads for gliclazide oral delivery, etc. [10]. Alginates have also been utilized for drug-delivery systems based on composite technology. For example, montmorillonite-alginate nanocomposites have been developed for sustained delivery of vitamin B1 and B6 [11]. Modulated drug release was achievable by incorporating pH-independent hydrocolloids gelling agents or by addition of chitosan [12].

Large number of mucoadhesive systems based on alginates have been developed, such as a mucoadhesive vaginal tablet of acriflavine for veterinary purposes. The main drawbacks of alginate formulations are their rapid erosion at

neutral pH and reduction in mucoadhesion on cross-linking with divalent cations. In order to strengthen the mucoadhesive property of alginates, these have been chemically derivatized; for example, alginate-polyethyleneglycol acrylate has gelation ability of alginate combined with mucoadhesive strength of acrylate functionality of polyethylene glycol [13]. Laurienzo *et al.* attempted modification of sodium alginate with amines and/or acid moieties that resulted in optimization of drug delivery properties, namely, the drug release rate, modulation of polysaccharide erosion pattern and adhesion to the biological substrates [14]. Bernkop *et al.* demonstrated an improvement of mucoadhesive properties and the release retardant properties of sodium alginate due to covalent linkage of cysteine [15]. The sustainment of drug release and improved mucoadhesion is exemplified by matrix tablets based on sodium alginate–cysteine conjugate containing tramadol hydrochloride as a model drug [16]. Furthermore, the low toxicity of these new excipients provides immense scope for utilization of thiolated polymers in mucoadhesive drug-delivery systems.

Adhesive proteins

Mussel adhesive proteins are recognized as powerful adhesives, which are stronger compared with the polymer-based adhesives. Most importantly, mussel adhesive proteins retain adhesive capacity in wet environments, which is not demonstrated by polymer-based adhesives. To date no polymer-based adhesives have been produced that can retain adhesion in an underwater environment. The strong adhesion of marine mussels under the sea inspired the development of several water-resistant adhesives. The catechol groups are present in large quantities in mussel adhesive proteins, which contribute to the outstanding adhesion of mussels on many different surfaces [17]. Catechols interact with biological surfaces, including mucus. These findings inspired researchers to examine catechol-chitosan mucoadhesive systems for drug delivery via oral, buccal and rectal routes. Catechol-modified chitosan hydrogel crosslinked by genipin is a promising mucoadhesive and biocompatible hydrogel system for buccal drug

delivery [18]. Chitosan-catechol mucoadhesive gel allowed sulfasalazine delivery by rectal route more effectively and safely compared with oral administration [19].

It may become imperative for the researchers to amalgamate several adhesive proteins to develop improvised bioadhesive materials for novel applications including drug, protein and gene delivery. Novel drug delivery formulations consisting of polyphenolic proteins from mussels and marine origin polysaccharides are promising, especially as adhesive in ophthalmic therapies.

Marine exopolysaccharides

Exopolysaccharides are obtained from marine bacteria. However, most of these are poorly understood and only a few have been fully characterized. Of the various pharmaceutical roles of microbial exopolysaccharides, assistance in attachment to sea surfaces is of particular interest. Exopolymers of marine *Vibrio* MH3 are involved in reversible attachment. The cross-linking of adjacent polysaccharide chains aids in permanent adhesion [20]. Exopolysaccharides are yet to be explored for drug delivery. Interest is being directed toward extreme marine environments, which could represent a large source of unidentified bacteria.

Dedicated research by marine scientists has afforded discovery and production of many marine bioadhesives of pharmaceutical interest. The possibility of chemical modification, addition of biodegradable additives and production of hybrid bioadhesives permits modulation of properties of bioadhesives and new possibilities, particularly in the pharmaceutical area.

Financial & competing interests disclosure

The author has no relevant affiliations or financial involvement with any organization or entity with a financial interest in or financial conflict with the subject matter or materials discussed in the manuscript. This includes employment, consultancies, honoraria, stock ownership or options, expert testimony, grants or patents received or pending, or royalties.

No writing assistance was utilized in the production of this manuscript.

References

1. Waite JH . Nature's underwater adhesive specialist. *Int. J. Adhes. Adhes.*7, 9–14 (1987).

| [Web of Science ®](#) | [Google Scholar](#)

2. Paola L . Marine polysaccharides in pharmaceutical applications: an overview. *Mar. Drugs*8, 2435–2465 (2010).

| [PubMed](#) | [Web of Science ®](#) | [Google Scholar](#)

3. Ali A , AhmedS. A review on chitosan and its nanocomposites in drug delivery. *Int. J. Biol. Macromol.*109, 273–286 (2018).

| [PubMed](#) | [Web of Science ®](#) | [Google Scholar](#)

4. Ways TMM , LauWM , KhutoryanskiyV. Chitosan and its derivatives for application in mucoadhesive drug-delivery systems. *Polymers*10, 267 (2018).

[PubMed](#) | [Web of Science ®](#) | [Google Scholar](#)

5. Watts P , SmithA , HinchcliffeM. ChiSys® as a chitosan-based delivery platform for nasal vaccination. *Mucos. Deliv. Biopharmaceut.*499–516 (2014).

[Google Scholar](#)

6. Bonengel S , Bernkop-SchnürchA. Thiomers – from bench to market. *J. Control. Rel.*195, 120–129 (2014).

[PubMed](#) | [Web of Science ®](#) | [Google Scholar](#)

7. Patil SB , SawantKK. Development, optimization and in vitro evaluation of alginate mucoadhesive microspheres of carvedilol for nasal delivery. *J. Microencapsul.*26(5), 432–443 (2009).

[PubMed](#) | [Web of Science ®](#) | [Google Scholar](#)

8. Hua S , MaH , LiX et al. pH-sensitive sodium alginate/poly(vinyl alcohol) hydrogel beads prepared by combined Ca²⁺ crosslinking and freeze–thawing cycles for controlled release of diclofenac sodium. *Int. J. Biol. Macromol.*46, 517–523 (2010).

[PubMed](#) | [Web of Science ®](#) | [Google Scholar](#)

9. Chatterjee B , AmalinaN , SenguptaP , MandalUK. Mucoadhesive polymers and their mode of action: recent update. *J. Appl. Pharm. Sci.*7(5), 195–203 (2017).

[Google Scholar](#)

10. Nayak AK , PalD. Formulation optimization and evaluation of jackfruit seed starch-alginate mucoadhesive beads of metformin HCl. *Int. J. Biol. Macromol.*49, 264–272 (2013).

| [Google Scholar](#)

11. Pal D , NayakAK. Novel tamarind seed polysaccharide-alginate mucoadhesive microspheres for oral gliclazide delivery: in vitro–in vivo evaluation. *Drug Deliv.*19, 123–131 (2012).

| [PubMed](#) | [Web of Science ®](#) | [Google Scholar](#)

12. Kevadiya BD , JoshiGV , PatelHA , IngolePG , ModyHM , BajajHC. Montmorillonite–alginate nanocomposites as a drug-delivery system: intercalation and in vitro release of vitamin B1 and vitamin B6. *J. Biomater. Appl.*25, 161–177 (2010).

| [PubMed](#) | [Web of Science ®](#) | [Google Scholar](#)

13. Tapia C , EscobarZ , CostaEet al. Comparative studies on polyelectrolyte complexes and mixtures of chitosan-alginate and chitosan-carrageenan as prolonged diltiazem chlorhydrate release systems. *Eur. J. Pharm. Biopharm.*57, 65–75 (2004).

| [PubMed](#) | [Web of Science ®](#) | [Google Scholar](#)

14. Davidovich-Pinhas M , Bianco-PeledH. Alginate-PEGAc: a new mucoadhesive polymer. *Acta Biomater.*7, 625–633 (2011).

| [PubMed](#) | [Web of Science ®](#) | [Google Scholar](#)

15. Laurienzo P , MalinconicoM , MattiaGet al. Novel alginate-acrylic polymers as a platform for drug delivery. *J Biomed. Mater. Re. A.*78, 523–531 (2006).
[PubMed](#) | [Google Scholar](#)
16. Bernkop-Schnürch A , ClausenAE , HnatyszynM. Thiolated polymers: synthesis and in vitro evaluation of polymer-cysteamine conjugates. *Int. J. Pharm.*226, 185–194 (2001).
[PubMed](#) | [Web of Science ®](#) | [Google Scholar](#)
17. Jindal AB , WasnikMN , NairHA. Synthesis of thiolated alginate and evaluation of mucoadhesiveness, cytotoxicity and release retardant properties. *Indian J. Pharm. Sci.*72(6), 766–774 (2010).
[PubMed](#) | [Web of Science ®](#) | [Google Scholar](#)
18. Dove J , SheridanP. Adhesive protein from mussels: possibilities for dentistry, medicine, and industry. *J. Am. Dent. Assoc.*112, 879–883 (1986).
[PubMed](#) | [Web of Science ®](#) | [Google Scholar](#)
19. Xu J , StrandmanS , ZhuJX , BarraletJ , CerrutiM. Genipin-crosslinked catechol-chitosan mucoadhesive hydrogels for buccal drug delivery. *Biomaterials*37, 395–404 (2015).
[PubMed](#) | [Web of Science ®](#) | [Google Scholar](#)
20. Xu J , TamM , SamaeiSet al. Mucoadhesive chitosan hydrogels as rectal drug delivery vessels to treat ulcerative colitis. *Acta Biomater.*48, 247–257 (2017).

[Download PDF](#)

Related research

Recommended articles

Cited by

[Cytotoxic activity of the crude polysaccharides/exopolysaccharides of *Coprinus comatus* and *Coprinellus truncorum*](#) >

Kristina Atlagić et al.

Natural Product Research

Published online: 2 Sep 2022

[Construction of protein-, polysaccharide- and polyphenol-based conjugates as delivery systems](#) >

Shizhang Yan et al.

Critical Reviews in Food Science and Nutrition

Published online: 18 Dec 2023

[Construction of lipid-biomacromolecular compounds for loading and delivery of carotenoids: Preparation methods, structural properties, and absorption-enhancing mechanisms](#) >

Yunjun Liu et al.

Critical Reviews in Food Science and Nutrition

[View more](#)

Information for

Authors

R&D professionals

Editors

Librarians

Societies

Opportunities

Reprints and e-prints

Advertising solutions

Accelerated publication

Corporate access solutions

Open access

Overview

Open journals

Open Select

Dove Medical Press

F1000Research

Help and information

Help and contact

Newsroom

All journals

Books

Keep up to date

Register to receive personalised research and resources by email

 Sign me up



ScienceDirect®

Heliyon

Volume 5, Issue 8, August 2019, e02247

Effect of cisplatin on pancreas and testes in Wistar rats: biochemical parameters and histology

Yogesh Chand Yadav  

Show more 

 Outline |  Share  Cite

<https://doi.org/10.1016/j.heliyon.2019.e02247> 

[Get rights and content](#) 

Under a Creative Commons [license](#) 

open access

Referred to by [Corrigendum to “Effect of cisplatin on pancreas and testes in Wistar rats: biochemical parameters and histology” \[Heliyon 5 \(8\) \(2019\) e02247\]](#)

Heliyon, Volume 6, Issue 4, April 2020, Pages e03688

Yogesh Chand Yadav



[View PDF](#)

Abstract

Objective

To investigate effect of cisplatin on biochemical parameter and histology of pancreas and testis in Wistar rats.

Material and methods

Single dose cisplatin (10 mg/kg) was injected by intraperitoneal route in Wistar rats. Blood was withdrawn on 7th day from cisplatin treated rats by retro-orbital sinus for biochemical estimation. Further rats were scarified and dissected out their pancreases and testes for estimation of antioxidant enzymes and histopathological study.

Results

The cisplatin-treated group showed a significantly ($P < 0.01$) increased blood glucose level, Glycosylated hemoglobin in blood on the 7th day as compared to the control group. Whereas cisplatin-treated group showed significantly ($p < 0.001$) increased lipid peroxidation and decreased reduced glutathione, superoxide dismutase, catalase in pancreatic and testicular tissue as compared to the control group. Histopathological sections of the pancreatic tissue showed marked vasoconstriction and micro infiltration were observed however testicular tissue showed degeneration in some somniferous tubules and also greatly depleted of germ cells in cisplatin treated group.

Conclusion

These findings demonstrated that the cisplatin could be induced diabetes and testicular toxicity due to their free radical mediated oxidative stress.



Keywords

Toxicology; Biochemical parameters and histology; Rats; Testis; Cisplatin; Pancreas

1. Introduction

Cisplatin is a prominent and most potent anticancer drugs and it used to treat metastatic testicular and ovarian cancer [1]. It is also used for treatment on various type cancer like lung, urine bladder, head, neck, esophageal, stomach, skin prostate, lymphoma and neuroblastoma, sarcoma, cervical, myeloma, mesothelima and osteosarcoma. In spite of its significant anticancer activity, cisplatin is often dose limited undesirable side effects such as nephrotoxicity [2]. Recent studies has been reported that nephrotoxicity and hepatotoxicity are cisplatin induced is reported that cisplatin and others around the world suggested hepatotoxicity is also a major dose-limiting side effect in cisplatin-based chemotherapy [3, 4, 5, 6]. Cisplatin can induce heptotoxicity after administered at high doses [7, 8]. Metallothionein protects against liver injury induced by high doses of cisplatin in mice [9]. Selenium and high dose of vitamin E administration protect against cisplatin-induced oxidative damage to liver [10]. Komdeur et al (2007) has been reported that Cisplatin-induced hyperglycemic hyperosmolar coma [11]. Amin et al (2007) has well documented that effect of Roselle and Ginger on cisplatin-induced reproductive toxicity in rats [12].

With this background, the present study has designed to investigate whether have any effect of cisplatin on pancreas and testes in Wistar rats.

2. Materials and methods

2.1. Drug and reagents

5,5-dithiobis 2-nitrobenzoic acid (Merck pvt. Ltd., India). Thiobarbuturic acid (Loba chemicals pvt.ltd. India). Superoxide Dismutase (sigma Aldrich chemicals pvt. Ltd. India).

2.2. Animals

The Wistar rats were allowed to have an access to water and food ad libitum, and maintained under constant (25 ± 1 °C), humidity (65 ± 10 %) and a 12 h light/dark cycle. The experiment was carried out in accordance to the guidelines mentioned in the CPCSEA, and institution animal ethical committee of Sumandeep Vidyapeeth University was approved the experiment protocols. The experiment was conducted in accordance with accepted standard guidelines for the care and use of animals in scientific research.

2.3. Cisplatin-induced toxicity

Two groups of rats (n = 6) used, in which 1st group administered 5 ml/kg normal saline throughout the experiment for 7 days; 2nd group (cisplatin treated) with single dose of cisplatin (10 mg/kg i.p.) on 1st day and keep animals up to 7 days. On the 7th day all animals were anaesthetized with diethyl ether. Blood sample (1–1.5 ml) was collected at once from the retro orbital plexus of rats under light diethyl ether anaesthesia, for biochemical parameter estimation. Pancreas and testes were subjected to histopathological study.

2.4. Biochemical analysis

2.4.1. Determination blood glucose level

The Blood glucose was determined by the method of O-toluidine using the modified reagent [13] and Glycosylated hemoglobin (gly Hb) was determined by the method of Sudhakar and Pattabiraman [14].

2.4.2. Determination reduced glutathione (GSH)

GSH Levels in pancreas and testis were estimated by the method (Beutler et al. 1963). 10% (w/v) homogenate prepared by added 5% trichloroacetic acid solution. It was centrifuged at 3500 rpm for 10 min, 50 µL supernatant was mixed with 0.32 mol/L disodium hydrogen phosphate and 0.04% 5,5-dithiobis 2-nitrobenzoic acid (DTNB) solution. The yellow-colored substance formed by the reaction of GSH and DTNB was measured at 412 nm. The results were expressed as GSH mg/g tissue weight [15].

2.4.3. Determination of malondialdehyde (MDA)

MDA levels were estimated by the method of (Satoh 1978). 10% (weight/volume) homogenate of pancreas and testis was prepared by added 0.1 mol/L phosphate buffer. It was centrifuged at 4 °C, 3500 rpm for 10 min. 0.2 mL supernatant was mixed with 0.67% 2-thiobarbuturic acid (TBA) and 20% trichloroacetic acid solution, and heated in a boiling water bath for 30 min. The pink-coloured chromogen formed by the reaction of TBA with MDA was measured at 532 nm. The results were expressed as MDA nmol/mg protein [16].

2.4.4. Determination of superoxide dismutase (SOD)

Superoxide dismutase (SOD) activity in pancreas and testis homogenate was determined according to the method (Minami and Yoshikawa 1979). The homogenate was centrifuged at 2500 rpm for 15 minutes at 4 °C. The 0.25 ml of supernatant was mixed with 0.5 ml of tris cacodylic buffer, and 0.1 ml of 16% triton x- 100 and 0.25 ml NBT. The reaction was started by the addition of 0.01 ml diluted pyrogallol. It was kept on Incubation for 5 minutes at 37 °C. The reaction was stopped by the addition of 0.3 ml of 2 M formic acid. The formazan colour developed was determined spectrophotometrically (Spectronic 501, Shimadzu). Enzymatic activity (SOD) was expressed as U/g of tissue [17].

2.5. Histopathological examination

The Wistar rats were sacrificed on the day of blood withdrawal. Pancreas and testis were isolated, processed, and embedded in paraffin wax. The sections were stained in haematoxylin and eosin and permanently mount for viewing and reporting [18].

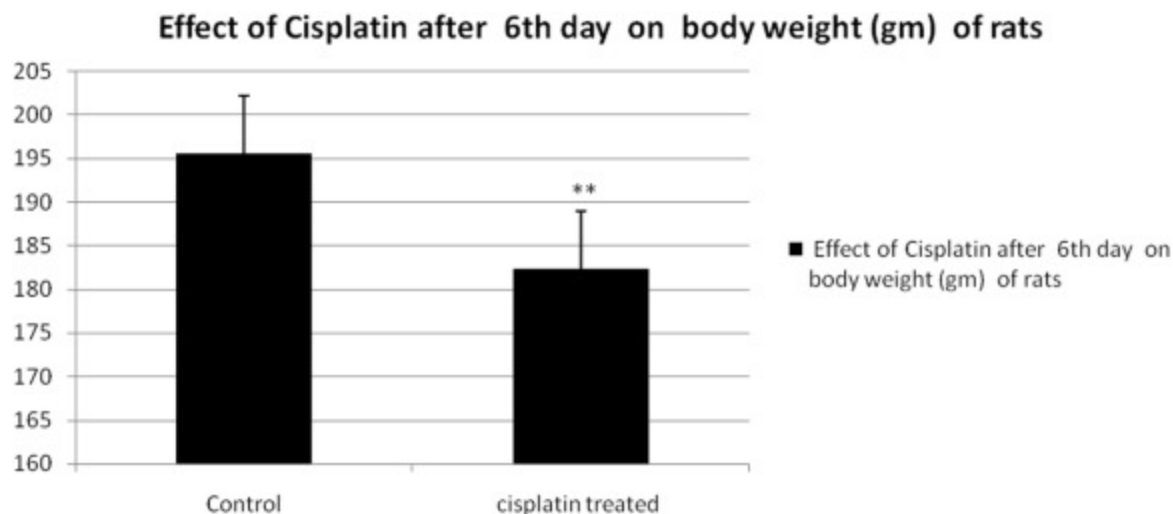
2.6. Statistical analysis

Result were expressed as mean +SEM, Statistical Analysis were performed with unpaired t test. P value less than <0.05 was considered.

3. Results

3.1. Changes of body weight of rats

Cisplatin treated group showed significantly ($p < 0.001$) decreased body wt of rats as compared control group (Fig.1).



[Download : Download high-res image \(142KB\)](#)

[Download : Download full-size image](#)

Fig. 1. Effect of Cisplatin after 6th day on body weight (gm) of rats. Each group represents mean \pm SD of six animals as compared to control treated group. ** $p < 0.01$ as compared to the control control.

3.2. Alteration of biochemical parameters

The cisplatin-treated group showed significantly ($p < 0.001$) increased glucoses, gly Hb in blood on the 7th day as compared to the control group (Table 1).

Table 1. Effect of cisplatin on biochemical parameters in serum.

Parameters	Control groups	Cisplatin treated group
Glucose	83.83 \pm 3.71	194.64 \pm 2.36 ***

Parameters	Control groups	Cisplatin treated group
Gly Hb	5.96 ± 0.5	8.65 ± 0.60 *
Total protein	8.56 ± 1.35	5.24 ± 0.86**

***P < 0.01, **P < 0.01 and *P < 0.05 as compared to the Control.

In term of tissue homogenate biochemical estimation, it was found that the cisplatin-treated group showed significantly ($p < 0.001$) increased lipid peroxidation (Table 2), whereas significantly ($p < 0.001$) decreased GSH, SOD, CAT in pancreatic and testicular tissue (Tables 2 and 3) as compared to the control group.

Table 2. Levels of GSH, SOD, CAT and MDH in pancreatic tissues of control and cisplatin treated group of rats.

Parameters	Control group	Cisplatin treated group
GSH(μmol/g)	11.45 ± 1.35	7.57 ± 1.35**
MDH(nmol/g)	24. ± .85	74.84 ± 1.42**
SOD(U/g)	15.46 ± 1.66	7.63 ± 1.33**
CAT(μmol H ₂ O ₂ /g)	298 ± 1.84	185 ± 3.45**

**P < 0.01 as compared to the Control.

Table 3. Levels of GSH, SOD, CAT and MDH in testicle tissue of control and cisplatin treated group of rats.

Parameters	Control group	Cisplatin treated group
GSH(μmol/g)	55 ± 2.45	42.48 ± 2.68**
MDH(nmol/g)	44. ±1 .64	65.38 ± 2.24**

Parameters	Control group	Cisplatin treated group
SOD(U/g)	28.46 ± 2.25	15.25 ± 2.24**
CAT(μmol H ₂ O ₂ /g)	225 ± 2.54	105 ± 2.34**

**P < 0.01 as compared to the Control.

3.3. Histopathological examination

Histopathological sections of the pancreatic tissue showed marked vasoconstriction and micro infiltration were observed cisplatin treated group II [Fig.2 Plates 1(B)] as compared to control group [Fig.2 Plates 1(A)].

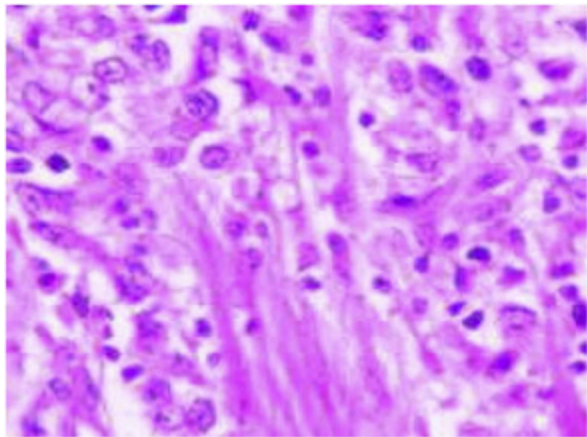


Plate 1 (A)

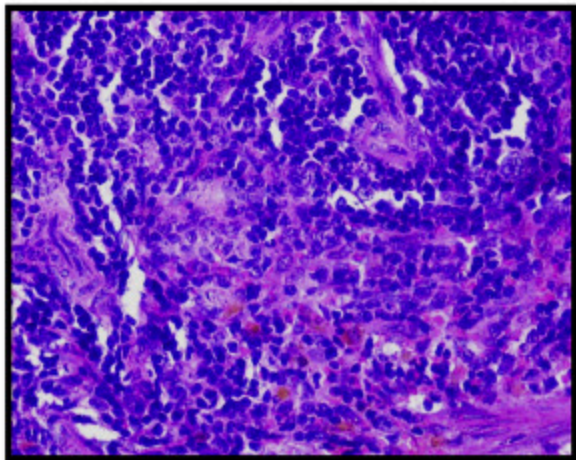


Plate 1 (B)

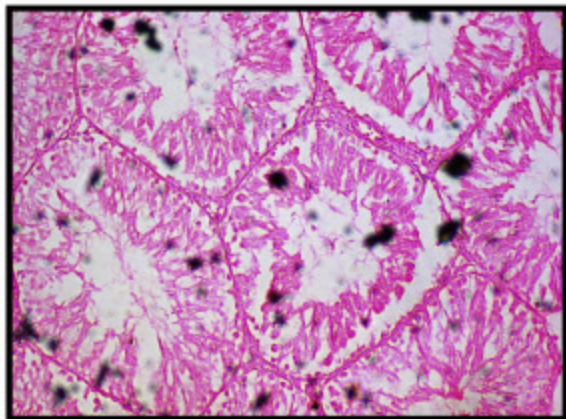


Plate 1 (C)

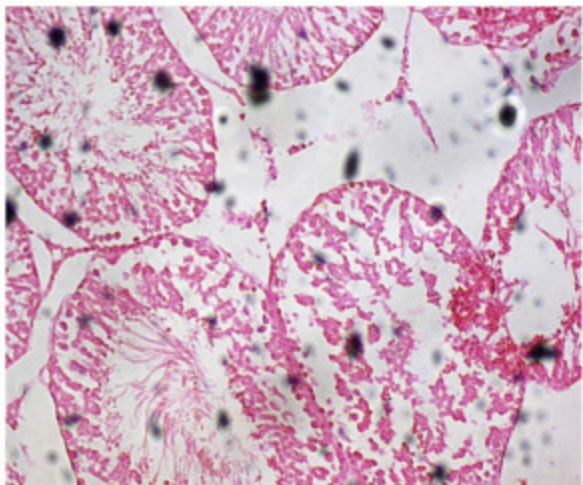


Plate 1 (D)

[Download : Download high-res image \(2MB\)](#)

[Download : Download full-size image](#)

Fig.2. Plate 1(A) Photograph of Pancreas in control group rat, Plate 1(B) Photograph of pancreas Cisplatin treated rat. Plate 1(C) Photograph of testis in control group rat. Plate 1 (D) Photograph of testes in cisplatin treated rat.

Histopathological sections of testicular tissue showed degeneration in some somniferous tubules and were also greatly depleted of germ cells in cisplatin treated group II [Fig.2 Plates 1(D)] as compared to control group [Fig.2 Plates 1(C)].

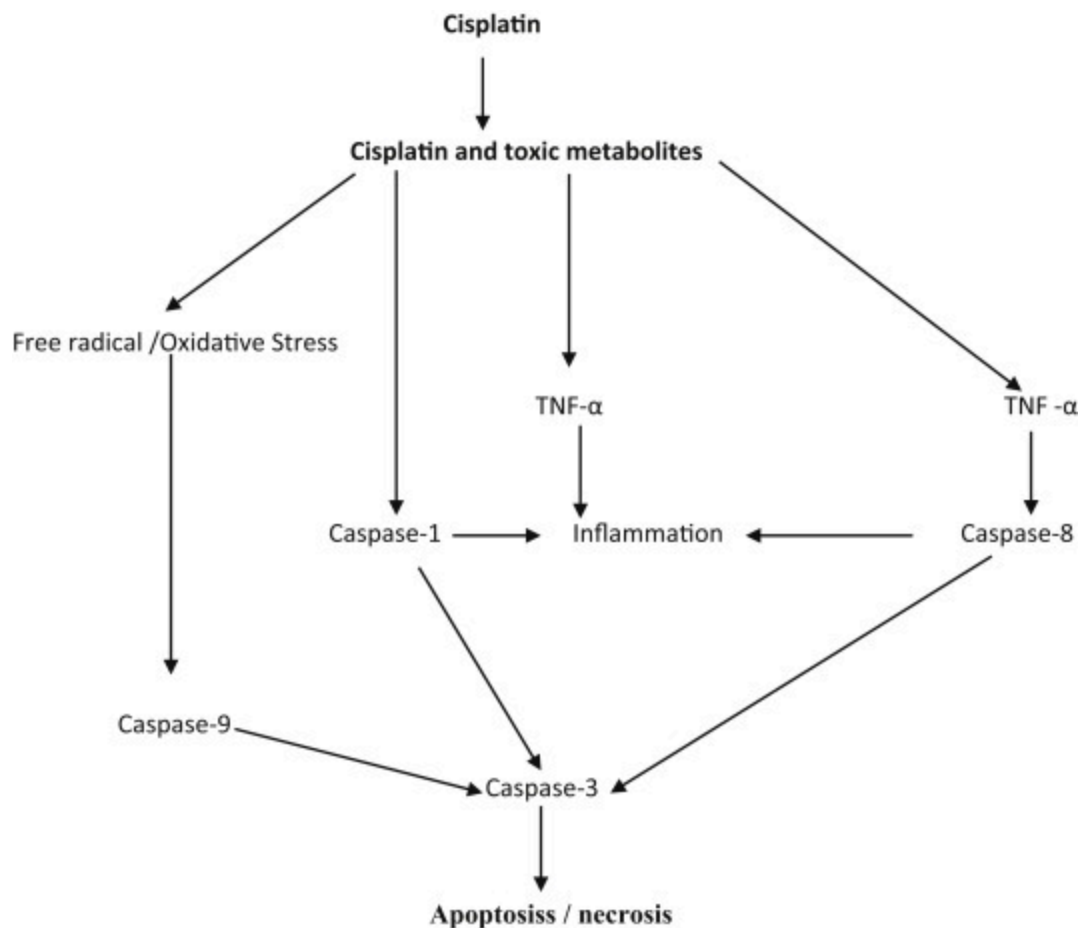
4. Discussion

The present study to investigate the effect of cisplatin on body wt of rats, biochemical parameters and histology of pancreas and testes.

After single dose of 10 mg/kg the cisplatin-treated showed a significant decreased body wt of rats as compared control group. The loss body wt of rats due to cisplatin induced gastrointestinal toxicity. Shahid et al (2018) has been reported that cisplatin induced gastrointestinal dysfunction due to concurrently utilized cisplatin with plant-derived agents [19].

After single dose of 10 mg/kg the cisplatin-treated showed a significant increase glucoses and gly Hb in serum me be due their emetogenic, glucocorticoids effect. The glucocorticod induces diabetes via impaired glucose metabolism.

In the present study, Cisplatin treated groups showed significantly increased lipid peroxidation and GSH, SOD, CAT were significantly decreased in pancreatic and testicular tissue as compared control group. The instantaneously significant decrease of antioxidants enzyme in cisplatin-induced tissues could potentiate elucidates the upregulation of lipid peroxidation [20]. It has been also well documented about a relationship between cisplatin-induced complications and lipid peroxidation [21]. Actually, cisplatin reacts with water and generated free radical. It's free radical oxidative stress induced toxicity pancreatic and testicular tissue (Fig.3).



[Download : Download high-res image \(194KB\)](#)

[Download : Download full-size image](#)

Fig.3. Mechanism of cisplatin induces pancreatic and testicle toxicity.

There are many previous studies have been well documented that cisplatin induces toxicity in liver [22] kidney [23, 24], due their free radical oxidative stress by interacting with DNA [25].

In vitro and in vivo Previous studies reported that cisplatin induces apoptotic cell death at low dose and it produces both necrosis and apoptosis at higher dose [26, 27]. There are numerous apoptotic pathways which are mediated by TNF receptors

as an extrinsic pathway and the mitochondrial and endothelium stress as an intrinsic pathway [28].

Histopathological sections of the pancreatic tissue showed marked vasoconstriction and micro infiltration which was indicates cisplatin could be indicated diabetes. It was also suggested by Goldstein et al [29], Nan et al (2003) and Komdeur et al [30].

Histopathological sections of testicular tissue showed degeneration in some somniferous tubules and were also greatly depleted of germ cells in cisplatin treated could be showed testicular toxicity. The present study is supported by Amr et al (2006) which are reported as effects of Roselle and Ginger on cisplatin-induced reproductive toxicity in rats [31].

Hence, cisplatin-induced pancreas and testicular damage due to their free radical mediated oxidative necrosis of tissue.

5. Conclusion

Finally on the basis of these investigations, it is concluded that cisplatin could be induced diabetes and testicular toxicity due to their cytotoxic and sever free radical oxidative stress effect. Actually, Cisplatin induces toxicity due their free radical oxidative stress by interacting with DNA. Further more studies needed for next generation.

Declarations

Author contribution statement

Yogesh Chand Yadav: Conceived and designed the experiments; Performed the experiments; Analyzed and interpreted the data; Contributed reagents, materials, analysis tools or data; Wrote the paper.

Funding statement

This research did not receive any specific grant from funding agencies in the public, commercial, or not-for-profit sectors.

Competing interest statement


The authors declare no conflict of interest.

Additional information

No additional information is available for this paper.

[Special issue articles](#) [Recommended articles](#)

References

- [1] T. Thigpen, R. Vance, L. Punekey, T. Khansurt
Chemotherapy in advanced ovarian carcinoma: current standards of care based on randomized trials
Gynecol. Oncol., 55 (1994), pp. 597-607
[Google Scholar](#) ↗
- [2] N.E. Madias, J.T. Harrington
Platinum nephrotoxicity
Am. J. Med., 65 (1978), pp. 307-314
 [View PDF](#) [View article](#) [View in Scopus](#) ↗ [Google Scholar](#) ↗
- [3] Y.J. Liao, H. Tang, Y.P. Jin
Study of toxic effects on hearing, kidney and liver of mice induced by anticancer agent of cisplatin and their mechanisms
Chin. Pharmacol. Bull., 20 (1) (2004), pp. 82-87
[View in Scopus](#) ↗ [Google Scholar](#) ↗
- [4] K.O. Hong, J.K. Hwang, K.K. Park, S.H. Kim
Phosphorylation of c-Jun N-terminal Kinases (JNKs) is involved in the preventive effect of xanthorrhizol on cisplatin-induced hepatotoxicity

Arch. Toxicol., 79 (4) (2005), pp. 231 2-23136

[Google Scholar ↗](#)

- [5] J. Liu, LiuY, S.S. Habeebu, C.D. Klaassen
Metallothionein (MT)-null mice are sensitive to cisplatin-induced hepatotoxicity

Toxicol. Appl. Pharmacol., 149 (1998), pp. 24-31

 [View PDF](#) [View article](#) [View in Scopus ↗](#) [Google Scholar ↗](#)

- [6] R. Pratibha, R. Sameer, P.V. Rataboli, D.A. Bhiwgade, C.Y. Dhume
Enzymatic studies of cisplatin induced oxidative stress in hepatic tissue of rats

Eur. J. Pharmacol., 532 (2006), pp. 290-293

 [View PDF](#) [View article](#) [View in Scopus ↗](#) [Google Scholar ↗](#)

- [7] R.J. Cersosimo
Hepatotoxicity associated with cisplatin chemotherapy

Ann. Pharmacother., 27 (1993), pp. 438-441

[CrossRef ↗](#) [View in Scopus ↗](#) [Google Scholar ↗](#)

- [8] C.F. Pollera, F. Meglio, M. Nardi, G. Vitelli, P. Marolla
Cisplatin-induced hepatic toxicity

J. Clin. Oncol., 5 (1987), pp. 318-319

[View in Scopus ↗](#) [Google Scholar ↗](#)

- [9] J. Liu, LiuY, S.S. Habeebu, C.D. Klaassen
Metallothionein (MT)-null mice are sensitive to cisplatin-induced hepatotoxicity

Toxicol. Appl. Pharmacol., 149 (1998), pp. 24-31

 [View PDF](#) [View article](#) [View in Scopus ↗](#) [Google Scholar ↗](#)

- [10] M. Naziroglu, A. Karaoglu, A.O. Aksoy

Selenium and high dose vitamin E administration protects cisplatin-induced oxidative damage to renal, liver and lens tissues

Toxicology, 195 (2004), pp. 221-230

 [View PDF](#) [View article](#) [View in Scopus ↗](#) [Google Scholar ↗](#)

- [11] R. Komdeur, J. Derksen, M.C. Legdeur, B.S. Hylkema
Cisplatin induces hyperglycaemic and hyperosmolar coma

J. Med., 65 (1) (2007), pp. 36-37

[View in Scopus ↗](#) [Google Scholar ↗](#)

- [12] Amr Amin, Alaa Eldin, A. Hamza
Effects of Roselle and Ginger on cisplatin-induced reproductive toxicity in rats

Asian J. Androl., 8 (5) (2006), pp. 607-612

[CrossRef ↗](#) [View in Scopus ↗](#) [Google Scholar ↗](#)

- [13] T. Sasaki, S. Mastsy, A. Sonae
Effect of acetic acid concentration on the colour reaction in the O-toluidine boric acid method for blood glucose estimation

Rinsho Kagaku, 1 (1972), pp. 346-353

[View in Scopus ↗](#) [Google Scholar ↗](#)

- [14] Pattabiraman Sudhakar
Anew colorimetric method for the estimation of glycosylated haemoglobin

Clin. Chem. Acta, 109 (1981), pp. 267-274

[Google Scholar ↗](#)

- [15] E. Beutler, O. Duron, B.M. Kelly
Improved method for the determination of blood glutathione

J. Lab. Clin. Med., 61 (1963), pp. 882-890

[View in Scopus ↗](#) [Google Scholar ↗](#)

- [16] K. Satoh
Serum lipid peroxide in cerebrovascular disorders determined by new colorimetric method

Clin. Chim. Acta, 90 (1978), pp. 37-43

[Google Scholar ↗](#)

- [17] M. Minami, H. Yoshikawa
Asimplified assay method of superoxide dismutase activity for clinical use

Clin. Chim. Acta, 92 (1979), pp. 337-342

[Google Scholar ↗](#)

- [18] S.K. Chandrasekaran, H. Benson, J. Urquhart
Methods to achieve controlled drug delivery: the biochemical engineering approach

J.R. Robinson (Ed.), Sustained and Controlled Drug Delivery Systems, Marchel Dekker, New (1978), pp. 557-593

[Google Scholar ↗](#)

- [19] F. Shahid, Z. Farooqui, F. Khan
Cisplatin-induced gastrointestinal toxicity: an update on possible mechanisms and on available gastroprotective strategies

Eur. J. Pharmacol., 827 (2018), pp. 49-57

15

 [View PDF](#) [View article](#) [View in Scopus ↗](#) [Google Scholar ↗](#)

- [20] P. Kaur, M.P. Bansal
Influence of selenium induced oxidative stress on spermatogenesis and lactate dehydrogenase-X in mice testis

Asian J. Androl., 6 (2004), pp. 227-232

[View in Scopus ↗](#) [Google Scholar ↗](#)

- [21] L.M. Antunes, J.D. Darin, L. Bianchi Nde
Effects of the antioxidants curcumin or selenium on cisplatin-induced nephrotoxicity and lipid peroxidation in rats
Pharmacol. Res., 43 (2001), pp. 145-150
[CrossRef ↗](#) [Google Scholar ↗](#)
- [22] Yogesh Chand Yadav
Effect of *Ficus religiosa* latex on cisplatin induced liver injury in Wistar rats
Revista Brasileira de Farmacognosia, 25 (2015), pp. 278-283
[Google Scholar ↗](#)
- [23] Yogesh Chand Yadav, D.N. Srivastava
Nephroprotective and curative effects of *Ficus religiosa* latex extract against cisplatin induced acute renal failure
Pharm. Biol., 51 (11) (2013), pp. 1480-1485
[Google Scholar ↗](#)
- [24] Yogesh Chand Yadav
Effect of *Ficus benghalensis* L. Latex extract (FBLE) on cisplatin induced hypotension and renal impairment in Wistar rats
Biochem. Pharmacol., 5 (2016), p. 216
[Google Scholar ↗](#)
- [25] H. Masuda, T. Tanaka, U. Takahama
Cisplatin generates superoxide anion by interaction with DNA in a cell-free system
Biochem. Biophys. Res. Commun., 203 (1994), pp. 1175-1180
 [View PDF](#) [View article](#) [View in Scopus ↗](#) [Google Scholar ↗](#)
- [26] W. Lieberthal, V. Triaca, J. Levine

Mechanisms of death induced by cisplatin in proximal tubular epithelial cells: apoptosis vs. necrosis

Am. J. Physiol. Renal. Physiol., 270 (1996), pp. F700-F708

[CrossRef ↗](#) [View in Scopus ↗](#) [Google Scholar ↗](#)

[27] R.H. Lee, J.M. Song, M.Y. Park, S.K. Kang, Y.K. Kim, J.S. Jung

Cisplatin-induced apoptosis by translocation of endogenous Bax in mouse collecting duct cells

Biochem. Pharmacol., 62 (2001), pp. 1013-1023

[Google Scholar ↗](#)

[28] F. Shiraishi, L. Curtis, L. Truong, K. Poss, G. Visner, K. Madsen, H. Nick, A. Agarwal

Heme oxygenase-1 gene ablation or expression modulates cisplatin-induced renal tubular apoptosis

Am. J. Physiol. Renal. Physiol., 278 (2000), pp. F726-F736

[CrossRef ↗](#) [View in Scopus ↗](#) [Google Scholar ↗](#)

[29] R.S. Goldstein, G.H. Mayor, R.L. Gingerich, J.B. Hook, R.W. Rosenbaum, J.T. Bond

The effects of cisplatin and other divalent platinum compounds on glucose metabolism and pancreatic endocrine function

Toxicol. Appl. Pharmacol., 69 (1983), pp. 432-441

 [View PDF](#) [View article](#) [View in Scopus ↗](#) [Google Scholar ↗](#)

[30] D.N. Nan, M. Fernandez-Ayala, M.E. Vega Villegas, *et al.*

Diabetes mellitus following cisplatin treatment

Acta Oncol., 42 (2003), pp. 75-78

[View in Scopus ↗](#) [Google Scholar ↗](#)

[31] A. Amr, Alaa Eldin A. Hamza

Effects of Roselle and Ginger on cisplatin-induced reproductive toxicity in rats

Asian J. Androl., 8 (5) (2006), pp. 607-612

[Google Scholar ↗](#)

Cited by (18)

[Hesperidin ameliorates cisplatin induced hepatotoxicity and attenuates oxidative damage, cell apoptosis, and inflammation in rats](#)

2022, Saudi Journal of Biological Sciences

Citation Excerpt :

...Cisplatin (CIS) is one of the most common and potent anti-neoplastic agents used against a broad range of malignancies including testicular, ovarian, cervical, bladder, head, neck as well as the lung. Despite its beneficial application as an anti-neoplastic agent, CIS causes several toxicities that limit its clinical use including nephrotoxicity, hepatotoxicity, cardiotoxicity, neurotoxicity, and ototoxicity (Hassan et al., 2020; Yadav, 2019; Neamatallah et al., 2018). Many experimental studies documented the common toxic side effects associated with CIS, especially nephrotoxicity (Tahoon, 2017)...

[Show abstract](#) 

[Nucleosides rich extract from Cordyceps cicadae alleviated cisplatin-induced neurotoxicity in rats: A behavioral, biochemical and histopathological study](#)

2022, Arabian Journal of Chemistry

Citation Excerpt :

...Cisplatin induced ROS and oxidative stress impairs mitochondrial function and integrity, enhances apoptosis through the activation of several caspase dependent pathways and eventually causes damages to the blood brain barrier, and thus inhibit the proliferation of neuronal stem cells (Gomaa et al., 2020; Kütük et al., 2019; Blanchette and Fortin, 2011). In addition, cisplatin toxicity impairs antioxidant defence efficiency, causing an imbalance in the prooxidant/antioxidant system (Yadav, 2019). Cells/tissues innate enzymatic antioxidant defence are the first line of antagonism against biological molecules damages induced by free radicals....

[Show abstract](#) 

Effects of chemotherapeutic agents on male germ cells and possible ameliorating impact of antioxidants

2021, Biomedicine and Pharmacotherapy

Citation Excerpt :

...Yadav has reported a significant increase in lipid peroxidation and a decrease in reduced glutathione (GSH), superoxide dismutase (SOD), and catalase (CAT) in the testes of rats following treatment with cisplatin. He has also reported degenerative changes in several seminiferous tubules and germ cell depletion following such exposure, implying the harmful impact of this agent on testicular cells through induction of free radical-associated oxidative stress [14]. Notably, extracts of *H. sabdariffa* and *Z. officinale* have been shown to decrease the magnitude of cisplatin-associated harmful effects on spermatogenesis in rats....

[Show abstract](#) 

Reproductive and developmental toxicities of 5-fluorouracil in model organisms and humans [↗](#)

2022, Expert Reviews in Molecular Medicine

The impact of apelin-13 on cisplatin-induced endocrine pancreas damage in rats: an in vivo study [↗](#)

2024, Histochemistry and Cell Biology

Comparative Analysis of Epigallocatechin-3-Gallate and TNF-Alpha Inhibitors in Mitigating Cisplatin-Induced Pancreatic Damage Through Oxidative Stress and Apoptosis Pathways [↗](#)

2024, Biological Trace Element Research



[View all citing articles on Scopus](#) [↗](#)

© 2019 Published by Elsevier Ltd.



All content on this site: Copyright © 2024 Elsevier B.V., its licensors, and contributors. All rights are reserved, including those for text and data mining, AI training, and similar technologies. For all open access content, the Creative Commons licensing terms apply.





Home ▶ All Journals ▶ Drug Development and Industrial Pharmacy ▶ List of Issues ▶ Volume 45, Issue 12
▶ Curcumin loaded mesoporous silica nanopa

Drug Development and Industrial Pharmacy >

Volume 45, 2019 - Issue 12

405 | 38

Views | CrossRef citations to date | Altmetric

0

Research Articles

Curcumin loaded mesoporous silica nanoparticles: assessment of bioavailability and cardioprotective effect

Yogesh Chand Yadav , Satyanarayan Pattnaik & Kalpana Swain

Pages 1889-1895 | Received 15 May 2019, Accepted 20 Sep 2019, Published online: 07 Oct 2019

 Cite this article  <https://doi.org/10.1080/03639045.2019.1672717>



 Sample our Bioscience journals, sign in here to start your access, Latest two full volumes FREE to you for 14 days

 Full Article

 Figures & data

 References

 Citations

 Metrics

 Reprints & Permissions

Read this article

Abstract

Rhizomes of the plant *Curcuma longa* has been traditionally used in medicine and culinary practices in India. It possesses various pharmacological effect, namely, antioxidant, hepatoprotective, anti-inflammatory, anti-thrombosis, and anti-apoptotic. The study was undertaken to assess the effect of curcumin and curcumin loaded mesoporous

silica nanoparticles (MSNs) against doxorubicin (DOX)-induced myocardial toxicity in rats. Furthermore, the study also included the bioavailability estimation of curcumin delivered alone and delivered via mesoporous technology. Cardiotoxicity was produced by cumulative administration of DOX (2.5 mg/kg for two weeks). Curcumin and curcumin loaded mesoporous nanoparticles (MSNs) each 200 mg/kg, po was administered as pretreatment for two weeks and then for two alternate weeks with DOX. The repeated administration of DOX induced cardiomyopathy associated with an antioxidant deficit and increased level of cardiotoxic biomarkers. Pretreatment with curcumin (alone and via MSNs) significantly protected myocardium from the toxic effects of DOX by significantly decreased the elevated level of malondialdehyde and increased the reduced level of reduced glutathione (GSH), superoxide dismutase (SOD) and catalase (CAT) in cardiac tissue. MSNs based delivery was found superior compared to curcumin delivered alone. Moreover, the results of bioavailability assessment in rats clearly indicated higher C_{max} and AUC values in rats when curcumin was administered via MSNs indicating superior bioavailability. The bioavailability of curcumin loaded MSNs, biochemical and histopathology reports support the good cardioprotective effect of curcumin which could be attributed to its increased bioavailability lead to good antioxidant and anti-inflammatory activity.

Q Keywords: Cardiotoxicity curcumin MSNs RP-HPLC bioavailability

Disclosure statement

We wish to confirm that there are no known conflicts of interest associated with this publication and there has been no significant financial support for this work that could have influenced its outcome.

Log in via your institution

➤ [Access through your institution](#)

Log in to Taylor & Francis Online

➤ [Log in](#)

Restore content access

➤ [Restore content access for purchases made as guest](#)

Purchase options *

[Save for later](#)

PDF download + Online access

- 48 hours access to article PDF & online version
- Article PDF can be downloaded
- Article PDF can be printed

USD 65.00

 [Add to cart](#)

Issue Purchase

- 30 days online access to complete issue
- Article PDFs can be downloaded
- Article PDFs can be printed

USD 1,085.00

 Add to cart

* Local tax will be added as applicable

Related Research

People also read



Recommended articles

Cited by
38

Information for

[Authors](#)

[R&D professionals](#)

[Editors](#)

[Librarians](#)

[Societies](#)

Opportunities

[Reprints and e-prints](#)

[Advertising solutions](#)

[Accelerated publication](#)

[Corporate access solutions](#)

Open access

[Overview](#)

[Open journals](#)

[Open Select](#)

[Dove Medical Press](#)

[F1000Research](#)

Help and information

[Help and contact](#)

[Newsroom](#)

[All journals](#)

[Books](#)

Keep up to date

Register to receive personalised research and resources by email

 [Sign me up](#)



Review

Comprehensive review on current developments of quinoline-based anticancer agents

[Shweta Jain](#)^a, [Vikash Chandra](#)^b, [Pankaj Kumar Jain](#)^c, [Kamla Pathak](#)^b, [Devendra Pathak](#)^b, [Ankur Vaidya](#)^b  

Show more 

 Outline |  Share  Cite

<https://doi.org/10.1016/j.arabjc.2016.10.009> 

[Get rights and content](#) 

Under a Creative Commons [license](#) 

open access

Abstract

Among heterocyclic compounds, quinoline scaffold has become an important construction motif for the development of new drugs. Quinoline and its derivatives possess many types of biological activities and have been reported to show significant anticancer activity. Quinoline compounds play an important role in anticancer drug development as they have shown excellent results through different mechanism of action such as growth inhibitors by cell cycle arrest, apoptosis, inhibition of angiogenesis, disruption of cell migration and modulation. A number of quinoline derivatives have been reported till date for

their anticancer activity. The present review, summarizes various mono-, di-, tri-, tetra- and heterocyclic substituent quinoline derivatives with potential anticancer activity. Their mechanism of action and possible structure activity relationship has also been discussed.



Abbreviations

CNS, central nervous system; DNA, deoxy ribonucleic acid; EZH, Enhancer of Zeste Homologue; FU, Fluorouracil; HDACIs, histone deacetylases inhibitors; IR, Infrared; JNK, Jun N-terminal kinase; GJIC, gap junction inter-cellular communication; MRP, multidrug resistance-related protein; Pgp, P-glycoprotein; ROS, reactive oxygen species; SAR, structure-activity relationship; THF, tetrahydro furan

Keywords

Anticancer; Quinoline; Quinoline derivatives; Structure-activity relationship

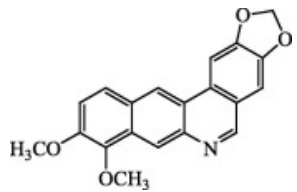
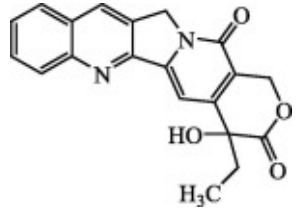
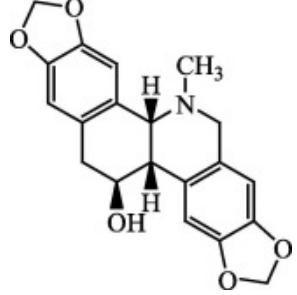
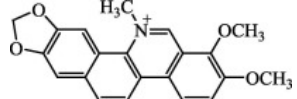
1. Introduction

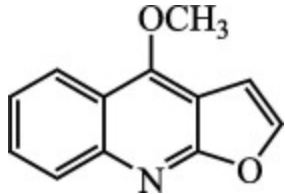
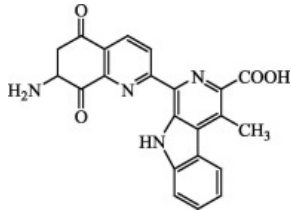
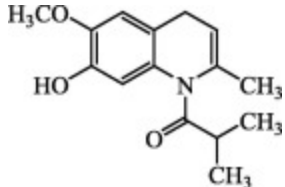
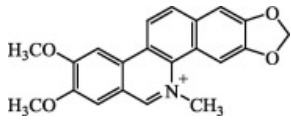
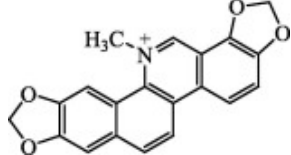
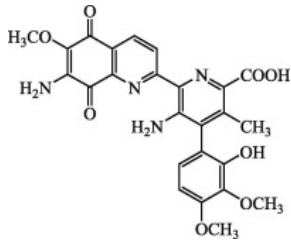
Quinoline is a heterocyclic aromatic organic compound having molecular formula C_9H_7N , characterized by a double-ring structure that contains a benzene ring fused to pyridine at two adjacent carbon atoms. Quinoline is also known as, benzopyridine, benzo[b]pyridine, 1-benzazine and benzazine. It is a hygroscopic, yellowish oily liquid, slightly soluble in water, soluble in alcohol, ether and many other organic solvents. Isoquinoline is a congener of quinoline and differs from quinoline in nitrogen position (at 2nd position) ([Ferlin et al., 2005](#)).

Quinoline and isoquinoline alkaloids obtained from natural sources show remarkable biological activities and relatively simple structures have attracted great interest in the scientific community, especially researchers involved in the chemistry

of natural products. Quinoline and its congeners have also attracted the interest of synthetic organic chemists due to the need to obtain increased amounts aimed at additional biological research. Quinoline alkaloids derived from flowering plants, animals and microorganisms possessed numerous biological activity. Some source of the quinoline or its derivatives and their biological activities are summarized in [Table 1](#).

Table 1. Natural quinoline and its congener possess antitumor/anticancer activity.

Com. No.	Reference	Structure	Quinoline derivative/user name	Source	Use
1	Ortiz et al. (2014)		Berberine	Family of <i>Berberidaceae</i>	Colon cancer
2	Wall et al. (1966)		Camptothecin	<i>Camptotheca acuminata</i> , <i>Notihapodytes Foetida</i>	Topoisomerase inhibitor (anticancer agent)
3	Haseeb et al. (2007)		Chelidonium	<i>Celandine</i>	Lung and pancreatic cancer
4	Haseeb et al. (2007)		Chelerythrine	<i>Celandine</i>	Lung and pancreatic cancer

Com. No.	Reference	Structure	Quinoline derivative/user name	Source	Use
5	Abdel et al. (2014)		Dictamine	<i>Dictaminus albus</i>	Cytotoxicity to HepG2 cells
6	Cai et al. (2010)		Lavendamycin	<i>Streptomyces lewendulae</i>	Antitumor antibiotic
7	Djerassi et al. (1958)		Lophocereine	<i>Lophocereus schotti</i>	Antitumor antibiotic
8	Tan et al. (1991)		Nitidine	<i>Zanthoxylum nitidum</i>	Topoisomerase inhibitor (anticancer agent)
9	Zhihu et al. (2014)		Sanguinarine	<i>Sanguinaria</i>	Lung and pancreatic cancer
10	Rao et al. (1963)		Streptonigrin	<i>Streptomyces flocculus</i>	Antitumor antibiotic

Various quinoline derivatives have been synthesized and reported for different activities. Quinoline derivatives are widely used as “parental” compounds to synthesize molecules with medical benefits, especially with anti-malarial and anti-

microbial activities. A number of quinoline and its derivatives are known to possess antimicrobial, antitumor, antifungal, hypotensive, anti HIV, analgesics and anti-inflammatory activities. Quinoline and its analogues have recently been examined for their modes of function in the inhibition of tyrosine kinases, proteasome, tubulin polymerization, topoisomerase and DNA repair. Substitution of the group in a suitable position of a bioactive molecule is found to exert a profound pharmacological effect ([Gasparotto et al., 2006](#)). The quinoline nucleus has naturally stirred in many alkaloids with swaying antitumor activity, for example, camptothecin ([Wall et al., 1966](#)). [Srivastava et al. \(2005\)](#) obtained a patent for an isolation procedure of camptothecin a quinoline analogous from *Nothapodytes Foetida*.

Applications of quinoline derivatives are fast spreading from anticancer drugs to almost every branch of medicinal chemistry. Quinoline derivatives represent a large number of antiproliferative agents exhibiting cytotoxicity through DNA intercalation, causing interference in the replication process ([Ryckebusch et al., 2008](#)). Actinomycin D, doxorubicin, mitoxantrone and streptonigrin are quinoline analogues possessing antibacterial or anti-cancer activity through DNA intercalation. Most of these drugs are currently used in the treatment of human malignancies target topoisomerase (types II) enzymes. Topoisomerase inhibitors designated as “poisons” interact with DNA to form cleavable complexes, causing permanent DNA damage that triggers a series of cellular events finally inducing apoptosis or other types of cell death. Topoisomerases are nuclear enzymes that regulate topological and conformational changes in DNA, critical to cellular processes such as replication, transcription, chromosome segregation and mitosis. There are two classes of DNA topoisomerase: (i) type I enzyme breaks one DNA strand for the passage of a second strand, and (ii) type II enzyme breaks both strands of one DNA duplex for the passage of a second DNA double strand. DNA topoisomerases (types II) are the primary target for a number of quinoline derivatives, including doxorubicin and mitoxantrone etc. Most of the anticancer drugs currently used in the treatment of human malignancies, as well as several new series of drugs under development, are targeted at topoisomerase II enzymes. Most of the quinoline based anticancer drugs currently used in the treatment of human malignancies, as well as several new series of drugs under development, are targeted at topoisomerase enzymes ([Schmidt et al., 2008](#)).

Among the many possible strategies for improving the therapeutic effectiveness of anticancer drugs, one of the most important is the synthesis of new derivatives with modified structure. In the search for new derivatives with advantageous biological properties many structural modifications have already been attempted. Such modifications appear to be a promising way for improvement of biological properties in comparison with those of the parent anticancer compounds,

because such modifications exhibited lower toxicity and were found to be highly cytotoxic to several neoplastic cell lines with multidrug resistance.

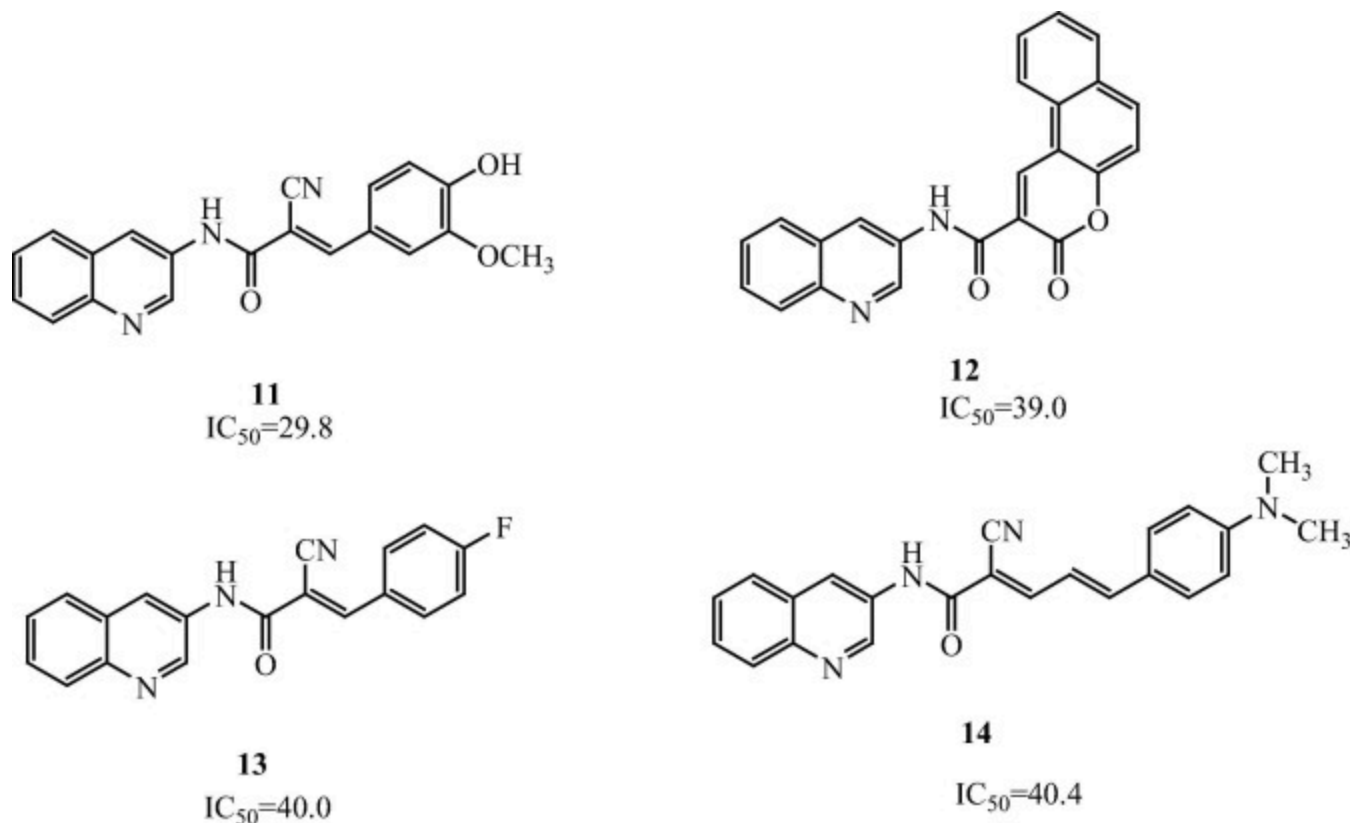
In the present review, we have summarized our knowledge on quinoline derivatives with respect to their anticancer activities, mechanisms of action, structure-activity relationship (SAR), and selective and specific activity against various cancer drug targets. In particular, we focus our review on *in vitro* and *in vivo* anticancer activities of quinoline derivatives in the context of cancer drug development and refinement.

2. Monosubstituted quinoline derivatives

2.1. 3-Quinoline derivatives

Several quinoline derivatives, isolated from natural sources or prepared synthetically, are important for medicinal chemistry and biomedical use. The quinoline derivatives that intercalate DNA are of growing interest in the field of anticancer drugs. A number of research programs directed toward developing new approaches to a variety of heterocyclic ring systems for anticancer activity, especially those containing 3-quinoline derivatives have been widely reported.

[Ghorab et al. \(2015\)](#) reported a series of 3-quinoline derivatives. Compounds were synthesized *via* reaction of 3-aminoquinoline with ethyl cyanoacetate followed by reaction with substituted aldehydes. The structures of the newly synthesized compounds were confirmed by elemental analyses, and spectroscopic techniques. All the newly synthesized compounds were evaluated for their cytotoxic activity against a human tumor breast cancer cell line (MCF7). It was found that the compounds 2-Cyano-3-(4-hydroxy-3-methoxyphenyl)-N-(quinolin-3-yl) acrylamide (**11**), 3-Oxo-N-(quinolin-3-yl)-3H-benzol[*f*]chromene-2-carboxamide (**12**), 2-Cyano-3-(4-fluorophenyl)-N-(quinolin-3-yl) acrylamide (**13**) and 2-Cyano-5-(4-(dimethylamino) phenyl)- N-(quinolin-3-yl) penta-2,4-dienamide (**14**) exhibited higher activity with IC₅₀ values of 29.8, 39.0, 40.0, 40.4 μmolL⁻¹, respectively. These compounds showed remarkable cytotoxic activity compared to doxorubicin as a positive control ([Fig. 1](#)).



Download : [Download high-res image \(261KB\)](#)

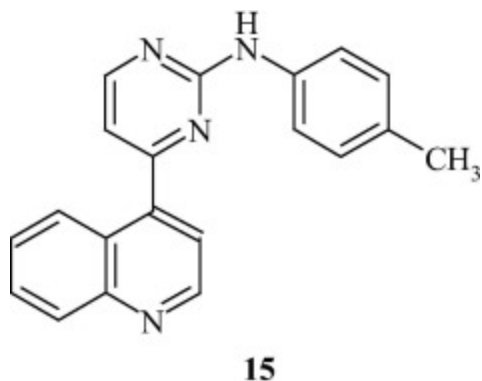
Download : [Download full-size image](#)

Figure 1. Structures of 3-quinoline derivatives (**11–14**) show cytotoxic activity against breast cancer cell line (MCF7).

2.2. 4-Quinoline derivatives

Reyes et al. (2010) synthesized a series of 4-quinoline substituted aminopyrimidine and 2-methylimidazo[1,2-a]pyridine derivatives. The synthesized compounds were evaluated for their cytotoxic activity against U251 (glioma), PC-3 (prostate), K562 (leukemia), HCT-15 (colon), MCF7 (breast) and SK-LU-1 (lung) cancer cell lines. Results showed that quinolin-4-yl-substituted compound (**15**), persists cytotoxic activity and is the most effective and selective against CDK1/CycA than against CDK2/CycB, while quinolin-3-yl-substituted compound is devoid of any cytotoxic activity (Fig. 2). This result constituted a

new lead of quinolin-4-yl-substituted compounds for their cytotoxic and CDK inhibitory activity from which more compelling and selective inhibitors can be designed.



Download : [Download high-res image \(54KB\)](#)

Download : [Download full-size image](#)

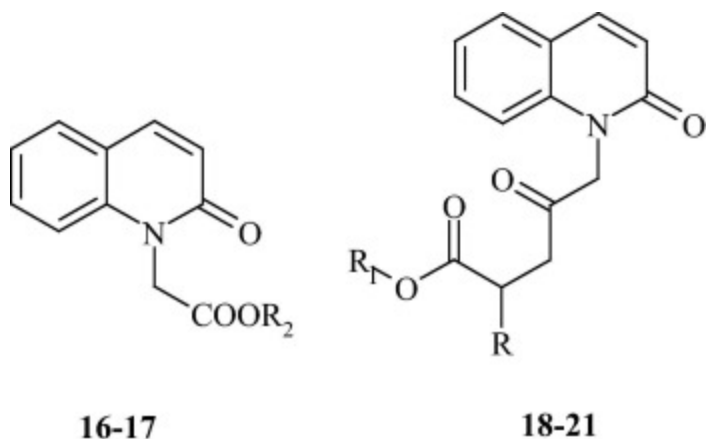
Figure 2. Structure of compound 4-(Quinolin-4-yl)-N-p-tolylpyrimidin-2-amine (**15**), possessing cytotoxic and CDK inhibitory activity.

3. Disubstituted quinoline derivatives

3.1. N-alkylated, 2-oxoquinoline derivatives

N-alkylated quinoline derivatives exhibited a wide spectrum of pharmacological activities, such as antiplasmodial, cytotoxic, antibacterial, antiproliferative, antimalarial, and anticancer activity. The incorporation of oxygen at second position in quinoline (i.e. 2-Oxoquinoline) may alter the biological response of quinoline ([Ryckebusch et al., 2003](#)). [Sagheer et al. \(2013\)](#) reported N-alkylated, 2-oxoquinoline derivatives as cytotoxic agents. The quinoline was N-alkylated by the bromoacetic acid and then oxidized with an alkaline potassium ferricyanide solution to get N-alkylated quinolone. Six new quinoline derivatives (**16–21**) with high purity were synthesized and tested for their cytotoxic activity on the HEp-2 cell line (tumor of the larynx) with inhibitory concentration percent of (IC%) range ([Fig. 3](#)). The results of cytotoxic studies showed that all the

synthesized compounds have IC_{50} (%) value in the range of 49.01–77.67%. The result of cytotoxicity confirms the anticancer activity of N-alkylated, 2-oxoquinoline derivatives.



$IC_{50}=49.01 - 77.67$

Download : [Download high-res image \(101KB\)](#)

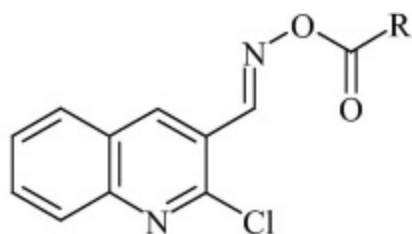
Download : [Download full-size image](#)

Figure 3. Structure of compounds N-alkylated, 2-oxoquinoline derivatives (**16–21**) shows good cytotoxic activity on the HEP-2 cell line (tumor of larynx).

3.2. 2,3-Disubstituted quinoline derivatives

Recently, photodynamic therapy is an emerging method of non-invasive treatment of cancer in which drugs such as Photofrin show localized toxicity on photoactivation at the tumor cells leaving the healthy cells unaffected. There has been increased interest in the discovery and investigation of compounds that damage DNA upon irradiation, also known as photonuclases, exhibited a large potential for therapeutic applications chiefly in cancer disease ([Armitage et al., 1998](#)). Importantly, the type and the efficiency of the photo cleavage reaction will depend on the binding affinity and the binding site that the photonuclase occupies. A number of 2,3-disubstituted quinoline oxime derivatives have been reported for their anticancer activity by means of DNA cleavage activity in cancerous cells.

Bindu et al. (2012) reported the simple, convenient and high yielding synthesis of 2-chloro-3-formyl quinoline oxime esters derivatives. The electrophoretic data showed concentration and substitution dependent nucleolytic activities of 2-chloro-3-formyl quinoline oxime esters. The DNA photo cleavage studies were performed by neutral agarose gel electrophoresis at different concentrations (40 μ M and 80 μ M) which indicated that few of quinoline oxime esters (**22–27**) converted into supercoiled pUC19 plasmid DNA to its nicked or linear form (Fig. 4). The structure activity studies concluded that the electron donating groups are highly reactive radical and thus possessed remarkable anticancer activity, while the molecules having halogen and nitro groups were less active. These electrons donating groups abstracts hydrogen atoms efficiently at C-40 of 2-deoxyribose in B-DNA.



22–27: *p*-ClC₆H₄; *p*-BrC₆H₄; *p*-NO₂C₆H₄; *p*-FC₆H₄
o-FC₆H₄; *m*-dinitro-C₆H₃

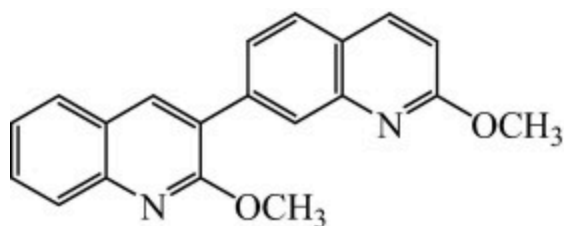
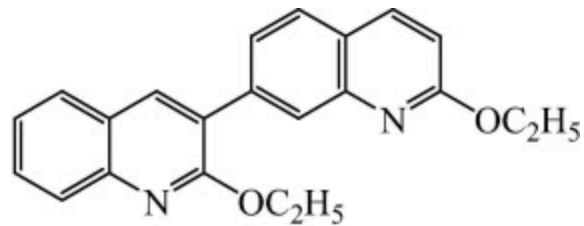
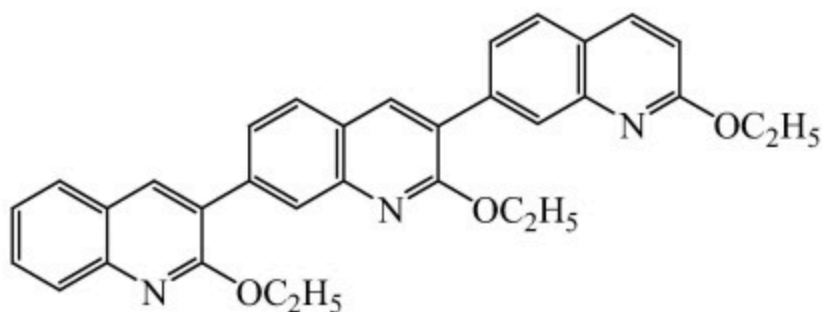
Download : [Download high-res image \(92KB\)](#)

Download : [Download full-size image](#)

Figure 4. Structure of compounds 2-chloro-3-formyl quinoline oxime esters derivatives having good anticancer properties.

In the continuous search of new 2,3-disubstituted quinoline derivatives for anticancer activity, Broch et al. (2010) designed and synthesized new quinoline derivatives. The synthesized compounds were evaluated for their *in vitro* antiproliferative activity toward a human fibroblast primary culture and two human solid cancer cell lines (MCF-7 breast and PA 1, ovarian carcinoma). Results showed that the dimeric analogous (2,2'-Dimethoxy-3,7'-biquinoline **28** and 2,2'-Diethoxy-3,7'-biquinoline **29**) were slightly active toward PA1 and MCF-7 cell lines with IC₅₀ values in the range of 36–54 μ M, and possessed better cytotoxicity toward these two human solid cancer cell lines as compared to trimeric compound (2,2',2''-

triethoxy-3,7'-3',7''-terquinoline **30**). The trimeric analogue (**30**) showed mild activity against the PA1 cell line with an IC_{50} value of $50\mu M$. The proposed reason for better activity of dimeric analogues is due to its enhanced solubility over trimeric analogues, and thus better cellular penetration (Fig. 5). The SAR studies showed that the introduction of various substituents on the heteroaromatic nucleus improved the solubility of compounds and results better biological profile.

**28** $IC_{50}=36-54$ **29** $IC_{50}=36-54$ **30** $IC_{50}=50$

[Download : Download high-res image \(274KB\)](#)

[Download : Download full-size image](#)

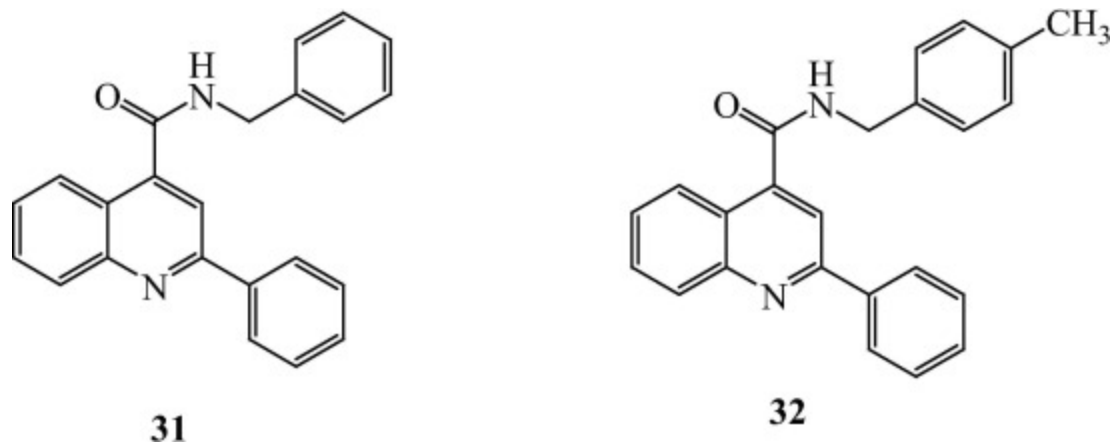
Figure 5. Structures of dimeric (**28**, **29**) and trimeric (**30**) analogues of 2,3-disubstituted quinoline derivatives having improved cytotoxicity against PA1/MCF-7 and PA1 cell line respectively.

3.3. 2,4-Disubstituted quinoline derivatives

Quinoline ring having 2,4-disubstitution plays an important role in the search of new anti-cancer agents as these derivatives have shown excellent results through different mechanism of action such as growth inhibitors by cell cycle arrest, apoptosis, inhibition of angiogenesis, disruption of cell migration, and modulation of nuclear receptor responsiveness (Lu et al., 2008).

Kouznetsov et al. (2012) reported a series of 2,4-disubstituted quinoline compounds, for their cytotoxic activity. The studies were further extended by the same research group Ilango et al. (2015). Various 2,4-disubstituted quinolines derivatives were synthesized from the reaction of aniline with benzaldehyde and pyruvic acid to formed 2-phenylquinolin-4-carboxylic acid, which converted to 2-phenylquinolin-4-carbonyl chloride, and on the subsequent reaction with substituted amines gave 2-phenylquinoline-4-substituted phenylcarboxamide. The syntheses of compounds were confirmed by spectroscopic techniques. The results of spectroscopy confirmed the synthesis of desired compounds with adequate purity.

The newly synthesized compounds were screened for cytotoxic activity by Trypan blue dye exclusion technique using Neubauer Hemocytometer. The Ara-c in a concentration of 10 µg/ml was used as standards. Among the synthesized compounds, nine compounds showed % mortality above 50. However, three compounds were found to have a 70% mortality when compared with Ara-c against the tumor cells. In spite of cytotoxic activity, all the newly synthesized compounds also showed good antibacterial and antifungal activities. Among newly synthesized derivatives, compounds N-2-diphenyl quinolin-4-carboxamide (**31**) and N-*p*-tolylquinolin-4-carboxamide (**32**) were found to possess maximum cytotoxicity (Fig. 6). The proposed reason for the superior cytotoxicity of these two compounds was the presence of bulky aryl groups at 2 and 4 positions which enhanced the activity of synthesized quinoline derivatives. The research group also proposed that the incorporation of the amido group in quinoline derivatives enhanced their cytotoxic and antimicrobial activities, but the presence of electron donating and electron withdrawing groups on the two aryl rings did not make any significant difference in their activity.



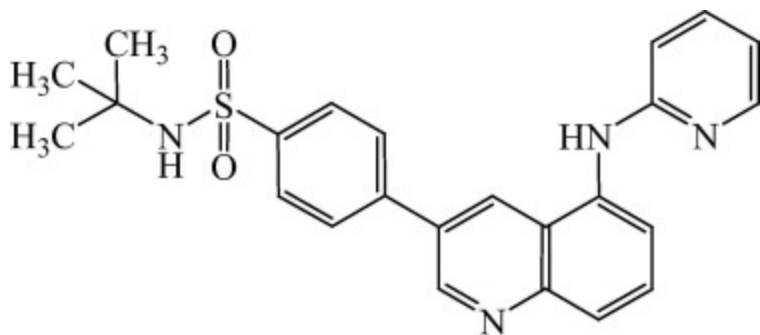
Download : [Download high-res image \(127KB\)](#)

Download : [Download full-size image](#)

Figure 6. Structure of compounds N-2-diphenyl quinolin-4-carboxamide (**31**) and N-p-tolylquinolin-4-carboxamide (**32**) shows best cytotoxicity among 2, 4-disubstituted quinoline compounds.

3.4. 3,5-Disubstituted quinoline derivatives

3,5-Disubstituted quinolines have been reported as potent c-Jun N-terminal kinase (JNKs) inhibitors and lead to produced anticancer activity. Three distinct genes encoding JNKs have been identified (*jnk1*, *jnk2*, and *jnk3*). JNK3 has been shown to mediate neuronal apoptosis and make inhibiting this isoform a promising therapeutic target for neurodegenerative diseases such as Parkinson's disease, Alzheimer's disease, and other CNS disorders. Currently JNK3 becomes primary target for number of therapeutics for anticancer activity (Zhang and Zhang, 2005, Kuan et al., 2003). Jiang et al. (2007) reported the synthesis of a novel series as potent c-Jun N-terminal kinase (JNK) inhibitors with selectivity against p38. The structures of 3,5-disubstituted quinolines were derived from 4-(2,7-phenanthrolin-9-yl)phenol. The X-ray crystal structure of inverse sulfonamide *t*-butyl analogue (**33**) in JNK3 revealed an unexpected binding mode for this new scaffold with protein and possessed a remarkable inhibition ($0.15\ \mu\text{M}$ IC₅₀) against JNK3 and devoid of inhibition against p38 (Fig. 7).

**33** $IC_{50}=0.15$

[Download : Download high-res image \(101KB\)](#)

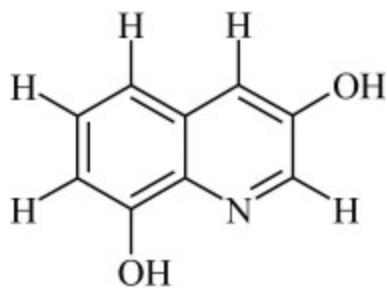
[Download : Download full-size image](#)

Figure 7. Structure of inverse sulfonamide *t*-butyl analogue (**33**) showing unexpected JNK3 binding capability with remarkable inhibitory activity ($0.15\mu\text{M } IC_{50}$) against p38 cell line.

3.5. 3,8-Disubstituted quinoline derivatives

Scolopendra subspinipes has been traditionally used for treating febrile seizure, malignant tumor, neuralgia or diphtheria in oriental countries. The inventors have extracted a novel quinoline compound from *scolopendra subspinipes* termed as jineol, and found that the extracted quinoline compound has cytotoxicity to a cancerous cell. This quinoline alkaloid has an oxygen atom at 3-carbon position and is rare in the nature. Nowadays jineol a new 3-hydroxy quinolinic compound has been discovered. It is known that the cyclic peptide structure of 3-hydroxy quinoline has an anticancer activity and its derivative 3-hydroxy quinoline-2-carboxylic acid, which can be obtained from a microorganism also showed anticancer activity ([Matson et al., 1993](#)). The amount of jineol (**34**) extracted from *scolopendra subspinipes* is very limited for commercial use ([Fig. 8](#)). Thus [Cho et al. \(2008\)](#), developed methods for synthesis of jineol and its derivatives thereof which showed anticancer activity. Jineol and its derivatives were synthesized by the reduction of starting material 2-amino-3-

methoxybenzoic followed by acetylation then selective deacetylation. The reaction was further proceed by the oxidation and Friedlander condensation and hydrogenation yielded jineol 8-methyl ether or jineol 3-benzyl ether.



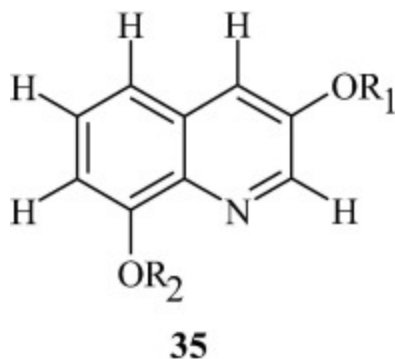
34

[Download : Download high-res image \(45KB\)](#)

[Download : Download full-size image](#)

Figure 8. Structure of jineol having anticancer activity.

The researchers patented a number of jineol derivatives having structure at 3,8-dihydroxy-quinoline derivatives (**35**) (Fig. 9). Jineol was extracted from *scolopendra subspinipes* with an organic solvent, and purifying an anticancerous activating portion by chromatography. Jineol showed cytotoxic activity of the cells, such as A-549 non-small cell lung cancer, SKOV-3 ovarian cancer, SK-Mel-2 melanoma, XP-498 central nervous system cancer and HCT-15 colon cancer. This jineol was utilized to derive its derivatives. The synthesized compounds were characterized by spectroscopic techniques. The cytotoxic activity of jineol derivatives was performed by SRB assay against A-549, SKOV-3, SK-Mel-2, XP-498 and HCT-15 cancer cell lines. Results showed enhanced cytotoxic activity of jineol and its derivatives as compared to carboplatin, cisplatin and adriamycin.



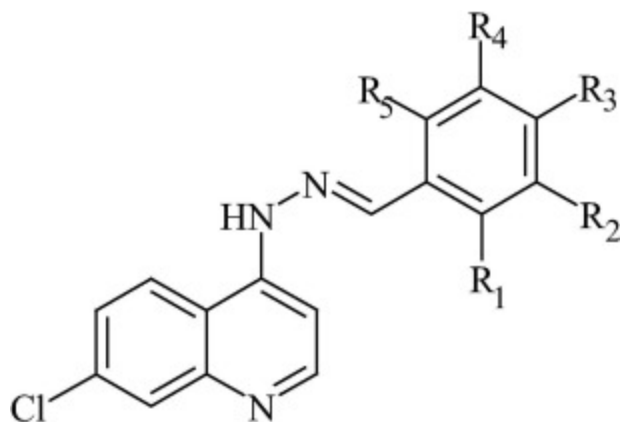
[Download : Download high-res image \(47KB\)](#)

[Download : Download full-size image](#)

Figure 9. Structure of 3,8-dihydroxy-quinoline derivatives (**35**) shows remarkable cytotoxic activity using SRB assay.

3.6. 4,7-Disubstituted quinolines derivatives

[Bispo et al. \(2015\)](#) reported a new and potent class of 7-chloro-4-quinolinyldrazones derivatives (**36**) as anticancer agents ([Fig. 10](#)). The synthesized compounds were screened against cancer cell lines using the MTT assay. The results of anticancer activity showed that compounds exhibited good cytotoxic activity against at least three cancer cell lines (SF-295, central nervous system; HTC-8 colon and HL-60, leukemia), with IC_{50} values between 0.314 and 4.65 $\mu\text{g}/\text{cm}^3$. Results showed that the compounds having 2,6-dichloro hydrazone derivative were more active as compared to monochloro, while di or trimethoxy hydrazone derivatives were more active than monomethoxy. Results also showed that 3rd position substituted hydrazone showed best cytotoxic activity while N-methylation increased biological activity of quinoline. However, 7-chloro substitution on the quinoline ring decreased cytotoxic activity.

**36** $IC_{50}=0.314-4.65$

[Download : Download high-res image \(93KB\)](#)

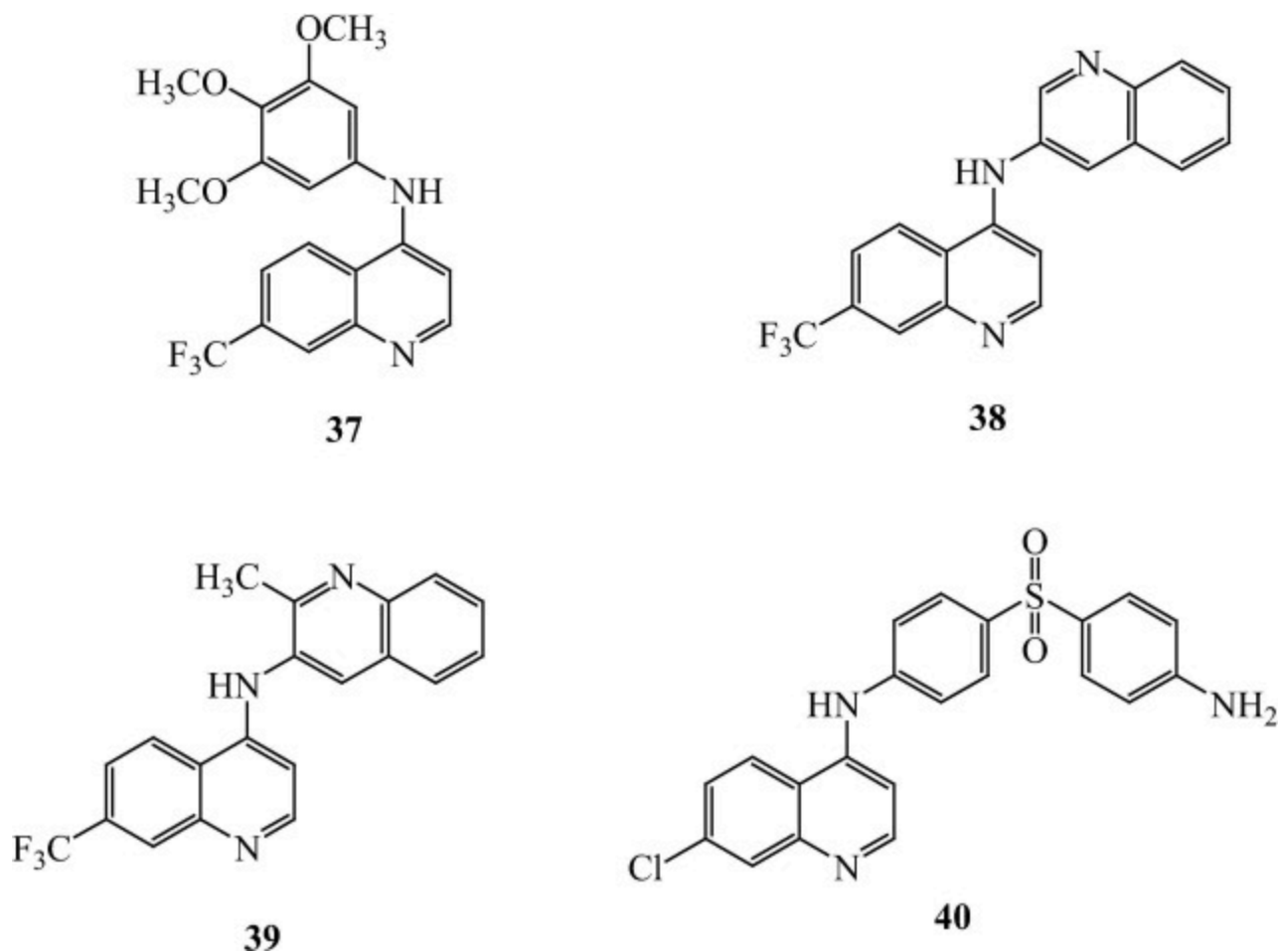
[Download : Download full-size image](#)

Figure 10. Structure of 7-chloro-4-quinolinylhydrazone derivatives (**36**) shows improved cytotoxic activity using MTT assay.

A plethora of the researcher's findings suggests that 4-amino, 7-substituted-quinoline derivatives bear numerous biological activities. These include anticancer, antioxidant, anti-proliferative, and anti-inflammatory properties. [Mcchesney et al. \(1962\)](#) employed structure activity relationship of 4-aminoquinoline derivatives for antimalarial activity. Consideration has been given to the potential role of metabolic transformations in the *in vivo* activation of 8-aminoquinoline.

[Ghorab et al. \(2014\)](#) designed and synthesized nineteen compounds based on a 4-aminoquinoline scaffold. The synthesized compounds bear *N*-substituted at the 4-position by aryl or heteroaryl, quinolin-3-yl, 2-methylquinolin-3-yl, thiazol-2-yl, dapsone moieties and bis-compounds. The synthesized compounds were assayed for *in vitro* using sulforhodamine B stain (SRB) method of the antiproliferative activity against the MCF-7 breast cancer cell line. Out of nineteen, seventeen compounds showed moderate activity than the reference drug doxorubicin, while compounds 7-(trifluoromethyl)-*N*-(3,4,5-trimethoxyphenyl)quinolin-4-amine (**37**), *N*-(7-(trifluoromethyl)quinolin-4-yl)quinolin-3-amine (**38**), 2-methyl-*N*-(7-

trifluoromethyl)quinolin-4-yl) quinolin-3-amine (**39**) and *N*-(4-(4-aminophenylsulfonyl) phenyl)-7-chloroquinolin-4-amine (**40**) were reported almost twice to thrice as potent as doxorubicin (Fig. 11). The result of *in vitro* studies strongly recommended that the 4-amino, 7-substituted-quinoline derivatives possess antiproliferative activity.



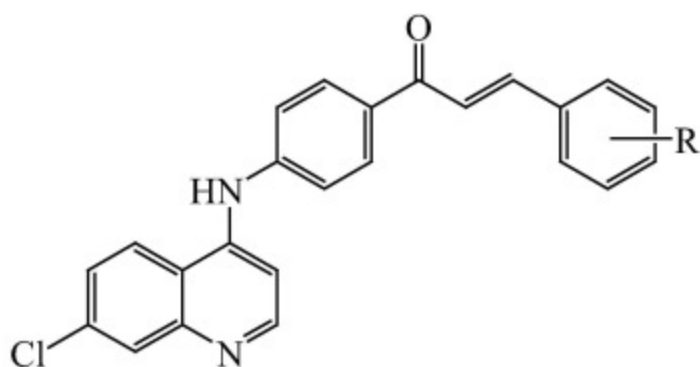
[Download : Download high-res image \(274KB\)](#)

[Download : Download full-size image](#)

Figure 11. Structure of 4-amino, 7-substituted-quinoline derivatives (**37–40**) showing improve antiproliferative activity against the MCF-7 breast cancer cell line using sulforhodamine B stain (SRB) method, with respect to doxorubicin.

Recently the combination of quinolines with chloroquine has been reported as the most apoptosis-inducing agent used against MCF-7 human breast cancer cells (Martirosyan et al., 2004). All differentiation-inducing quinolines caused growth suppression in MCF-7 and MCF10A cells by strong suppression of E2F1 which results cell cycle arrest.

Ferrer et al. (2009) reported a series of new [(7-Chloroquinolin-4-yl)amino]chalcone derivatives and were tested *in vitro* antiproliferative activity against human prostate LNCaP tumor cells. Compounds (2E)-3-(4-Chlorophenyl)-1-{3-[(7-chloroquinolin-4-yl)amino]phenyl}prop-2-en-1-one (4-chloro-3'-[(7-chloroquinolin-4-yl)amino]chalcone (**41**), (2E)-1-{3-[(7-Chloroquinolin-4-yl)amino]phenyl}-3-(3-fluorophenyl)prop-2-en-1-one (3'-[(7-chloroquinolin-4-yl)amino]-3-fluorochalcone (**42**) and (2E)-1-{3-[(7-Chloroquinolin-4-yl)amino]phenyl}-3-phenylprop-2-en-1-one (3'-[(7-chloroquinolin-4-yl)amino]chalcone, (**43**) exhibited potential inhibitors of human prostate cancer cell proliferation with IC₅₀ values of 7.93±2.05, 7.11±2.06 and 6.95±1.62 µg/mL respectively (Fig. 12). Results showed that the presence of hydrogen or a halogen on position 3rd or 4th in the aromatic ring improved the antiproliferative activity of the reported compounds.



41: R=4-Cl; **42:** R=3-F; **43:**R=H

41: IC₅₀=7.93 ± 2.05; **42:** IC₅₀=7.11 ± 2.06; **43:**IC₅₀=6.95 ± 1.62

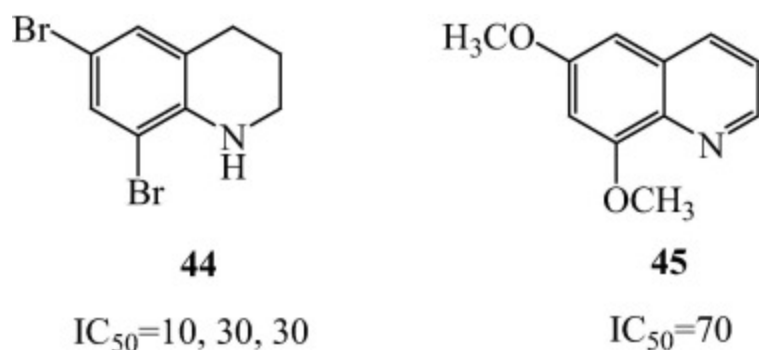
Download : [Download high-res image \(144KB\)](#)

Download : [Download full-size image](#)

Figure 12. Structure of compounds [(7-Chloroquinolin-4-yl)amino]chalcone (**41–43**) exhibits potential antiproliferative activity against prostate LNCaP tumor cells.

3.7. 6,8-Disubstituted quinoline derivatives

The quinoline and 6,8-disubstituted quinoline skeletons are often used in the designs of many synthetic compounds with diverse pharmacological properties. [Okten et al. \(2013\)](#) described an easy route for synthesis of 6,8-disubstituted quinoline derivatives since 6,8-dibromoquinolines. The reaction starts with synthesis of 6,8-dibromoquinolines followed by metal bromine exchange leading to produce various 6,8-disubstituted quinoline derivatives. The synthesized compounds were characterized by spectroscopic techniques. The synthesized compounds were screened for antiproliferative activity against several tumor cell lines. The results showed that compound 6,8-dibromo-1,2,3,4-tetrahydroquinoline (**44**) showed comparable antiproliferative activity against HeLa (cervical epithelioid carcinoma cells), HT-29 (colon cells) and C6 (brain tumor cells) in a concentration of 10 μ g/mL, 30 μ g/mL and 30 μ g/mL respectively with respect to 5-FU. Compound 6,8-dimethoxyquinoline (**45**) also showed significant activity against HT-29 cells in the concentration of 70 μ g/mL with respect to 5-FU. The proposed reaction procedure avoids shortcoming of numerous conventional methods (i.e. Skraup, Friedlander, Doebner-von Miller, Pfitzinger, Conrad-Limpach, and Combes) including limited homogeneity and substitution on the quinoline ring system ([Fig. 13](#)).



[Download : Download high-res image \(86KB\)](#)

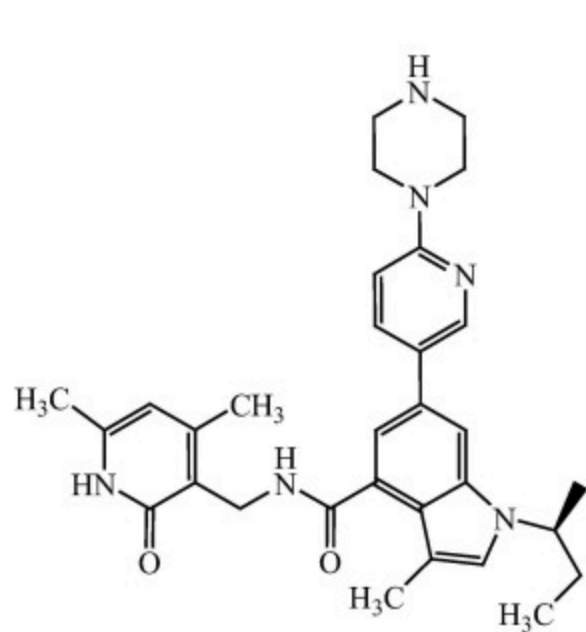
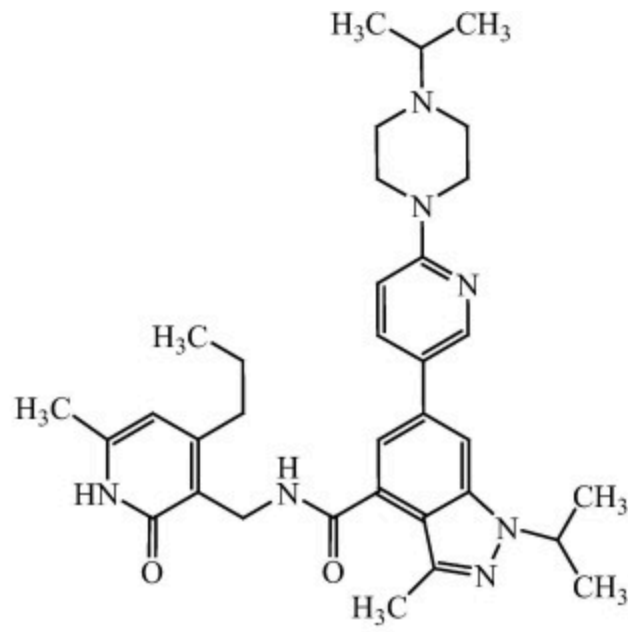
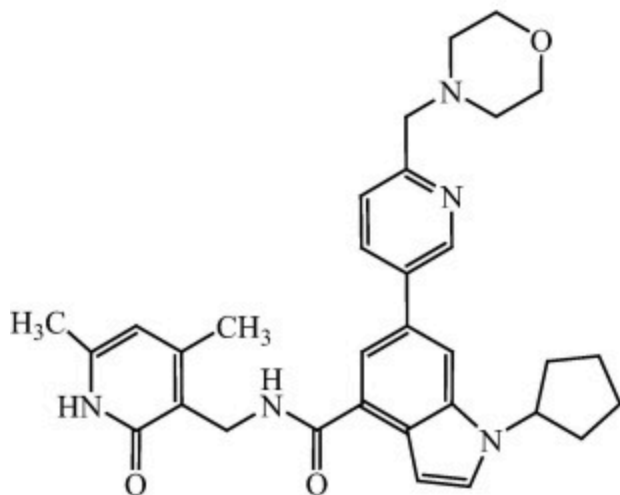
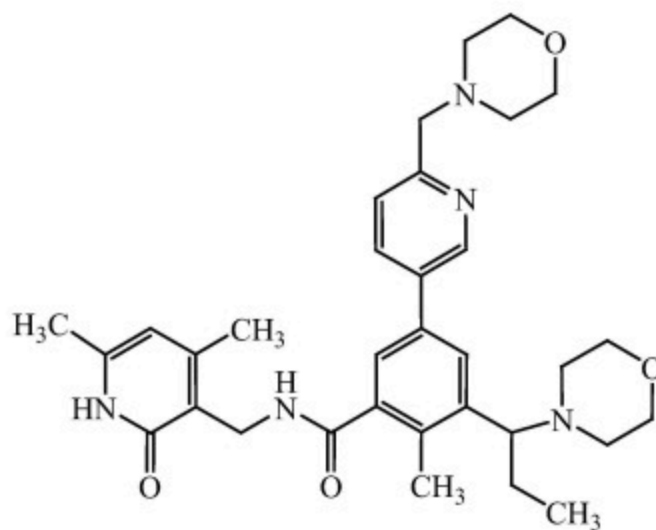
[Download : Download full-size image](#)

Figure 13. Structure of compounds 6,8-dibromo-1,2,3,4-tetrahydroquinoline (**44**) and 6,8-dimethoxidequinoline (**45**) showing comparable antiproliferative activity against HeLa/HT-29/C6 and HT-29 cancer cell lines respectively.

4. Trisubstituted quinoline derivatives

4.1. 2,4,5-Trisubstituted quinoline derivatives

Enhancer of Zeste Homologue 2 (EZH2) is a member of the histone-lysine *N*-methyltransferase (HKMT) family, which methylates K9 and K27 of histone H3, leading to transcriptional repression of the affected target genes. EZH2 has been found to be over-activated or over-expressed in many cancer types including colon, prostate, breast, and lung cancer ([Kleer et al., 2003](#)). Recently EZH2 has become a choice of target for a number of researchers for the treatment of cancer. EZH2 inhibitors had been discovered by many pharmaceutical companies and academic institutes exposed in the treatment of cancer. To date, a number of EZH2 inhibitors ([Fig. 14](#)) have been reported ([Nasveschuk et al., 2014](#), [Bradley et al., 2014](#)). Unfortunately, the known EZH2 inhibitors have very limited scaffold structures.

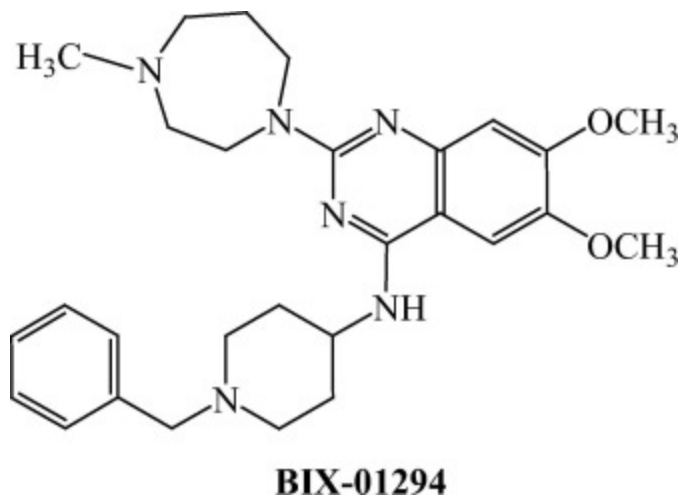
**GSK 126****UNC 1999****EPZ005687****EPZ 6438/E7438**

[Download : Download high-res image \(437KB\)](#)

[Download](#) : [Download full-size image](#)

Figure 14. Structure of typical EZH2 inhibitors.

In the search of new potent EZH2 inhibitors [Xiang et al. \(2015\)](#) discovered a new class of 5-methoxyquinoline derivatives a congener of BIX-01294 (2-(hexahydro-4-methyl-1*H*-1,4-diazepin-1-yl)-6,7-dimethoxy-*N*-[1-(phenylmethyl)-4-piperidinyl]-4-quinazolinamine, ([Fig. 15](#)). BIX-01294 is a well-known histone methyltransferase G9a/GLP inhibitor containing a 1-benzylpiperidin-4-ylamino group ([Kubicek et al., 2007](#)).



[Download](#) : [Download high-res image \(101KB\)](#)

[Download](#) : [Download full-size image](#)

Figure 15. Structure of compound 2-(hexahydro-4-methyl-1*H*-1,4-diazepin-1-yl)-6,7-dimethoxy-*N*-[1-(phenylmethyl)-4-piperidinyl]-4-quinazolinamine (BIX-01294), a potent EZH2 inhibitors.

5-Methoxyquinoline derivatives were prepared by cyclization of 2-bromo-5-methoxyaniline and malonic acid, using POCl₃ as catalyst and solvent. The intermediate 8-bromo-2,4-dichloro-5-methoxyquinoline was prepared which on subsequent reactions with *n*-BuLi in THF and CH₃OH followed on reaction with a variety of primary or secondary amines at the 4-position of the quinoline moiety and finally on nucleophilic substitution reaction with amines at the 2-position of the

quinoline moiety in *i*-PrOH under microwave conditions, using TFA as an acid catalyst gave the desired series of compounds. The quinoline derivatives were assayed for their anticancer activity which was based on both enzymatic and cellular assays, in which the enzymatic activities were determined by the AlphaLISA (EZH2) method, and the cell growth inhibition potencies were evaluated on the HCT-15 (colon) and MD-MBA-231 (breast) cell lines by the MTT method. The results of these studies showed that compound 5-methoxy-2-(4-methyl-1,4-diazepan-1-yl)-N-(1-methylpiperidin-4-yl)quinolin-4-amine (**46**), displayed an IC_{50} value of $1.2\mu M$ against EZH2, decreased global H3K27me3 level in cells and also showed good anti-viability activities against both HCT15 and MD-MBA-231 tumor cell lines ([Fig. 16](#)). Studies also indicated that methoxy groups at the 5-position might be more important for the potency of the compounds, and single or double substitutions at other positions would not contribute to the potency. Selectivity studies of compound (**46**) were also done on different proteins, including SMYD3, G9a, SUV39H1, SETDB1, PRMT1 and SETD8. Results of selectivity showed that the compound (**46**) is highly selective for EZH2. Researchers concluded that the compound (**46**) could be a lead compound deserving further structural optimization due to the fact that it represents a new scaffold and possesses low molecular weight.

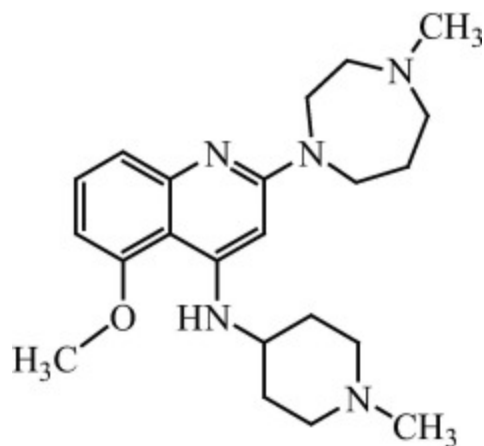
**46** $IC_{50}=1.2$ [Download : Download high-res image \(79KB\)](#)[Download : Download full-size image](#)

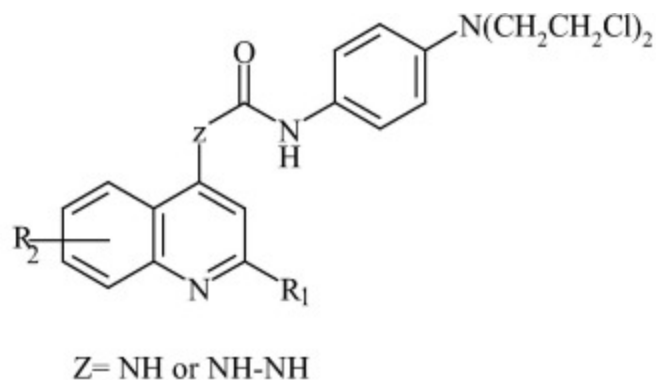
Figure 16. Structure of compound 5-methoxy-2-(4-methyl-1,4-diazepan-1-yl)-N-(1-methylpiperidin-4-yl)quinolin-4-amine (**46**) showing good anti-viability activities against both HCT15 and MD-MB-231 tumor cell lines.

4.2. 2,4,6-Trisubstituted quinolines

DNA alkylating agents have been widely used in chemotherapy. Recently, the investigation of new alkylating agents for cancer chemotherapy via the designing of DNA-directed alkylating agents or prodrug becomes a key area to overcome the general drawbacks of alkylating agents. DNA-directed alkylating agents are generally synthesized by linking alkylating pharmacophores (such as N-mustard residue) to DNA-affinic molecules (such as DNA intercalating agents or DNA minor groove binder) (Gourdie et al., 1990). These agents showed higher cytotoxicity and better therapeutic efficacy than the corresponding untargeted alkylating agents. Studies on the structure–activity relationships of these conjugates suggest that the selection of the DNA-affinic molecule (carrier), N-mustard residue (alkyl or phenyl N-mustard) and the spacer (type and length) greatly affect their antitumor activity. For example, Tallimustine a proposed anticancer drug candidate for this new class of cytotoxic compounds. It was evaluated in Phases I and II clinical trials and expressed a promising anticancer activity both *in vivo* and *in vitro* (Pezzoni et al., 1991).

Till date a number of DNA-directed alkylating agents, having N-mustard residue have been reported. In the search of new N-mustard alkylating agents Kakadiya et al. (2010) reported a series of phenyl N-mustard quinoline conjugates as potent DNA-directed alkylating agents. In his study quinolines were chosen as a DNA-affinic molecule, as they are DNA minor groove binders. New N-mustard–quinoline conjugates were synthesized, using urea or hydrazinecarboxamide as stabilizing spacers. The new targets derivatives were subjected to antitumor evaluation against a variety of human tumor cell growth *in vitro*, therapeutic efficacy *in vivo*, and their capability of DNA interstrand cross-linking. Results showed that compounds having hydrazinecarboxamide as a linker showed increased cytotoxic activity in comparison with the corresponding compounds bearing a urea spacer. The therapeutic efficacy against human tumor xenografts in animal model study clearly exposed the complete tumor remission in nude mice bearing human breast carcinoma MX-1 xenograft by N-{4-[Bis(2-chloroethyl)amino]phenyl}-N0-(2-methyl-4-quinoliny)urea (**47**); N-{4-[Bis(2-chloroethyl)amino]phenyl}-N0-[6-methoxy-2-(3-methoxy-phenyl)-4-quinoliny]urea (**48**); N-{4-[Bis(2-chloroethyl)amino]phenyl}-2-(6-methyl[1,3]-dioxolo[4,5-g]quinolin-8-yl)-hydrazinecarboxamide (**49**) and N-{4-[Bis(2-chloroethyl)amino]phenyl}-2-[6-(dimethylamino)-2-methyl-

4-quinolinyl]-hydrazinecarboxamide (**50**). The study concluded that the both linkers were able to lower the chemically reactive N-mustard pharmacophore and thus the newly synthesized conjugates possessed a long half-life in rat plasma (Fig. 17).



47: R₁ = Me, R₂ = H; **48:** R₁ = 3-MeO-C₆H₄, R₂ = 6-MeO

49: R₁ = Me, R₂ = 6,7-(OCH₂O); **50:** R₁ = Me, R₂ = 6-NMe₂

[Download : Download high-res image \(135KB\)](#)

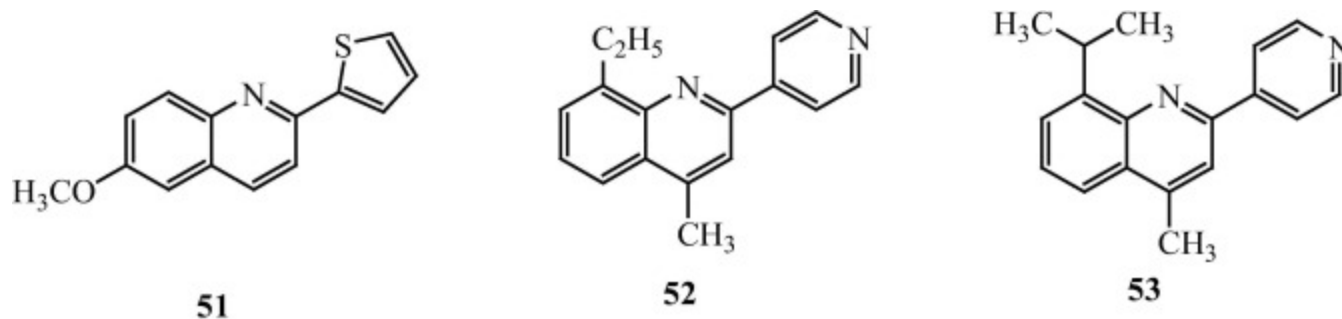
[Download : Download full-size image](#)

Figure 17. Structure of N-mustard–quinoline conjugates (**47–50**) showing improvement of anticancer activity against human breast carcinoma MX-1 xenograft.

4.3. 2,4,8-Trisubstituted quinoline derivatives

It is known that diverse polyfunctionalized quinoline molecules are used as potential anticancer agents. As a part of a medicinal chemistry program devoted to the search of new anticancer compounds, 2,4,8-trisubstituted quinoline derivatives could serve as models for the development of new antitumor drugs. It was reported that chemical modulation at the C-2 position of quinoline would alter the biological activity of the new quinoline compounds. The introduction of a hetaryl moiety in the C-2 position of the quinoline ring would possibly enhance the lipophilicity and DNA-quinoline binding properties of the prepared compounds and thus may augment the anticancer activity. [Kouznetsov et al. \(2012\)](#) accounted C-2

quinoline derivatives that possessed good cytotoxic activity. They identified structural similarities between sixteen C-2-substituted quinolines compounds and reported structures as anticancer. The synthesized compounds were tested in specific human cancer cell lines (MCF-7, H-460 and SF-268) and against nonspecific Vero cell lines and THP-1 monocyte macrophages, which indicated that 2- α -furyl- and 2- γ -pyridinyl quinoline derivatives 6-Methoxy-2-(thiophen-2-yl)quinoline (**51**); 8-Ethyl-4-methyl-2-(pyridin-4-yl)quinoline (**52**) and 8-Propyl-4-methyl-2-(pyridin-4-yl)quinoline (**53**) are active against the three specific cancer cell lines (MCF-7, H-460 and SF-268) and, at the same time, were devoid of cytotoxic effect on nonspecific Vero cell lines and THP-1 monocyte macrophages when compared to adriamycin and camptothecin as standard drugs (Fig. 18). Biological activity and SAR results were compared with different molecular descriptors determined in silico using online available software, in an attempt to show a relationship with the possible mode of action of these quinoline derivatives.



[Download : Download high-res image \(132KB\)](#)

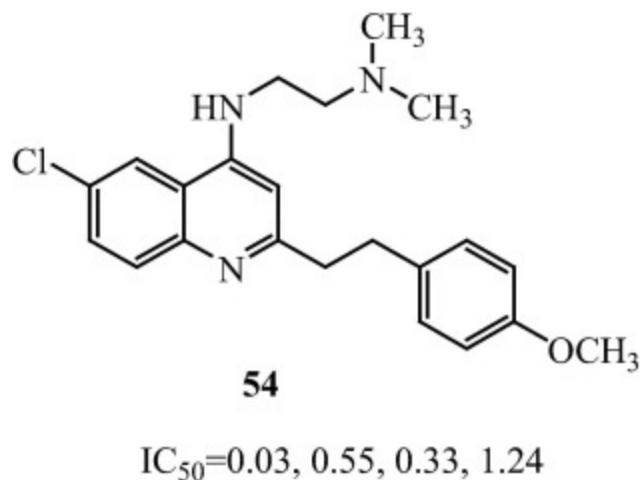
[Download : Download full-size image](#)

Figure 18. Structures of compounds 6-Methoxy-2-(thiophen-2-yl)quinoline (**51**); 8-Ethyl-4-methyl-2-(pyridin-4-yl)quinoline (**52**) and 8-Propyl-4-methyl-2-(pyridin-4-yl)quinoline (**53**) show excellent cytotoxicity against the specific human cancer cell lines (MCF-7, H-460 and SF-268).

4.4. 2-Substituted-4-amino-6-halogenquinoline derivatives

Gefitinib and pelitinib the 4-aminoquinazoline and 4-aminoquinoline skeletons respectively, are considered to be the promising nucleus for antitumor drug development. As a result, a great number of novel 4-aminoquinazoline and 4-

aminoquinoline derivatives have been developed in succession. Two series of novel 2-substituted-4-amino-6-halogenquinolines were designed, synthesized and evaluated by Jiang et al. (2012) for their antiproliferative activity against H-460 (lung), HT-29 (colon), HepG2 (liver) and SGC-7901 (stomach) cancer cell lines *in vitro*. The pharmacological results indicated that most compounds with 2-arylvinyl substituents exhibited good to excellent antiproliferative activity. Among them, the compound (E)-N¹-(6-Chloro-2-(4-methoxystyryl)quinolin-4-yl)-N²,N²-dimethylethane-1,2-diamine (**54**) (with a 4-methoxystyryl group at the C-2 position and a dimethylaminoalkylamino substituent at the C-4 position) was considered promising lead for further structural modifications with IC₅₀ values of 0.03 μM, 0.55 μM, 0.33 μM and 1.24 μM, against H-460, HT-29, HepG2 and SGC-7901 cancer cell lines respectively which was 2.5- to 186-fold more active than gefitinib (Fig. 19). The prelude SARs showed that the improved activity depended strongly on the introduction of an ethylene linkage between the nucleus and aryl moiety.



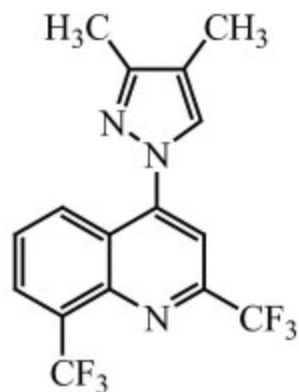
Download : [Download high-res image \(94KB\)](#)

Download : [Download full-size image](#)

Figure 19. Structure of compound (E)-N¹-(6-Chloro-2-(4-methoxystyryl)quinolin-4-yl)-N²,N²-dimethylethane-1,2-diamine (**54**) shows improve antiproliferative activity over H-460, HT-29, HepG2 and SGC-7901 cancer cell lines.

4.5. 2,8-Bis(trifluoromethyl)-4-substituted quinoline derivatives

[Meshram et al. \(2012\)](#) synthesized various 2,8-bis(trifluoromethyl)-4-substituted quinoline derivatives since 4-substituted iodoquinoline on reaction with boronic acids in the presence of a palladium catalyst under basic conditions or by the use of Triton B as a base. Synthesized compounds were characterized by spectroscopic techniques. Cell proliferation or viability of the synthesized compounds were assayed via MTT [3-(4,5-dimethylthiazol-2-yl)-2,5-diphenyl tetrasolium bromide] assay against the HL-60 (myeloid leukemia) and U937 (leukemia monocyte lymphoma) cell lines using etoposide as a reference drug. Results of cytotoxicity studies showed that synthesized quinoline derivatives were toxic to human HL-60 and U937 cell lines in the concentration of 100–200 $\mu\text{g/ml}$. Compound (**55**) [4-(3,5-dimethyl-1H-pyrazol-4-yl)-2,8-bis (trifluoromethyl) quinoline] was found to be a most potent antiproliferative agent ([Fig. 20](#)). This compound possessed IC_{50} value $19.88 \pm 3.35 \mu\text{g/ml}$ and $43.95 \pm 3.53 \mu\text{g/ml}$ in HL-60 and U937 cell lines respectively.

**55**

$\text{IC}_{50} = 19.88 \pm 3.35, 43.95 \pm 3.53$

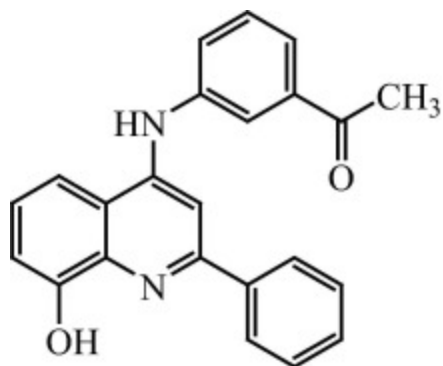
[Download : Download high-res image \(82KB\)](#)

[Download : Download full-size image](#)

Figure 20. Structure of compound 4-(3,5-dimethyl-1H-pyrazol-4-yl)-2,8-bis (trifluoromethyl) quinoline (**55**) shows highest anticancer activity against HL-60 and U937 cell lines.

4.6. 4-Anilino-8-hydroxy-2-phenylquinoline derivatives

Chen et al. (2006) reported the synthesis and antiproliferative evaluation of certain 4-anilino-8-methoxy-2-phenylquinoline and 4-anilino-8-hydroxy-2-phenylquinoline derivatives. The results showed that the antiproliferative activity of 4'-COMe-substituted derivatives decreased in an order of 6-OMe ($3.89\mu\text{M}$) > 8-OMe ($10.47\mu\text{M}$) > 8-OH ($14.45\mu\text{M}$), signifying that the position of substitution at the quinoline ring was crucial. For 3'-COMe derivatives, the antiproliferative activity of 8-OH (4-(3-Acetylanilino)-8-hydroxy-2-phenylquinoline) (**56**, $1.20\mu\text{M}$) was found to be more potent than its 8-OMe counterpart ($8.91\mu\text{M}$), indicating that a H-bond donating substituent was more favorable than that of a H-bonding accepting group. Similarly, for 8-OH derivatives, the antiproliferative effect of -COMe (**56**) was more potent than its oxime derivative ($2.88\mu\text{M}$), which in turn was more potent than the methyloxime counterpart ($5.50\mu\text{M}$) (Fig. 21). In continuation, the studies showed that the compound (**56**) was principally active against the growth of certain solid cancer cells, such as HCT-116 (colon cancer), MCF7 and MDA-MB-435 (breast cancer) with GI₅₀ values of 0.07, <0.01 and <0.01 μM , respectively.



21

IC₅₀=0.07, <0.01, <0.01

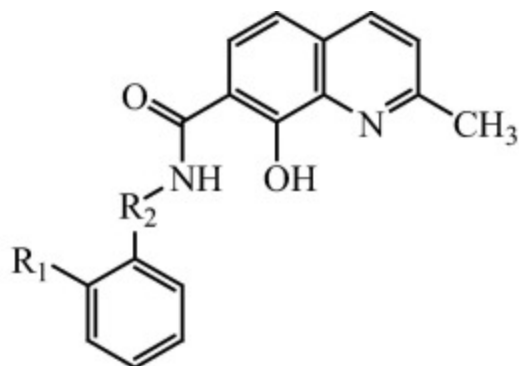
Download : [Download high-res image \(84KB\)](#)

Download : [Download full-size image](#)

Figure 21. Structure of compound 4-(3-Acetylanilino)-8-hydroxy-2-phenylquinoline (**56**) shows significant antiproliferative activity against HCT-116, MCF7 and MDA-MB-435 cancer cell lines.

4.7. 8-Hydroxy-2-methyl-7- substituted quinoline derivatives

Nowadays, researchers are focusing on biologically active quinoline analogues and fluorescent compounds capable of staining cancer cells. Researchers are trying to increase the lipophilicity of quinoline derivatives to enhance the permeability of the derivatives through the cell membranes, while their antiproliferative activities render them interesting as leading structures for anticancer agents or (in case of non-active compounds) as dying agents (Li et al., 2007). Spaczyńska et al. (2014) reported a series of 8-hydroxy-2-methylquinolone derivatives with benzylamide substitution and characterized by spectroscopic techniques. Compounds were investigated for fluorescent properties. Compounds 8-Hydroxy-2-methylquinoline-7-carboxylic acid (3- phenylbutyl)-amide (**57**) and 8-Hydroxy-2-methylquinoline-7-carboxylic acid phenethylamide (**58**) showed highest fluorescence, while remaining compounds also possessed remarkable fluorescence. The results of fluorescence studied showed that compounds having an unsubstituted aryl system or substituted —CH₃ or —F showed the best fluorescence intensity while substitution with —OCH₃ or —OH in the aryl ring decreased fluorescence. Synthesized compounds were also utilized for biological assays and were tested by the MTS assay against the wild type of human colon adenocarcinoma cell line (HCT116) and mutants with disabled TP53 gene (HCT116 p53). The synthesized compounds were also screened for their cytotoxicity against murine melanoma cell line (B16-F10) and normal human dermal fibroblasts. The compound 2-Hydroxybenzoic acid N'-(8-hydroxy-2-methylquinoline-7-carbonyl)-hydrazide (**59**) was found to possess highest cytotoxic activity and was active in inhibiting the proliferation of all tumor cell lines and possessed highest cytotoxic activity but very poor fluorescence, too weak for observations (Fig. 22).



57: $R_1=(CH_2)_4$, $R_2=H$; **58:** $R_1=(CH_2)_2$, $R_2=H$
59: $R_1=NH-CO$, $R_2=OH$

Download : [Download high-res image \(114KB\)](#)

Download : [Download full-size image](#)

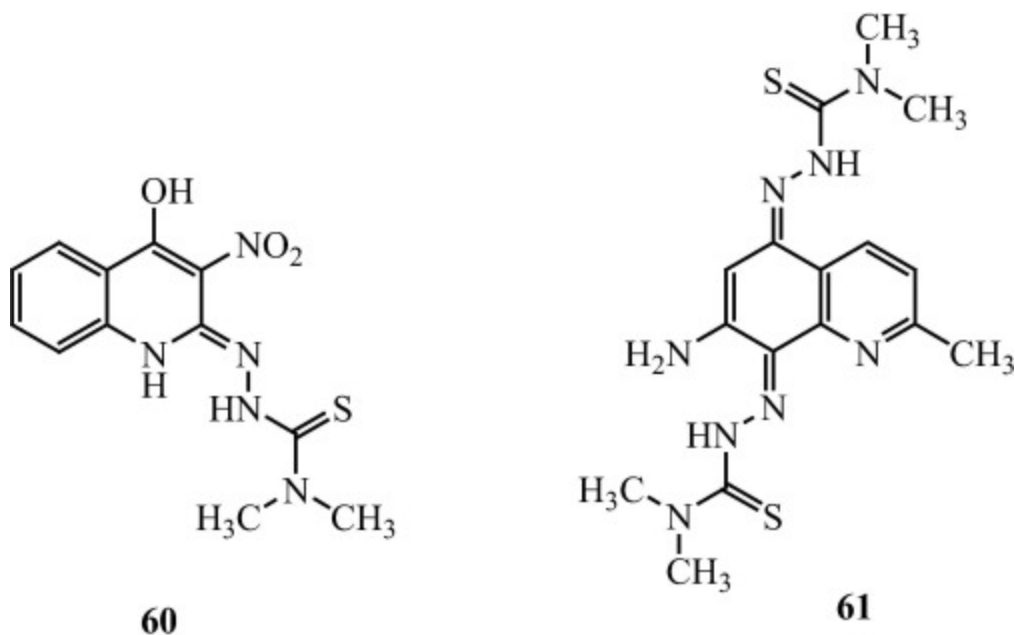
Figure 22. Structure of 8-hydroxy-2-methyl-quinolone derivatives (**57–59**) possesses highest cytotoxicity against B16-F10, NHDF cell lines but with very poor fluorescence.

4.8. Thiosemicarbazones based on quinoline scaffold

Thiosemicarbazones exhibit potent anticancer activity through the blocking of ribonucleotide reductase or by specific redox activity. [Serda et al. \(2010\)](#) showed that reduction of complex of Fe^{3+} -thiosemicarbazone lead to generation of reactive oxygen species (ROS) which may also be responsible for inhibition of ribonucleotide reductase as they are able to quench the tyrosyl radical of the R2 subunit of ribonucleotide reductase. Quinoline and its derivatives were also reported as a potent antiproliferative scaffold. Number of thiosemicarbazones based on quinoline compounds has been synthesized using microwave assisted techniques.

Microwave assisted chemistry carried most of the steps in efficient manner and green technique and also provide good (above 80%) yields of the main product. The proposed technique is time and cost efficient and allows obtaining a relatively wide group of compounds for biological tests. Structures of all new compounds were confirmed with spectroscopic techniques. The antiproliferative activity of thiosemicarbazones based quinoline compounds (**60** and **61**) was assessed by the

MTT assay against the HCT116 (human colon carcinoma) cell line (Fig. 23). Tested compounds exhibited improved antiproliferative activities against HCT116 cancer cells.



Download : [Download high-res image \(150KB\)](#)

Download : [Download full-size image](#)

Figure 23. Structure of thiosemicarbazones based quinoline compounds (**60**, **61**) shows good antiproliferative activity against the HCT116 cell line by MTT assay.

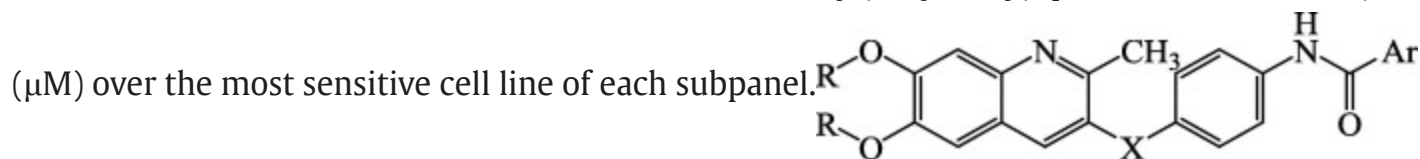
5. Tetrasubstituted quinoline derivatives

5.1. 2,3-Disubstituted-6,7-dimethoxy (dihydroxy) quinoline derivatives

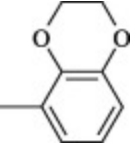
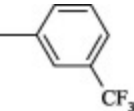
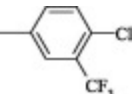
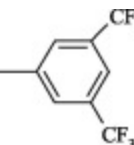
RAF (rapidly-growing fibrosarcoma) kinases are serine/threonine kinases, and they are part of the mitogen activated protein kinase signal transduction cascade. This cascade is vital for numerous cellular fates, including cell growth, differentiation,

proliferation and survival (Weber et al., 2000). Imatinib a diarylamides derivative was used in the treatment of gastrointestinal stromal tumors, thyroid cancer, breast cancer, meningioma, ovarian cancer, and nonsmall cell lung cancer in combination with other drugs (Wellbrock et al., 2004). Gamal et al. (2014) synthesized a new series of diarylamide derivatives possessing dimethoxy(dihydroxy)quinoline nucleus. The synthesized compounds were tested for *in vitro* antiproliferative activities over NCI-58 cancer cell line panel of nine different cancer types. Compounds 3,4-dichloro-N-(4-(6,7-dimethoxy-2-methylquinolin-3-yloxy)phenyl)benzamide (**62**); N-(4-(6,7-dimethoxy-2-methylquinolin-3-yloxy)phenyl)-2,3-dihydrobenzo[b][1,4]dioxine-5-carboxamide (**63**); 3-(Trifluoromethyl)-N-(4-(6,7-dimethoxy-2-methylquinolin-3-yloxy)phenyl)benzamide (**64**); 4-Chloro-3-(trifluoromethyl)-N-(4-(6,7-dimethoxy-2-methylquinolin-3-yloxy)phenyl)benzamide (**65**); N-(4-(6,7-dimethoxy-2-methylquinolin-3-yloxy)phenyl)-3,5-bis(trifluoromethyl)benzamide (**66**) showed the most promising results among all the synthesized compounds at a single-dose concentration of 10mM over 58 cell line panel. These compounds (**62–66**) were further tested in 5-dose testing mode in order to determine their IC₅₀ values, and the results were compared with those of imatinib and gefitinib which showed that the five compounds were more potent than imatinib against all the cell lines of nine different cancer types (Table 2). Compound **66** showed the highest inhibited activity and was further tested against C-RAF kinase inhibition. Results of C-RAF kinase inhibition showed 76.65% inhibition at 10mM. So it can be concluded that C-RAF kinase inhibition is a possible mechanism of the antiproliferative activity of this compound. The structure activity relationship (SAR) studies of synthesized compounds indicated that 6,7-dimethoxyquinoline scaffold was more favorable for activity than 6,7-dihydroxyquinoline. The O linker was optimal for the activity too. Taken together, they can give information about the pharmacophore of this series of compounds.

Table 2. Structures of the 2,3-disubstituted-6,7-dimethoxy (dihydroxy) quinoline derivatives (**60–64**) with their IC₅₀ values



Com. No.	R	X	Ar	Cancer cell lines								
				RPMI-8226 ^a	HOP-92 ^b	HCT-116 ^c	SF-295 ^d	SK-MEL-5 ^e	OVCAR-4 ^f	A498 ^g	PC-3 ^h	BT-549 ⁱ
62	CH ₃	O		3.70	16.10	4.26	1.59	4.99	5.26	20.60	4.77	3.91

Com. No.	R	X	Ar	Cancer cell lines								
				RPMI-8226 ^a	HOP-92 ^b	HCT-116 ^c	SF-295 ^d	SK-MEL-5 ^e	OVCAR-4 ^f	A498 ^g	PC-3 ^h	BT-549 ⁱ
63	CH ₃	O		2.98	3.93	3.42	2.91	2.92	3.32	2.06	2.49	1.71
64	CH ₃	O		3.67	3.08	3.22	2.73	2.45	3.68	1.78	2.85	3.31
65	CH ₃	O		5.43	13.60	4.18	2.28	10.60	5.58	2.42	4.30	8.86
66	CH ₃	O		1.57	1.82	1.56	1.64	2b.76	4.53	1.13	1.66	3.02
Imatinib				6.31	12.59	12.59	19.95	12.59	19.95	19.95	19.95	15.85
Gefitinib				6.31	0.32	3.16	10.00	3.16	6.31	0.63	5.01	3.16

a
Leukemia cell line.

b
Non-small cell lung cancer cell line.

c
Colon cancer cell line.

d
CNS cancer cell line.

e

Melanoma cell line.

f

Ovarian cancer cell line.

g

Renal cancer cell line.

h

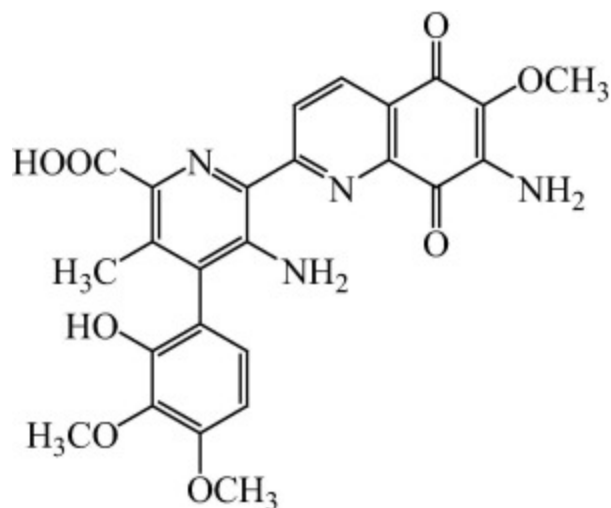
Prostate cancer cell line.

i

Breast cancer cell line.

5.2. 6,7-Substituted-5,8-quinolinequinone derivatives

5,8-Quinolinequinones derivatives reported to possess a wide spectrum of biological properties that include anti-tumor, anti-inflammatory and anti-bacterial activities ([Cheng et al., 2008](#), [Castellano et al., 2008](#)). Streptonigrin, isolated from the bacterium *Streptomyces flocculus* showed antitumor activity, having 5,8-quinolinequinones nub, which was one of the first compounds to be systematically modified in an attempt to correlate specific structural features with anti-cancer properties ([Fig. 24](#)) ([Rao et al., 1963](#)). Earlier structure–activity studies (SARs) concluded that the 7-aminoquinolinequinone-moiety of streptonigrin was crucial for anti-tumor activity; however, further studies showed that the addition of electron-withdrawing groups at the 6- and/or 7-positions of the quinolinequinone results enhanced rates of DNA degradation ([Rao, 1974](#), [Lown and Sim, 1976](#), [Shaikh et al., 1986](#)). Unfortunately, the high toxicity of streptonigrin has limited its therapeutic value ([Davis et al., 1978](#), [Bolzán and Bianchi, 2001](#)).



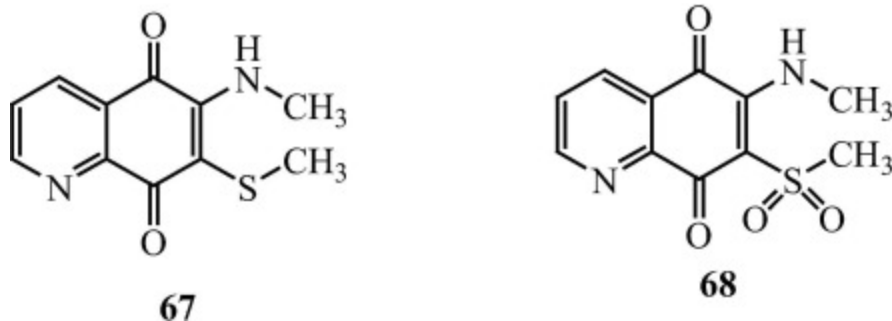
Streptonigrin

Download : [Download high-res image \(109KB\)](#)

Download : [Download full-size image](#)

Figure 24. Structure of streptonigrin, having antitumor activity, with 5,8-quinolinequinones nub.

[Mulchin et al. \(2010\)](#) reported a series of 6,7-substituted 5,8-quinolinequinones derivatives and identified their anti-cancer, anti-inflammatory or tuberculostatic activity. The starting material of synthesis was 8-hydroxyquinoline or 8-hydroxy-2-methyl-quinoline, which on the subsequent reaction with sodium chlorate gave oxidative product dichloro-quinones. These dichloro-quinones were then treated with a variety of amine nucleophiles to give the 6 and/or 7-substituted 5,8-quinolinequinolines products in good (65–96%) yield. The anti-cancer activity of the synthesized compounds was measured against HL60 cells (IC_{50}) and human T-cells (IC_{50}) from healthy volunteers using the MTT assay. These quinolinequinones showed promise as anti-cancer activity. Results showed that the introduction of a sulfur group at the 7-position of the quinolinequinone (6-methylamino-7-methylsulfanyl-5,8-quinolinequinone (**67**) and 6-amino-7-methylsulfonyl-5,8-quinolinequinone (**68**)) led to the discovery of a number of biologically active compounds that exhibited selectivity for leukemic cells over T-cells, a highly desirable property for an anti-cancer drug, while a di-chloro or di-thiol-substituted quinolinequinone gave better anti-inflammatory activity ([Fig. 25](#)).



Download : [Download high-res image \(95KB\)](#)

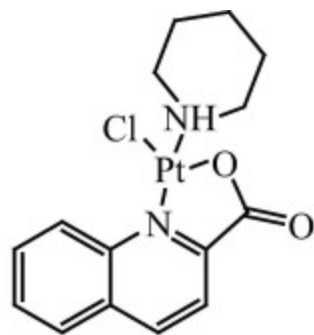
Download : [Download full-size image](#)

Figure 25. Structure of 6,7-substituted 5,8-quinolinequinones derivatives (**67**, **68**) shows significant anticancer activity against HL60 cells and human T-cells.

6. Heterocyclic fused quinoline derivatives

6.1. 1,2-Quinoline-platinum complex

The compound belonging to a series of platinum(II) complexes bearing piperidine (pip) as a ligand, exhibited notable antitumor activity (Da et al., 2001, Solin et al., 1982). Thanh et al. (2014) reported a [PtCl₂(pip)(quinoline)] complex, in which the quinoline ligand is replaced by an N,O-bidentate quinaldate ligand and quinoline-piperidine ligands are arranged in cis positions. The researchers also reported a new chlorido(piperidine-κN)-(quinoline-2-carboxylato-κ²N,O)platinum(II) compound (**69**) in which the quinoline ring of the quinaldate ligand occupies a transposition with respect to the piperidine ring (Fig. 26). The compound was synthesized in two steps. In a first step the quinaldic acid in its ionic form coordinates with PtII via the O atom of the carboxylate group first and in a cis position with respect to piperidine based on the trans effect, while in a second step, the quinaldic acid coordinates with PtII also via its N atom, resulting in the cyclic complex.

**69**

IC₅₀=4.46, 2.59, >10, 5.60

[Download : Download high-res image \(72KB\)](#)

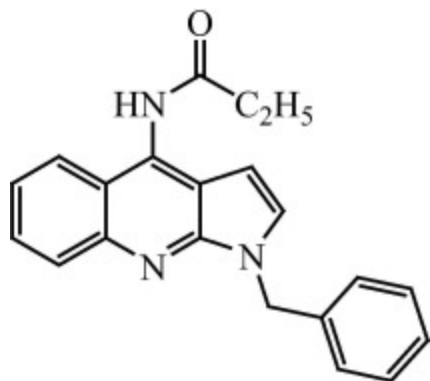
[Download : Download full-size image](#)

Figure 26. Structure of compound chlorido(piperidine- κ N)-(quinoline-2-carboxylato- κ^2 N,O)platinum(II) (**69**), shows significant cytotoxicity against human cancer cells of HepG2, RD, MCF7 and Fl.

The cytotoxic activity of the synthesized compound (**69**) was tested and recorded for four human cancer cells of HepG2, RD, MCF7 and Fl. The IC₅₀ values of the reported compound were found to be 4.46, 2.59, >10 and 5.60 μgml^{-1} respectively.

6.2. Pyrroloquinolines derivatives

Lee et al. (2004) identified a novel series of substituted pyrroloquinolines that selectively inhibited the function of P-glycoprotein (Pgp) without modulating multidrug resistance-related protein 1 (MRP 1). The synthesized compounds were screened for their toxicity toward drug-sensitive tumor cells (i.e. MCF-7, T24) and for their ability to antagonize Pgp mediated drug-resistant cells (i.e. NCI/ADR) and MRP 1 mediated resistant cells (i.e. MCF-7/VP). The results showed that the dihydropyrroloquinolines inhibited Pgp to varying degrees, without any significant inhibition of MRP 1. The compound Pgp-4008 (**70**) was found to be most potent in inhibition of Pgp *in vitro* (Fig. 27).



PGP-4008(70)

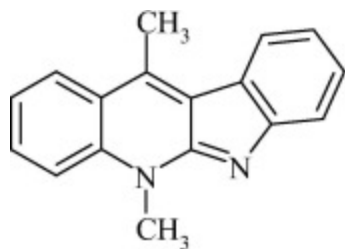
[Download : Download high-res image \(73KB\)](#)

[Download : Download full-size image](#)

Figure 27. Structure of compound Pgp-4008 (**70**), most potent in inhibition of *Pgp in vitro*.

6.3. Indolo[2,3-b]quinoline derivatives

5,11-Dimethyl-5H-indolo[2,3-b]quinoline (DiMIQ, **71**), the synthetic analogue of indolo[2,3-b]quinoline, reported high cytotoxic activity and inhibits the proliferation of mouth carcinoma KB cells (at a concentration of 1 mM) (Czoch et al., 1994) (Fig. 28). Moreover, its activity is similar to the cytotoxic activity of doxorubicin (0.8 mM against KB cells) a marketed anticancer drug (Kaczmarek et al., 1999). Unfortunately, DiMIQ (**71**) has limited practical applicability in the treatment of cancer, possibly due to its high toxicity, lack of selectivity and very low solubility in aqueous solutions, especially at neutral pH. The high toxicity and low bioavailability of DiMIQ (**71**), prompted researchers to look for new analogues which would conform to the high requirements necessary for anticancer drugs: potent and selective activity and low side effects.

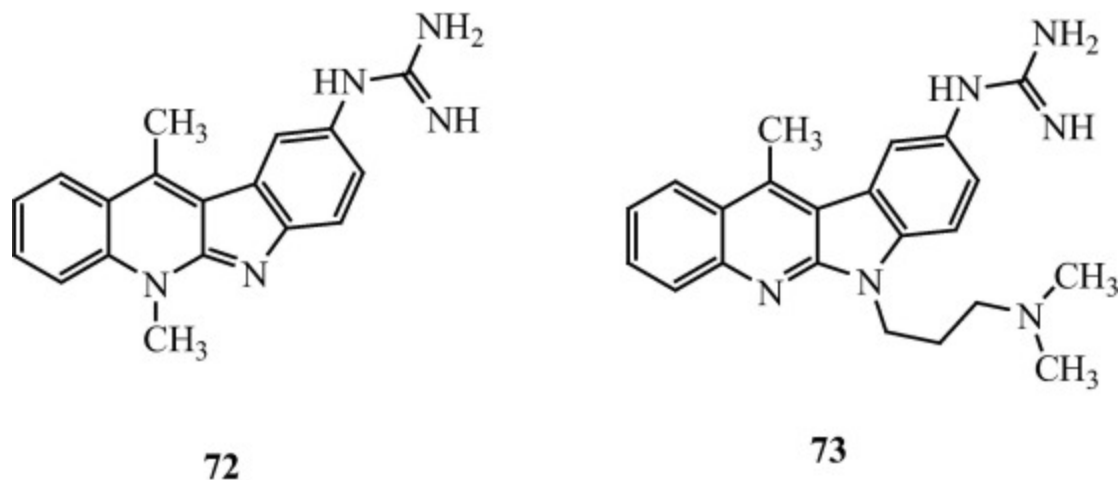
**DiMIQ (71)**

[Download : Download high-res image \(47KB\)](#)

[Download : Download full-size image](#)

Figure 28. Structure of compound 5,11-dimethyl-5H-indolo[2,3-b]quinoline (DiMIQ, **71**), a indolo derivative shows high cytotoxic activity and inhibits the proliferation of mouth carcinoma KB cells.

In the search of new DiMIQ congeners, [Sidoryk et al. \(2015\)](#) reported new indolo[2,3-b]quinoline derivatives containing guanidine, amino acid or guanylamino acid substituents. Results revealed that the attachment of the guanidine, or guanylamino acid chain directly to the DiMIQ or 6H-indolo[2,3-b]quinoline moiety significantly perked up its selective cytotoxicity against almost all cancer cell lines, while decreasing this activity against the normal cell line. Compounds N-guanyl-N-(5,11-dimethyl-5H-indolo[2,3-b]quinolin-9-yl)-amine dihydrochloride (**72**) and N-guanyl-N-[6-(2-dimethylaminoethyl)-11-methyl-6Hindolo[2,3-b]quinolin-9-yl]-amine tetrahydrochloride (**73**) showed highest *in vitro* cytotoxicity and possessed selectivity between normal and cancer cell lines ([Fig. 29](#)). The cytotoxicity of compound (**72**) was found to be about 600-fold lower against normal fibroblasts than against A549 and MCF-7 cancer cell lines. The mechanism of action of synthesized compounds was also studied for guanidine derivatives, which showed that compounds (**72** and **73**) were very effective inducers of apoptosis. The results of mechanism of action studies proved that the compounds (**72** and **73**) produced antiproliferative activity through DNA interactions probably lead to the inhibition of DNA synthesis and consequent arrest the cells in S cell cycle phase. Compound (**72**), interacted more strongly with DNA than that of compound (**73**), and was also more efficient in the induction of apoptosis. The studies concluded that the conjugates containing the guanidine group directly linked to the core structure confirmed highly potent and selective anticancer activity.



Download : [Download high-res image \(155KB\)](#)

Download : [Download full-size image](#)

Figure 29. Structure of indolo[2,3-b]quinoline derivatives (**72**, **73**) shows remarkable cytotoxicity against A549 and MCF-7 cancer cell lines.

6.4. Anilino-furo[2,3-b]quinoline derivatives

Chen et al. (2005) synthesized 4-anilino-furo[2,3-b]quinoline and angular 4-anilino-furo[3,2-c]quinoline derivatives and evaluated *in vitro* against the full panel of NCI's 60 cancer cell lines. Compound 1-(4-(furo[2,3-b]quinolin-4-ylamino)phenyl)ethanone (**74**) was found to be the most cytotoxic with a mean GI₅₀ value of 0.025 μM (Fig. 30). The results showed that substitution at either furo[2,3-b]quinoline ring (2a, 2b, and 5b) or 4-anilino moiety (3–7) decreased cytotoxicity.

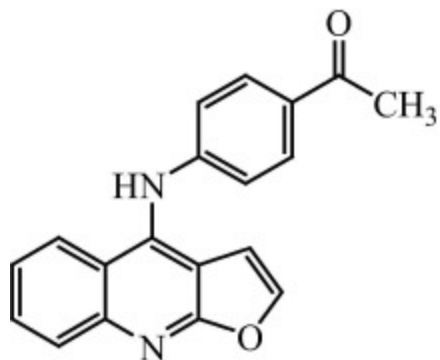
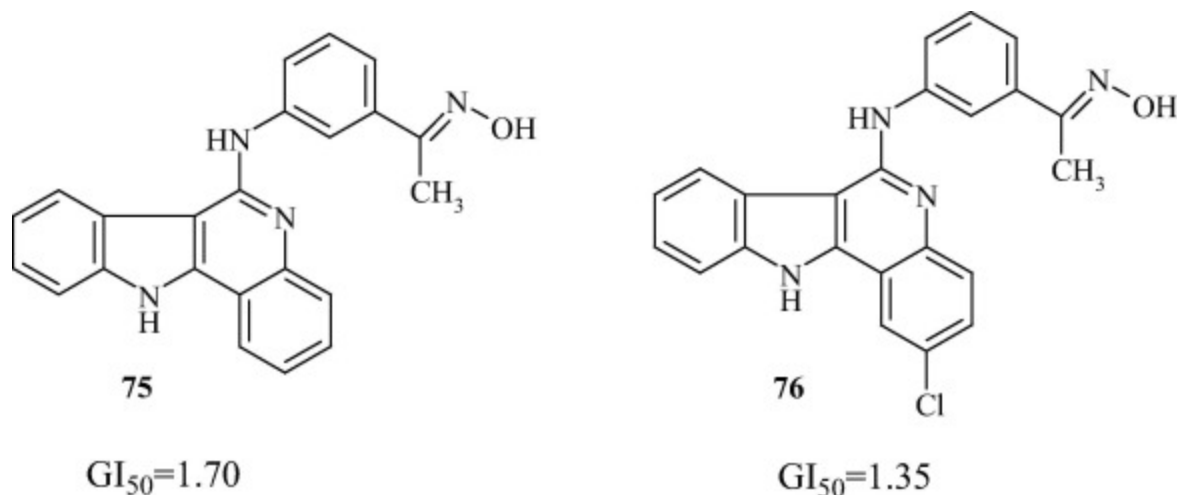
**74**GI₅₀=0.025[Download : Download high-res image \(70KB\)](#)[Download : Download full-size image](#)

Figure 30. Structure of compound 1-(4-(furo[2,3-b]quinolin-4-ylamino)phenyl) ethanone (**74**) shows most cytotoxicity against NCI's 60 cancer cell lines.

6.5. Indolo-, pyrrolo-, benzofuro and 6-anilinoindolo quinoline derivative

Chen et al. (2002) synthesized certain indolo-, pyrrolo-, and benzofuro-quinolin-2(1H)-ones and 6-anilinoindoloquinoline derivatives and evaluated *in vitro* against a three-cell line panel consisting of MCF7 (Breast), NCI-H460 (Lung), and SF-268 (CNS). The results have shown that cytotoxicity decreased in the order of 6-anilinoindoloquinolines > indoloquinolin-2(1H)-ones > pyrroloquinolin-2(1H)-ones > benzofuroquinolin-2(1H)-ones. Among them, 1-(3-(1H-indolo(3,2-c)quinolin-6-ylamino)phenyl) ethanone oxime hydrochloride (**75**) and its 2-chloro derivative (**76**) were most active, with a mean GI₅₀ values of 1.70 and 1.35 mM, respectively (Fig. 31). Both compounds (**75**, **76**) were also found to inhibit the growth of SNB-75 (CNS cancer cell) with a GI₅₀ value of less than 0.01 mM.



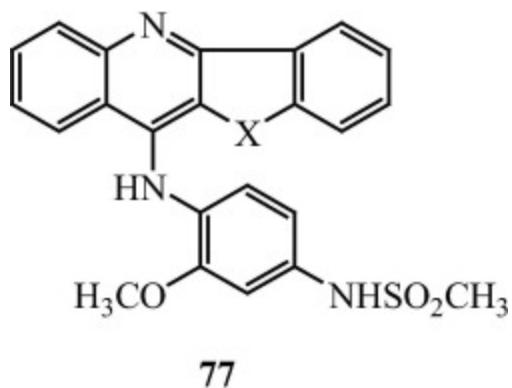
[Download : Download high-res image \(147KB\)](#)

[Download : Download full-size image](#)

Figure 31. Structure of compounds 1-(3-(11H-indolo(3,2-c)quinolin-6ylamino)phenyl) ethanone oxime hydrochloride (**75**) and its 2-chloro derivative (**76**) shows cytotoxicity against MCF7, NCI-H460, SNB-75 and SF-268 cancer cell lines.

[Atwell et al. \(1972\)](#) synthesized acridine derivatives having an amino group at position 9 of acridine, and found that some of them had the effect of inhibiting leukemia. [Cain et al. \(1974\)](#) reported the interrelation between the anticancer effect of the acridine derivatives and the specific kind of alkylamino group at position 9 of acridine, and found that the most effective derivative is N-(4-(9-acridinylamino)-3-methoxyphenyl)-methanesulfonamide (amsacrine). [Yamato et al. \(1988\)](#) obtained a patent for compounds having indenoquinoline, benzofuroquinoline or benzothienoquinoline *in lieu* of the acridine skeletal structure of amsacrine, the process for the preparation thereof. In the present structure X was O, S or CH₂ (**77**) ([Fig. 32](#)).

These compounds showed intensive antiproliferative activity. The antiproliferative activity was determined by measuring the 50% growth inhibition (ED₅₀) of KB-cells. The numbers of surviving cells were counted by a Kohlter's counter, and the counted number was compared to that of the control to find the concentration of the drug for inhibiting the growth by 50%, thus found concentration being estimated as the ED₅₀ value. *In vivo* activity showed the prolonging life of P-388 murine leukemia cell line with cancer and these synthesized compounds were found to be devoid of any acute toxicity.



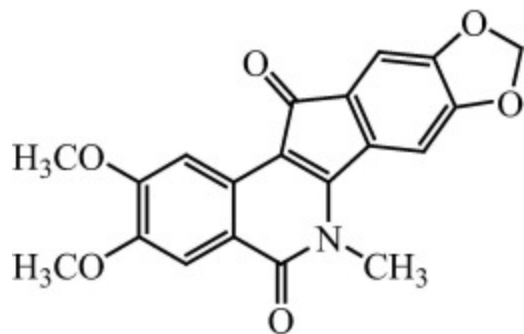
[Download](#) : [Download high-res image \(76KB\)](#)

[Download](#) : [Download full-size image](#)

Figure 32. Structure of compounds indenoquinoline, benzofuroquinoline or benzothienoquinoline derivatives (**77**) showing intensive antiproliferative activity against KB-cancer cells and prolonging the life of P-388 murine leukemia cell line with cancer.

6.6. Indeno [1,2-c]quinoline derivatives

Although the quinoline ring is found in a wide variety of biologically active compounds and is frequently condensed with various heterocycles leads to produce remarkable active multifaceted. Synthesis and biological evaluation of the indeno [1,2-c] quinoline skeleton attracts limited attention. NSC 314622 (**78**) an indenoquinoline analogue, was first identified as a novel Topoisomerase I inhibitor with better pharmacokinetic features than camptothecin (Fig. 33) (Antony et al., 2003). Since then, a number of indenoisoquinolines analogues especially indeno [1,2-c]isoquinoline derivatives have been synthesized and proved to possess DNA Top I inhibitory activity. These compounds bind to a transient Top I DNA covalent complex and inhibited the resealing of a single-strand nick that the enzyme creates to relieve superhelical tension in duplex DNA (Hsiang et al., 1985, Hertzberg et al., 1989).



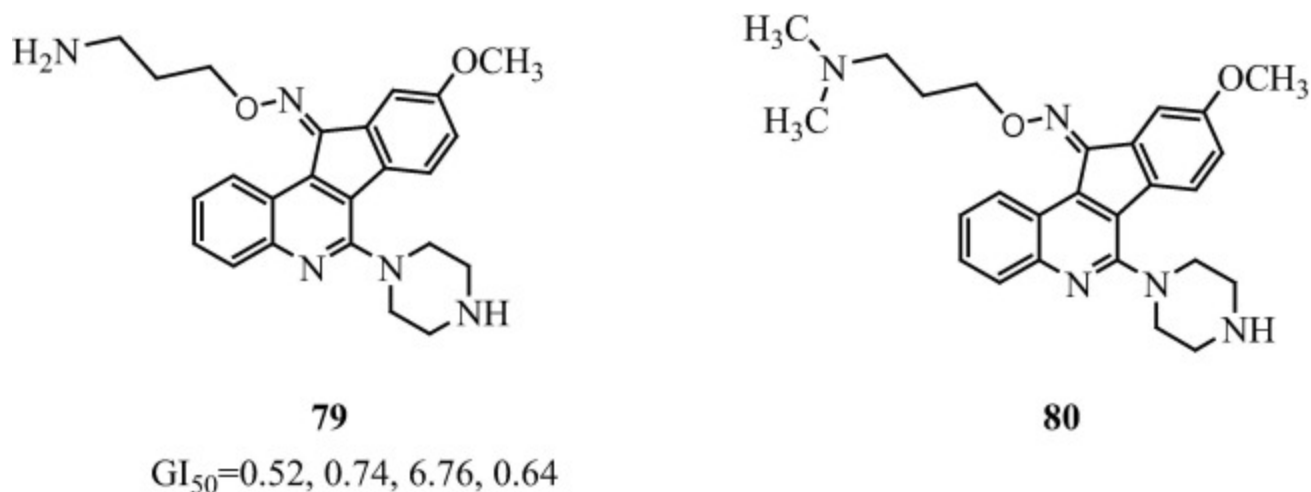
NSC 314622 (78)

[Download : Download high-res image \(88KB\)](#)

[Download : Download full-size image](#)

Figure 33. Structure of indenoquinoline analogue (NSC 314622, **78**) shows Topoisomerase I inhibitory activity.

In the search of new, potent indeno[1,2-*c*]quinoline derivatives, [Tseng et al. \(2008\)](#) synthesized some new indeno[1,2-*c*]quinoline derivatives and reported their antiproliferative evaluation against the growth of six cancer cell lines including human cervical epithelioid carcinoma (HeLa), oral squamous cell carcinoma (SAS), hepatocellular carcinoma (SKHep), human stomach adenocarcinoma (AGS), prostate cancer (PC-3), and non-small cell lung cancer (A549). All indeno[1,2-*c*]quinoline derivatives were derived from [isatin](#). The antiproliferative activity was measured by determining the concentration of substances that inhibited the growth of 50% of cells (GI_{50}). The results illustrated that the compound 9-Methoxy-6-(piperazin-1-yl)-11H-indeno[1,2-*c*]-quinolin-11-one O-3-aminopropyl oxime (**79**) was the most potent with GI_{50} values of 0.52, 0.74, 6.76, and 0.64 μ M against the growth of HeLa, SKHep, AGS, and A549 cells, respectively. The study also showed that the potency of synthesized compounds was decreased in an order of aminoalkoxyimino > hydroxyimino > alkoxyimino > carbonyl. Flowcytometric analysis indicated that the compound 9-Methoxy-6-(piperazin-1-yl)-11H-indeno[1,2-*c*]-quinolin-11-one O-3-(dimethylamino)propyl oxime (**80**) can induce cell cycle arrest in S phase, and DNA polyploidy (>4n) followed by apoptosis ([Fig. 34](#)).



Download : [Download high-res image \(176KB\)](#)

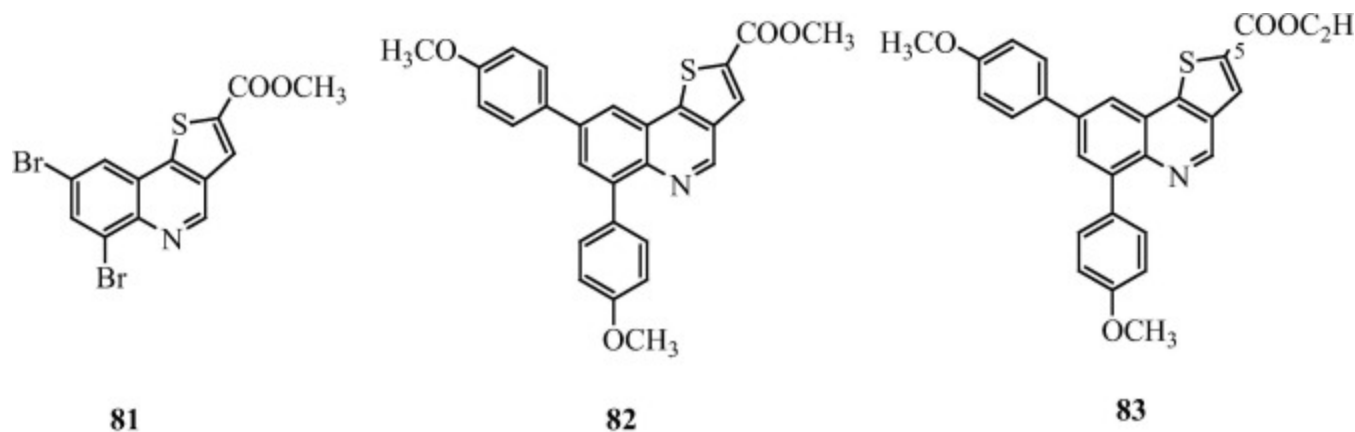
Download : [Download full-size image](#)

Figure 34. Structure of indeno[1,2-c]quinoline derivatives (**79–80**) shows significant antiproliferative activity against HeLa, SKHep, AGS, and A549 cancerous cells.

6.7. 6,8-Diarylthieno[3,2-c]quinoline-2-carboxylate scaffold

The 6,8-diarylthieno[3,2-c]quinoline-based compounds continue to attract a great deal of attention in the research because of their rich biological activities including antibacterial ([Castrillo et al., 2001](#)), anticancer ([Jarak et al., 2005](#)) and anti-inflammatory agents ([Cesare et al., 1999](#)). Recently a number of thieno[3,2-c]quinoline derivatives were found to inhibit protein kinases in cancer cells ([Beydoun and Doucet, 2012](#), [Pierre et al., 2011](#)). [Avetisyan et al. \(2007\)](#) reported a series of substituted 2,4-dimethyl-thieno[3,2-c]quinolones derivatives, which were prepared via intramolecular cyclization and subsequent aromatization of 3-(2-chloroprop-2-en-1-yl)- and 3-(2-oxopropyl)-2-methylquinolin-4-thiols. [Mphahlele et al. \(2014\)](#) produced [(6,8-diarylthieno[3,2-c]quinoline)]-2-carboxylates derivatives via direct one-pot base-promoted conjugate addition–elimination of 6,8-dibromo-4-chloroquinoline-3-carbaldehyde with methyl mercaptoacetate and subsequent cyclization afforded methyl [(6,8-dibromothieno[3,2-c]quinoline)]-2-carboxylate followed by Suzuki-Miyaura cross-coupling with arylboronic acids to yield desired compounds. These synthesized compounds were screened for their cytotoxicity

against the human breast cancer cell line MCF-7 using the MTT assay. Cytotoxicity of the synthesized compounds was also evaluated by measuring cell kinetics using the xCELLigence Real Time Cell Analysis (RTCA) system. Compounds Methyl [(6,8-Dibromothieno[3,2-c]quinoline)]-2-carboxylate (**81**); Methyl 6,8-bis(4-methoxyphenyl)thieno[3,2-c]quinoline-2-carboxylate (**82**) and Ethyl 6,8-bis(4-methoxyphenyl)thieno[3,2-c]quinoline-2-carboxylate (**83**) showed remarkable cytotoxic activity against human breast adenocarcinoma cell line (MCF-7 cells) either by using MTT assay or in Real Time Cell Analysis (Fig. 35). The compounds inhibited cancer cell growth in a dose- and time-dependent manner and their LC₅₀ values, were accountable to compare to nocodazole, a well-established cytotoxic drug. The structure-activity relationship analysis suggested that the cytotoxicity of the synthesized compounds seems to be dependent on the electronic effects and lipophilicity of the substituent on the *para* position of the 6- and 8-phenyl rings. The structure-activity relationship analysis provided a guideline for the readers to design new derivatives with increased activity.



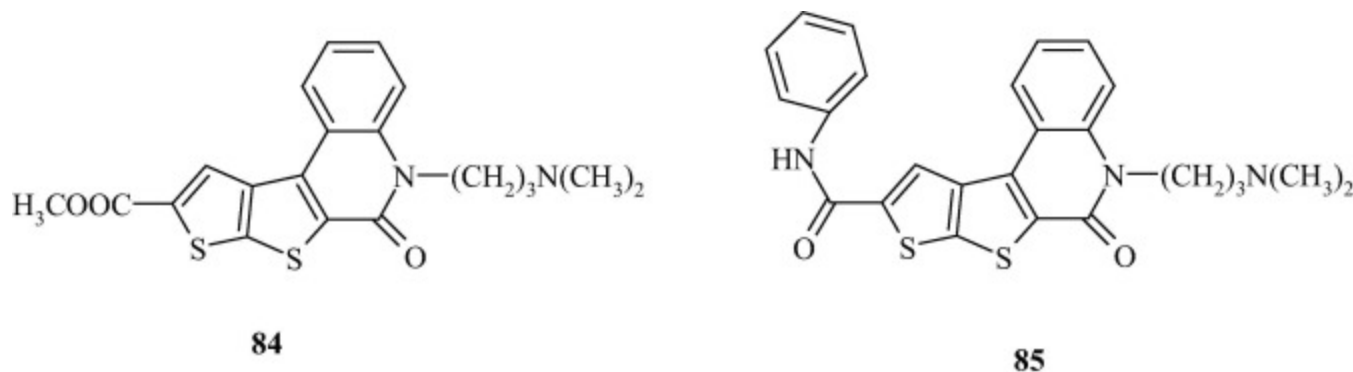
[Download : Download high-res image \(161KB\)](#)

[Download : Download full-size image](#)

Figure 35. Structure of [(6,8-diarylthieno[3,2-c]quinoline)]-2-carboxylates derivatives (**81–83**) showing remarkable cytotoxicity against MCF-7 cell line either by using MTT assay or in Real Time Cell Analysis.

6.8. Thieno (2,3)-quinolone derivatives

Koruznjak et al. (2002) reported the novel synthesis scheme of thieno (39,29:4,5)thieno(2,3)-quinolone derivatives and performed their cytostatic activities against malignant cell lines: pancreatic (MiaPaCa2), breast (MCF7), cervical (HeLa), laryngeal (Hep2), colon (CaCo-2), melanoma (HBL), and human fibroblast cell lines (WI-38). All tested compounds exhibited strong inhibitory activities against all cell lines tested. The results showed that the compound (**84**), which bears the 3-dimethylaminopropyl substituent on quinolone nitrogen and methoxycarbonyl substituent on quinolone position 9, exhibited marked antitumor activity. On the contrary, compound (**85**), which also bears the 3-dimethylaminopropyl substituent on the quinolone nitrogen, but anilido substituent on position 9, exhibited less antitumor activity than the others (Fig. 36).



Download : [Download high-res image \(136KB\)](#)

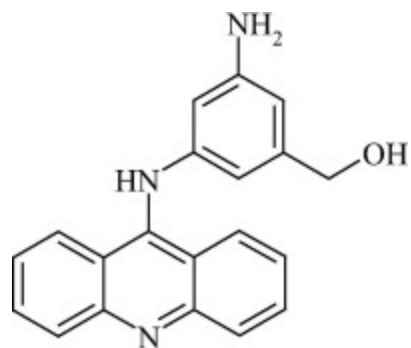
Download : [Download full-size image](#)

Figure 36. Structure of compounds thieno (39,29:4,5)thieno(2,3)-quinolone derivatives (**84** and **85**). Compound (**84**) shows best anticancer activity while compound (**85**) shows least anticancer activity against MiaPaCa2, MCF7, HeLa, Hep2, CaCo-2, HBL and WI-38 cell lines.

6.9. 6H-indolo [2,3-b]quinoline derivatives

9-Anilinoacridine derivatives have been extensively studied as potential chemotherapeutic agents due to their capability of intercalating DNA, leading to the inhibition of topoisomerase II. Su et al. (1995) stated that further structural modification lead to the discovery of an improved broad spectrum antitumor agent, 3-(9-acridinylamino)-5-(hydroxymethyl)aniline

(AHMA, **86**), is capable of inhibiting the growth of certain solid tumors such as mammary adenocarcinoma, melanoma and lung carcinoma in mice (Fig. 37).



AHMA (**86**)

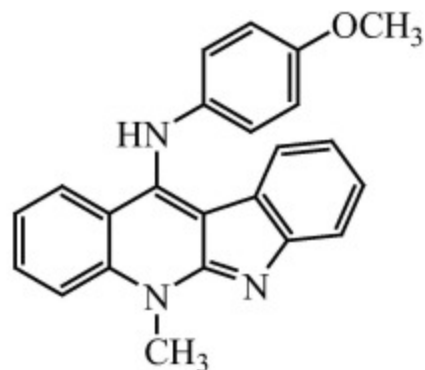
Download : [Download high-res image \(60KB\)](#)

Download : [Download full-size image](#)

Figure 37. Structure of compound 3-(9-acridinylamino)-5-(hydroxymethyl)aniline (AHMA, **86**), capable of inhibiting the growth of certain solid tumors.

These results promoted to synthesize and evaluate 4-anilino-furo[2,3-b]quinoline derivatives, which were structurally related to 9-Anilinoacridine derivatives.

Chen et al. (2004) synthesized and reported the anticancer evaluation of certain 11-substituted 6H-indolo[2,3-b]quinolines and their methylated derivatives. These 6H-indolo[2,3-b]quinoline derivatives were prepared from the commercially available 1,4-dihydroxyquinoline through alkylation, chlorination, nucleophilic reaction, and ring cyclization. The *in vitro* anticancer assay indicated that 5-methylated derivatives were more cytotoxic than their respective 6-methylated counterparts. Among them, 11-(4-methoxyanilino)-6-methyl-6H-indolo[2,3-b]quinoline (**87**) was the most cytotoxic with a mean GI_{50} value of $0.78\mu\text{M}$ and also exhibited selective cytotoxicities for HL-60 (TB), K-562, MOLT-4, RPMI-8226 and SR with GI_{50} values of 0.11, 0.42, 0.09, 0.14, and $0.19\mu\text{M}$, respectively (Fig. 38).



87

GI_{50} =0.78, 0.11, 0.42, 0.09, 0.14, 0.191

[Download : Download high-res image \(102KB\)](#)

[Download : Download full-size image](#)

Figure 38. Structure of compound 11-(4-methoxyanilino)-6-methyl-6H-indolo[2,3- b]quinoline (**87**) shows selective cytotoxicities for HL-60 (TB), K-562, MOLT-4, RPMI-8226 and SR cancer cells.

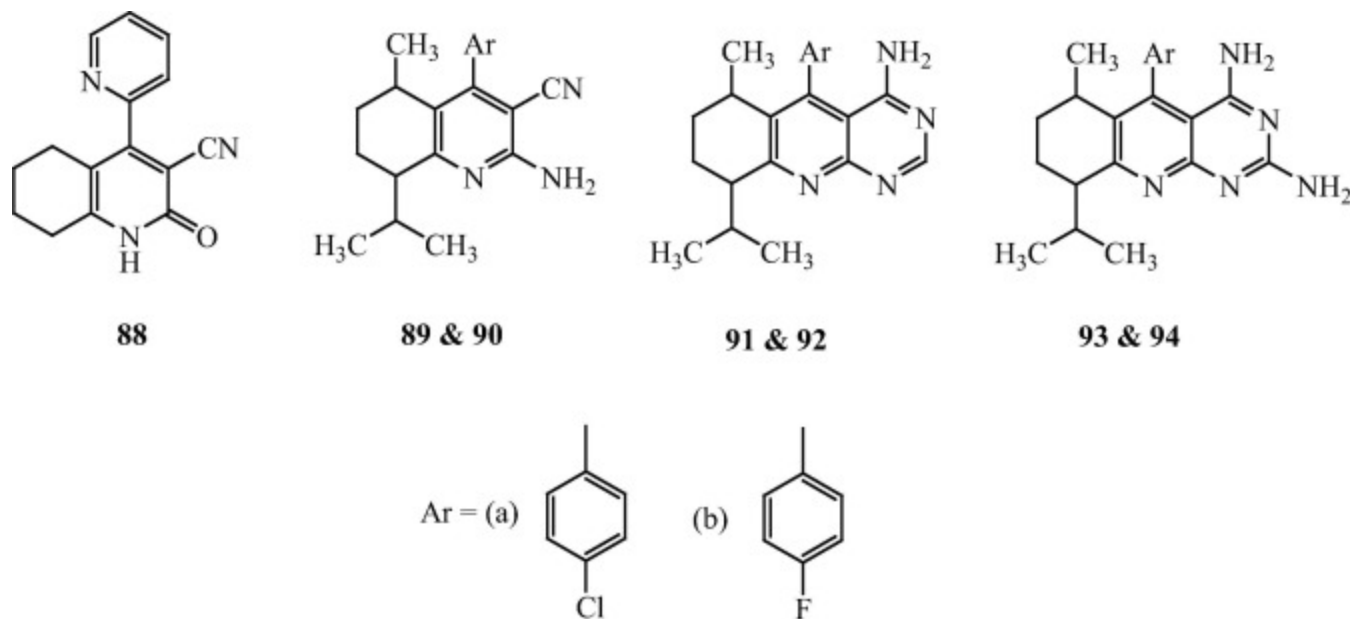
The studies were further extended by [Long et al. \(2005\)](#) who had synthesized various 4-anilino-furo[2,3-b]quinoline and 4-anilino-furo (3,2-c) quinoline derivatives and evaluated their cytotoxic activity against various cancerous cell lines.

6.10. Tetrahydroquinoline and tetrahydropyrimidoquinoline derivatives

Studies clearly revealed that the quinoline and pyrimidine nucleuses are an important pharmacophore in various antitumor agents ([Karthikeyan et al., 2015](#)). Nowadays pyrimidine based potent anticancer drugs are available in the market, for example, gefitinib (Iressa™) ([Wakeling et al., 2002](#)) and [erlotinib](#) (Tarceva™) ([Moyer et al., 1997](#)), and thus, it is considered as an attractive target for the design of new anticancer agents. Recently, several tetrahydroquinolines and their pyrimidine derivatives were synthesized and evaluated for their anticancer activity, and a number of tetrahydropyrimidoquinolines derivatives were reported for their anticancer activity ([Faidallah and Rostomb, 2013](#), [Alqasoumi et al., 2010](#)).

Taking into consideration the above findings, and in an effort to identify novel potent anticancer leads through the combination of the two active anticancer moieties, [Gedawy et al. \(2015\)](#) prepared and reported several tetrahydroquinolines with different groups at C-2 and C-4 positions. Several tetrahydropyrimidoquinolin-4-amines and tetrahydropyrimidoquinoline-2,4-diamines with different aryl groups at position number 5 to substantiate were also reported and also marked their anticancer activity against both human colon carcinoma (HCT116) and human breast adenocarcinoma (MCF7) cell lines.

The results of *in vitro* anticancer activity showed that seven compounds 2-Oxo-4-(pyridin-2-yl)-1,2,5,6,7,8-hexahydroquinoline-3-carbonitrile (**88**); 2-Amino-4-(4-chlorophenyl)-8-isopropyl-5-methyl-5,6,7,8-tetrahydro-quinoline-3-carbonitrile (**89**); 2-Amino-4-(4-fluorophenyl)-8-isopropyl-5-methyl-5,6,7,8-tetrahydro-quinoline-3-carbonitrile (**90**); 5-(4-Chlorophenyl)-9-isopropyl-6-methyl-6,7,8,9-tetrahydropyrimido-[4,5-b]quinolin-4-amine (**91**); 5-(4-Fluorophenyl)-9-isopropyl-6-methyl-6,7,8,9-tetrahydropyrimido-[4,5-b]quinolin-4-amine (**92**); 5-(4-Chlorophenyl)-9-isopropyl-6-methyl-6,7,8,9-tetrahydropyrimido-[4,5-b]quinoline-2,4-diamine (**93**) and 5-(4-Fluorophenyl)-9-isopropyl-6-methyl-6,7,8,9-tetrahydropyrimido-[4,5-b]quinoline-2,4-diamine (**94**) possessed potent anticancer activity against both HCT-116 (colon) and MCF7 (breast) cell lines with IC_{50} between 16.33 and 34.28 μ M ([Fig. 39](#)). All these compounds were also reported more potent than [imatinib](#) ($IC_{50}=34.40$ IM) and [tamoxifen](#) ($IC_{50}=34.30$ IM). Out of these seven compounds, compound (**94**) was the most active against HCT-116 cell line with 2.1-fold more potent antitumor activity than imatinib, while compounds (**88**, **90** and **91**) exhibited the highest anticancer activity against the MCF7 cell line, having 2–1.79-fold more potent anticancer activity than tamoxifen.



[Download : Download high-res image \(219KB\)](#)

[Download : Download full-size image](#)

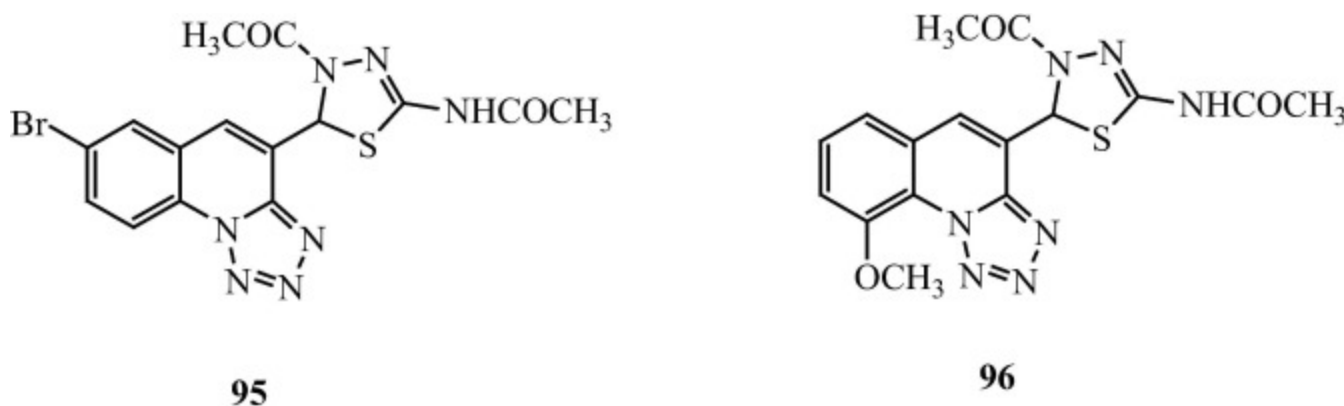
Figure 39. Structure of novel tetrahydroquinoline (**88–90**), and tetrahydropyrimidoquinoline derivatives (**91–94**) possesses potent anticancer activity against both HCT116 and MCF7 cancer cell lines.

On the basis of *in vitro* outcomes the researchers conclude that the anticancer activity of the synthesized quinoline and pyrimidoquinoline compounds appeared to be related to the cycloalkyl moiety fused to the pyridine ring, since the best activity was obtained by compounds bearing the branched cyclohexyl moiety (Compounds **91**, **92**, **93** and **94**).

It was clear that the substituents in quinoline derivatives, at position 2 had a marked effect on the anticancer activity, since the compounds with carbonyl or amino groups possessed potent anticancer activity, while those with the chloro group at C-2 position were inactive. Thus, it was concluded that the tetrahydroquinolines and their fused pyrimidine derivatives represented a novel and promising class of anticancer agents, so researcher proposed further studies to explore the mechanism of action and to optimize the anticancer activity of these derivatives.

6.11. 1,3,4-Thiadiazol, tetrazole and quinoline derivatives

1,3,4-Thiadiazol, tetrazole and quinoline derivatives have been reported as promising candidates for anticancer activity. Number of articles have been published for thiadiazol, tetrazole and quinoline containing compounds possessed anticancer activity. Understanding these facts [Sheetal et al. \(2012\)](#) reported N-[4-acetyl-5-(6, 7, 8-substituted-2-chloroquinolin-3-yl)-4,5-dihydro-1,3,4-thiadiazol-2-yl]-acetamides compound possessed anticancer and anti-tubercular activity. The researchers extended their study and introduced a new heterocyclic compound had tetrazole moiety with quinoline derivatized with 1,3,4- thiadiazolidine ring. The synthesized N- (4-acetyl-4,5-dihydro - 5- (7,8,9- substituted - tetrazolo [1,5-a] - quinolin-4-yl) - 1,3,4-thiadiazol -2- yl) acetamides compounds were screened for their *in vitro* cytotoxic activity against two cell lines viz., human breast cancer cell line MCF7 and human cervix cancer cell line HeLa. The GI₅₀, LC₅₀ and TGI values were evaluated. The DNA cleavage study was also reported. Compounds (**95** and **96**) with halogen substituent at 7th position of the target molecules showed potent cytotoxicity against human cervix cancer cell line HeLa ([Fig. 40](#)). DNA cleavage studies revealed that most of these compounds showed partial cleavage and few of them showed complete cleavage of DNA.



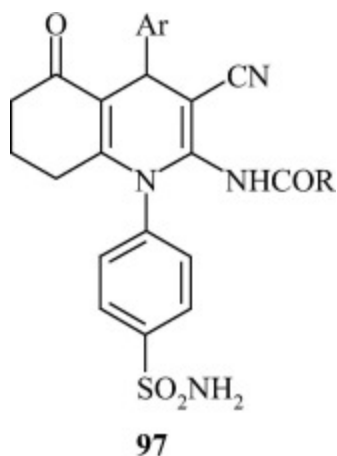
[Download : Download high-res image \(150KB\)](#)

[Download : Download full-size image](#)

Figure 40. Structure of N- (4-acetyl-4,5-dihydro - 5- (7,8,9- substituted - tetrazolo [1,5-a] - quinolin-4-yl) - 1,3,4-thiadiazol -2- yl) acetamide derivatives (**95** and **96**) with halogen substituent at 7th position showing potent cytotoxicity against HeLa cancer cell line.

6.12. Pyrimidoquinoline derivatives

[Al-Said et al. \(2011\)](#) reported in their study synthesis and investigation of the antiproliferative activity of new quinoline and pyrimidoquinoline derivatives containing a free sulfonamide moiety. Several compounds had been synthesized which exhibited significant anticancer activity. Quinoline compounds (**97**) having substituted benzamide, free amino group, butanamide, showed remarkable anticancer activity against Ehrlich Ascites Carcinoma (EAC) cells ([Fig. 41](#)). Docking of these synthesized compounds in the carbonic anhydrase active site suggested that the synthesized compounds may act as carbonic anhydrase inhibitors and this may contribute in part to their anticancer activity.



Download : [Download high-res image \(51KB\)](#)

Download : [Download full-size image](#)

Figure 41. Structure of pyrimidoquinoline derivatives (**97**) showing remarkable anticancer activity against Ehrlich Ascites Carcinoma (EAC) cells.

6.13. Quinoline sulfonamide derivative

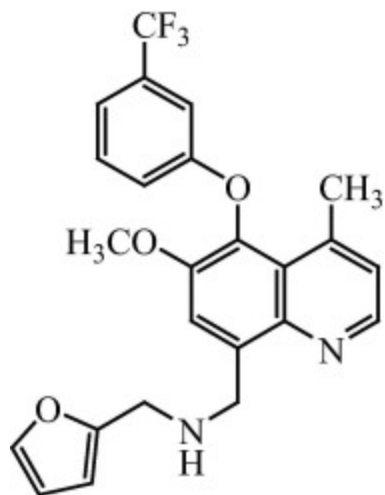
Quinoline and sulfonamide derivatives are important biologically active compounds that possess potent antitumor activity ([Kouznetsov et al., 2006](#)). Acetylation of histones in chromatin involved in the regulation of gene transcription and is tightly controlled by the balance of acetyltransferase (HATs) and deacetylase (HDAC) activities. HDACs mediate changes in

nucleosome conformation are important in the regulation of gene expression and also are involved in cell cycle progression and differentiation. Alterations of HDACs were identified in tumor cells and contributed to the massive perturbations of gene expression in numerous tumors. HDAC inhibition leads to differentiation, cell cycle arrest and apoptosis in tumor cells (Hsi et al., 2004). Recently new set of sulfonamide derivatives have been reported as potent histone deacetylases inhibitors (HDACIs) (Finn et al., 2005, Ghorab et al., 2007).

6.14. 6-Methoxy- 8- [(2-furanylmethyl)amino]- 4-methyl -5- (3 trifluoro-methylphenoxy) quinoline derivatives

Cancer cells have a tendency to reduce capacity of gap junction inter-cellular communication (GJIC). The enhancement of GJIC induced apoptosis, decreased cell viability, and attenuated tumor growth.

Heiniger et al. (2010) reported a second generation of PQ analogues [PQ7 i.e. 6- methoxy- 8- [(2-furanylmethyl)amino]- 4-methyl -5- (3 trifluoro-methylphenoxy) quinoline, **99**] and examined its activates GJIC activity mediated tumor growth inhibitory activity in xenograft T47D mice (Fig. 42). Scrape load/dye transfer and colony growth assays were performed to measure GJIC and tumor formation of T47D breast cancer cells. Results showed that PQ7 (**98**) at 500 nM induced a 16-fold increased in the GJIC in T47D cells, and 50% decreased of colony growth with 100 nM concentration. PQ7-treated nu/nu mice showed a 100% regression of xenograft tumor growth of T47D cells. The authors concluded that the second-generation PQ7 (**98**) had a promising role in exerting anti-tumor activity in human breast cancer cells.

**PQ7 (98)**

[Download : Download high-res image \(80KB\)](#)

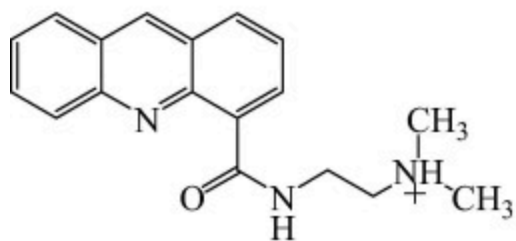
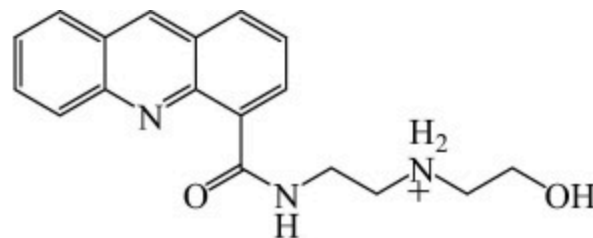
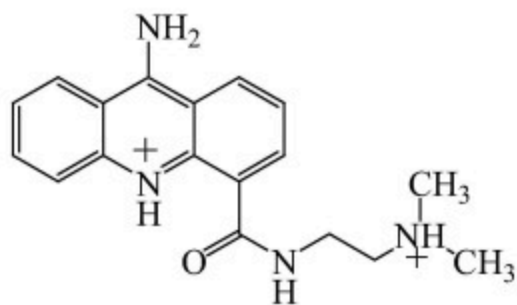
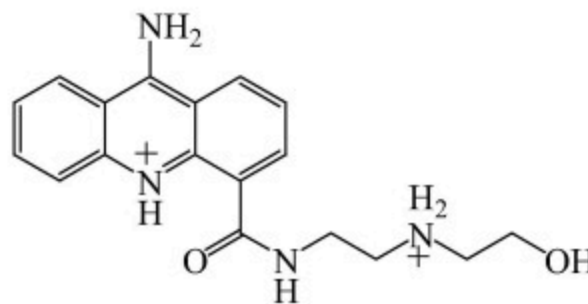
[Download : Download full-size image](#)

Figure 42. Structure of compound PQ7 (6- methoxy- 8- [(2-furanylmethyl)amino]- 4-methyl -5- (3 trifluoro-methylphenoxy) quinoline, **98**) having promising anticancer activity against T47D breast cancer cells.

6.15. N-2[4 Dimethylamino)ethyl]acridine-4-carboxamide derivatives

Acridine-4-carboxamides have been reported as a new generation of intercalators which are active against solid tumors and leukemia. A number of studies have been reported for their capacity to bind to DNA, for their DNA-damaging activity in whole cells and isolated nuclei, and for their inhibitory effect on RNA synthesis in a cell-free system ([Atwell et al., 1987](#), [Denny et al., 1987](#)). A model of the acridine-4-carboxamide-DNA complexes were proposed by [Wakelin and Denny \(1990\)](#), suggesting intercalation of acridine ring between base pairs with the 4-carboxamide moiety located in the minor groove. The proposed structure of the substituent at position 4 seems to be the important factor in the stabilization of the drug-DNA complex as well as in the GC specificity of these acridines ([Bailly et al., 1992](#)). An antitumor drug N-[2-(dimethylamino)ethyl]acridine-4-carboxamide (DACA, **99**) a acridine-4-carboxamide congener and its three close structural

analogues *N*-[2-(hydroxyethylamino)ethyl]acridine-4-carboxamide (DACA, **100**), *N*-[2-(dimethylamino)ethyl]-9-aminoacridine-4-carboxamide (amino-DACA, **101**), and *N*-[2-(hydroxyethylamino)ethyl]-9-aminoacridine-4-carboxamide (amino-DACA, **102**) were further studied by the same research group to determine their ability to inhibit RNA synthesis *in vitro* and to form topoisomerase II-mediated DNA lesions in relation to cell-killing activity (Fig. 43). Results showed that the stabilization of the cleavable complex of topoisomerase II with DNA by acridine-4-carboxamides is not as important for the cytotoxic action of these compounds, but the compounds which can penetrate cell membrane easily and are able to form a strong intercalative complex with DNA, for example amino-DACA, may enhance DNA cleavage by topoisomerase II. The enhancement of DNA cleavage occurs only when used at low doses while at higher concentrations they act as catalytic inhibitors. The results also suggested that the compound having 4-carboxamide chain attached with *N*-2-(dimethylamino)ethyl moiety resulted in more efficient transport through cell membranes, higher cytotoxicity, and DNA-damaging activity. Thus compound amino-DACA, which easily penetrates the cell membrane, fully inhibited DNA break formation, whereas other analogues exhibited a lower degree of protection when used at high concentration.

**DACA (99)****DACAH (100)****amino-DACA (101)****amino-DACAH (102)**

[Download : Download high-res image \(295KB\)](#)

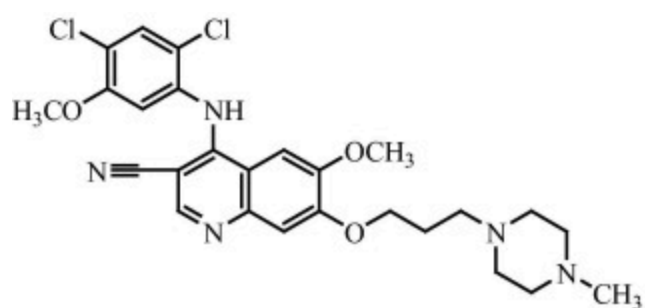
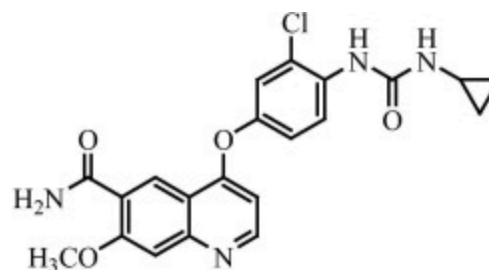
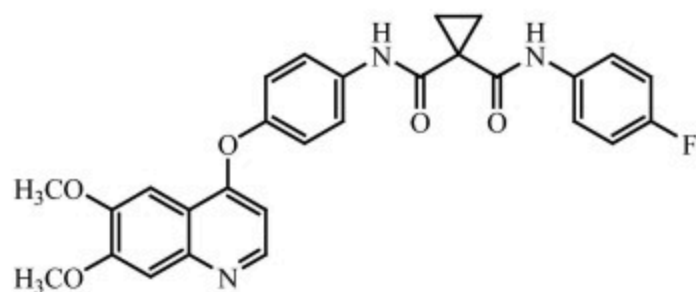
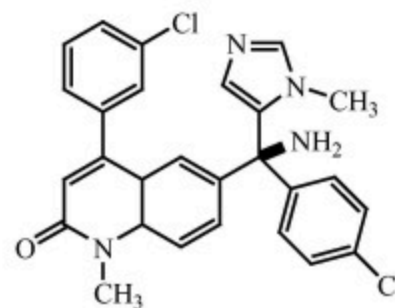
[Download : Download full-size image](#)

Figure 43. Structure of N-2[4 Dimethylamino)ethyl]acridine-4-carboxamide derivatives (**99–102**) having DNA cleavage property.

7. Future prospects of quinoline derivatives

Nowadays quinoline nucleus has gained popularity in the development of new anticancer drugs. Numbers of quinoline congeners have been synthesized daily and some of them showed excellent results on various types of cancer cells, through

different mechanisms of action. Recently, three protein kinase inhibitors (Bosutinib, Lenvatinib, and Cabozantinib) (**103–105**) and an inhibitor of farnesyltransferase (Tipifarnib) (**106**), considered as potential anticancer agents, entered into phase of clinical trials (Afzal et al., 2014) (Fig. 44).

**Bosutinib (103)****Lenvatinib (104)****Cabozantinib (105)****Tipifarnib (106)**

[Download : Download high-res image \(314KB\)](#)

[Download : Download full-size image](#)

Figure 44. Structure of compounds bosutinib (**103**), lenvatinib (**104**), cabozantinib (**105**) and tipifarnib (**106**) quinoline nucleus under clinical trial.

8. Conclusion

Quinoline or 1-aza-naphthalene is a weak tertiary base, composed of benzene and pyridine ring fused at two adjacent carbon atoms obtained by condensation of a benzene ring with pyridine. The quinoline ring plays an important role in biological and pharmacological activities. In recent years, large numbers of quinoline derivatives, including mono-, di-, tri-, tetra- and heterocyclic substituents have been synthesized and their cytotoxic activity reported. These quinoline and their derivatives possessed remarkable anticancer activity due to their structure diversity, which are responsible for their anticancer activities. Till date a large number of quinoline derivatives have been marketed for their cytotoxic activity and now scientist is also focusing to introduce new quinoline molecules in market to encompass anticancer activity.

Acknowledgments

This project was supported by Uttar Pradesh University of Medical Sciences, VC-UPUMS, for their encouragement and support.

[Recommended articles](#)

References

[Abdel et al., 2014](#) S.E. Abdel, A. Zaitoon, S.A.M. El, A.A. Bakhashwain
J. Egypt. Soc. Parasitol., 44 (2014), p. 771

[Afzal et al., 2015](#) O. Afzal, S. Kumar, M.R. Haider, M.R. Ali, R. Kumar, M. Jaggi, S. Bawa
Eur. J. Med. Chem., 97 (2015), p. 871

 [View PDF](#) [View article](#) [View in Scopus ↗](#)

[Alqasoumi et al., 2010](#) S.I. Alqasoumi, A.M. Al-Taweel, A.M. Alafeefy, E. Noaman, M.M. Ghorab
Eur. J. Med. Chem., 45 (2010), p. 738

 [View PDF](#) [View article](#) [View in Scopus ↗](#)

[Al-Said et al., 2011](#) M.S. Al-Said, G.M. Mostafa, A.D.S. Mohammed, H.M. Mostafa

Eur. J. Med. Chem., 46 (2011), p. 207

[Antony et al., 2003](#) S. Antony, M. Jayaraman, G. Laco, G. Kohlhagen, K.W. Kohn, M. Cushman, Y. Pommier

Cancer. Res., 63 (2003), p. 7428

[View in Scopus ↗](#)

[Armitage, 1998](#) B. Armitage

Chem. Rev., 98 (1998), p. 1171

[View in Scopus ↗](#)

[Atwell et al., 1972](#) G.J. Atwell, B.F. Cain, R.N. Seelye

J. Med. Chem., 15 (1972), p. 611

[CrossRef ↗](#) [View in Scopus ↗](#)

[Atwell et al., 1987](#) G.J. Atwell, G.W. Rewcastle, B.C. Baguley, W.A. Denny

J. Med. Chem., 30 (1987), p. 664

[CrossRef ↗](#) [View in Scopus ↗](#)

[Avetisyan et al., 2007](#) A.A. Avetisyan, I.L. Aleksanyan, K.S. Sargsyan

Russ. J. Org. Chem., 43 (2007), p. 422

[View in Scopus ↗](#)

[Bailly et al., 1992](#) C. Bailly, W.A. Denny, L.E. Mellor, L.P.G. Wakelin, M.J. Waring

Biochemistry, 31 (1992), p. 3514

[CrossRef ↗](#) [View in Scopus ↗](#)

[Beydoun and Doucet, 2012](#) K. Beydoun, H. Doucet

Eur. J. Org. Chem., 34 (2012), p. 6745

[CrossRef ↗](#) [View in Scopus ↗](#)

[Bindu et al., 2012](#) P.J. Bindu, K.M. Mahadevan, N.D. Satyanarayan, T.R.R. Naik

Bioorg. Med. Chem. Lett., 22 (2012), p. 898

 [View PDF](#) [View article](#) [View in Scopus](#) ↗

[Bispo et al., 2015](#) M.L.F. Bispo, C.C. Alcantara, M.O. Moraes, C.Ó. Pessoa, F.A.R. Rodrigues, C.R. Kaiser, S.M.S.V. Wardell, J.L. Wardell, M.V.N.

Souza

Montash. Chem., 146 (2015), p. 2041

[CrossRef](#) ↗ [View in Scopus](#) ↗

[Bolzán and Bianchi, 2001](#) A.D. Bolzán, M.S. Bianchi

Mutat. Res., 488 (2001), p. 25

 [View PDF](#) [View article](#) [View in Scopus](#) ↗

[Bradley et al., 2014](#) W.D. Bradley, S. Arora, J. Busby, S. Balasubramanian, V.S. Gehling, C.G. Nasveschuk, R.G. Vaswani, C.C. Yuan, C.

Hatton, F. Zhao, K.E. Williamson, P. Iyer, J. Méndez, R. Campbell, N. Cantone, S. Garapaty-Rao, J.E. Audia, A.S. Cook, L.A. Dakin, B.K. Albrecht, J.C. Harmange, D.L. Daniels, R.T. Cummings, B.M. Bryant, E. Normant, P. Trojer

Chem. Biol., 21 (2014), p. 1463

 [View PDF](#) [View article](#) [View in Scopus](#) ↗

[Broch et al., 2010](#) S. Broch, B. Aboab, F. Anizon, P. Moreau

Eur. J. Med. Chem., 45 (2010), p. 1657

 [View PDF](#) [View article](#) [View in Scopus](#) ↗

[Cai et al., 2010](#) W. Cai, M. Hassanib, R. Karki, E.D. Walter, K.H. Koelsch, H. Seradj, J.P. Lineswala, H. Mirzaei, J.S. York, F. Olang, M. Sedighi,

J.S. Lucas, T.J. Eads, A.S. Rose, S. Charkhzarrin, N.G. Hermann, H.D. Beall, M. Behforouz

Bioorg. Med. Chem., 18 (2010), p. 1899

 [View PDF](#) [View article](#) [View in Scopus](#) ↗

[Cain et al., 1974](#) B.F. Cain, R.N. Seelye, G.J. Atwell

J. Med. Chem., 17 (1974), p. 922

[CrossRef ↗](#) [View in Scopus ↗](#)

[Castellano et al., 2008](#) S. Castellano, A. Bertamino, I. Gomez-Monterrey, M. Santoriello, P. Grieco, P. Campiglia, G. Sbardella, E. Novellino
Tetrah. Lett., 49 (2008), p. 583

 [View PDF](#) [View article](#) [View in Scopus ↗](#)

[Castrillo et al., 2001](#) A. Castrillo, D.J. Pennington, F. Otto, P.J. Parker, M.J. Owen, L. Bosca
J. Exp. Med., 194 (2001), p. 231

[View in Scopus ↗](#)

[Cesare et al., 1999](#) P. Cesare, L.V. Dekker, A. Sardini, P.J. Parker, P.A. McNaughton
Neuron, 23 (1999), p. 617

 [View PDF](#) [View article](#) [View in Scopus ↗](#)

[Chen et al., 2006](#) Y.L. Chen, C.J. Huang, Z.Y. Huang, C.H. Tseng, F.S. Chang, S.H. Yang, S.R. Lin, C.C. Tzeng
Bioorg. Med. Chem., 14 (2006), p. 3098

 [View PDF](#) [View article](#) [View in Scopus ↗](#)

[Chen et al., 2002](#) Y.L. Chen, C.H. Chung, I.L. Chen, P.H. Chen, H.Y. Jeng
Bioorg. Med. Chem., 10 (2002), p. 2705

 [View PDF](#) [View article](#) [View in Scopus ↗](#)

[Chen et al., 2004](#) Y.L. Chen, H.M. Hung, C.M. Lu, Li, C. Kuang, C.C. Tzeng
Bioorg. Med. Chem., 12 (2004), p. 6539

 [View PDF](#) [View article](#) [View in Scopus ↗](#)

[Chen et al., 2005](#) Y.L. Chen, I.L. Chen, T.C. Wang, C.H. Han, C.C. Tzeng
Eur. J. Med. Chem., 40 (2005), p. 928

 [View PDF](#) [View article](#) [CrossRef ↗](#)

[Cheng et al., 2008](#) Y. Cheng, L.K. An, N. Wu, X.-D. Wang, X.Z. Bu, Z.S. Huang, L.Q. Gu

Bioorg. Med. Chem., 16 (2008), p. 4617



[View PDF](#)

[View article](#)

[View in Scopus](#) ↗

[Cho et al., 2008](#) S.C. Cho, M.Z. Sultan, S.S. Moon

Bull. Korean Chem. Soc., 29 (2008), p. 1587

[View in Scopus](#) ↗

[Czoch et al., 1994](#) W.P. Czoch, F. Pognan, L. Kaczmarek, J. Boraty

J. Med. Chem., 37 (1994), p. 3503

[Da et al., 2001](#) T.T. Da, D.B. Vu, N.H. Dinh

J. Pharm. Sci., 6 (2001), p. 6

[View in Scopus](#) ↗

[Davis et al., 1978](#) H.L.J. Davis, D.D. Von Hoff, J.E. Henney, M. Rozenzweig

Cancer. Chemother. Pharm., 1 (1978), p. 83

[View in Scopus](#) ↗

[Denny et al., 1987](#) W.A. Denny, G.J. Atwell, G.W. Rewcastle, B.C. Baguley

J. Med. Chem., 30 (1987), p. 658

[CrossRef](#) ↗ [View in Scopus](#) ↗

[Djerassi et al., 1958](#) C. Djerassi, G.W. Krakower, A.J. Lemin, L.H. Liu, J.S. Mills, R. Villotti

J. Am. Chem. Soc., 80 (1958), p. 6284

[CrossRef](#) ↗ [View in Scopus](#) ↗

[Faidallah and Rostomb, 2013](#) H.M. Faidallah, S.A.F. Rostomb

Eur. J. Med. Chem., 63 (2013), p. 133



[View PDF](#)

[View article](#)

[View in Scopus](#) ↗

[Ferlin et al., 2005](#) M.G. Ferlin, G. Chiarelto, V. Gasparotto, V.L. Dalla, V. Pezzi, L. Barzon, G. Palù, I. Castagliuolo

J. Med. Chem., 48 (2005), p. 3417

[CrossRef ↗](#) [View in Scopus ↗](#)

[Ferrer et al., 2009](#) R. Ferrer, G. Lobo, N. Gamboa, J. Rodrigues, C. Abramjuk, K. Jung, M. Lein, J.E. Charris

Sci. Pharm., 77 (2009), p. 725

[View in Scopus ↗](#)

[Finn et al., 2005](#) P.W. Finn, M. Bandara, C. Butcher, A. Finn, R. Hollin-shead, N. Khan, N. Law, S. Murthy, R. Romero, C. Watkins

Helv. Chim. Acta, 7 (2005), p. 1630

[CrossRef ↗](#) [View in Scopus ↗](#)

[Gamal et al., 2014](#) E.M.I. Gamal, M.A. Khan, M.S.A. Maksoud, M.M.G. El-Din, C.H. Oh

Eur. J. Med. Chem., 87 (2014), p. 484

[Gasparotto et al., 2006](#) V. Gasparotto, I. Castagliuolo, G. Chiarelto, V. Pezzi, D. Montanaro, P. Brun, G. Palu, G. Viola, M.G. Ferlin

J. Med. Chem., 49 (2006), p. 1910

[CrossRef ↗](#) [View in Scopus ↗](#)

[Gedawy et al., 2015](#) E.M. Gedawy, A.E. Kassab, A.A. El-Malah

Med. Chem. Res., 24 (2015), p. 3387

[CrossRef ↗](#) [View in Scopus ↗](#)

[Ghorab et al., 2007](#) M.M. Ghorab, F.A. Ragab, E. Noaman, H.I. Heiba, E.M. El-Hossary

Arzneimittelforschung, 57 (2007), p. 795

[View in Scopus ↗](#)

[Ghorab and Alsaid, 2015](#) M.M. Ghorab, M.S. Alsaid

Acta. Pharm., 65 (2015), p. 271

[CrossRef ↗](#) [View in Scopus ↗](#)

[Ghorab et al., 2014](#) M.M. Ghorab, M.S. Al-said, R.K. Arafa

Acta. Pharm., 64 (2014), p. 285

[CrossRef ↗](#) [View in Scopus ↗](#)

[Gourdie et al., 1990](#) T.A. Gourdie, K.K. Valu, G.L. Gravatt, T.J. Boritzki, B.C. Baguley, L.P.G. Wakelin, W.R. Wilson, P.D. Woodgate, W.A.

Denny

J. Med. Chem., 33 (1990), p. 1177

[CrossRef ↗](#) [View in Scopus ↗](#)

[Haseeb et al., 2007](#) A. Haseeb, R.S. Shannon, B. Jorien, A. Nihal

Can. lett., 249 (2007), p. 198

[View in Scopus ↗](#)

[Heiniger et al., 2010](#) B. Heiniger, G. Gakhar, K. Prasain, D.H. Hua, T.A. Nguyen

Antican. Res., 30 (2010), p. 3927

[View in Scopus ↗](#)

[Hertzberg et al., 1989](#) R.P. Hertzberg, M.J. Caranfa, S.M. Hecht

Biochemistry, 28 (1989), p. 4629

[CrossRef ↗](#) [View in Scopus ↗](#)

[Hsi et al., 2004](#) L.C. Hsi, X. Lotan, R. Xi, I. Shureiqi, S.M. Lippman

Cancer. Res., 64 (2004), p. 8778

[View in Scopus ↗](#)

[Hsiang et al., 1985](#) Y.H. Hsiang, R. Hertzberg, S. Hecht, L.F.J. Liu

Biol. Chem., 260 (1985), p. 14873

 [View PDF](#) [View article](#) [View in Scopus ↗](#)

[Ilango et al., 2015](#) K.I. Ilango, P.I. Valentina, K.I. Subhakar, M.K. Kathiravan

Austin. J. Anal. Pharm. Chem., 4 (2015), p. 1048

[Jarak et al., 2005](#) I. Jarak, M. Kralj, L. Suman, G. Pavlovic, J. Dogan, I. Piantaninda, M. Zinic, K. Pavelic, G. Karminski-Zamola
J. Med. Chem., 48 (2005), p. 2346

[CrossRef ↗](#) [View in Scopus ↗](#)

[Jiang et al., 2012](#) Jiang, N., Zhai, X., Li, T., Liu, D., Zhang, T., Wang, B., Gong, P., 2012. *Molecules*. 17, 5870.

[Google Scholar ↗](#)

[Jiang et al., 2007](#) R. Jiang, D. Duckett, W. Chen, J. Habel, Y.Y. Ling, P.L. Grasso, T.M. Kamenecka
Bioorg. Med. Chem. Lett., 17 (2007), p. 6378

 [View PDF](#) [View article](#) [View in Scopus ↗](#)

[Kaczmarek et al., 1999](#) L. Kaczmarek, W.P. Czoch, J. Osiadacz, M. Mordarski, A. Sokalski, J.B. Nski, H.E. Marcinkowska, G.S.K. Radzikowski
Med. Chem., 7 (1999), p. 2457

 [View PDF](#) [View article](#) [View in Scopus ↗](#)

[Kakadiya et al., 2010](#) R. Kakadiya, H. Dong, A. Kumar, D. Narsinh, X. Zhang, T.C. Chou, T.C. Lee, A. Shah, T.L. Su
Bioorg. Med. Chem., 18 (2010), p. 2285

 [View PDF](#) [View article](#) [View in Scopus ↗](#)

[Karthikeyan et al., 2015](#) C. Karthikeyan, C. Lee, J. Moore, R. Mittal, E.A. Suswam, K.L. Abbott, S.R. Pondugula, U. Manne, N.K. Narayanan,
P. Trivedi, A. Tiwari
Bioorg. Med. Chem., 23 (2015), p. 602

 [View PDF](#) [View article](#) [View in Scopus ↗](#)

[Kleer et al., 2003](#) C.G. Kleer, Q. Cao, S. Varambally, R. Shen, I. Ota, S.A. Tomlins, D. Ghosh, R.G.A.B. Sewalt, A.P. Otte, D.F. Hayes, M.S.
Sabel, D. Livant, S.J. Weiss, M.A. Rubin, A.M. Chinnaiyan
Proc. Natl. Acad. Sci. USA, 100 (2003), p. 11606

[View in Scopus ↗](#)

[Koruznjak et al., 2002](#) J.D. Koruznjak, N. Slade, B. Zamola, K. Paveli, G.K. Zamola

Chem. Pharm. Bull., 50 (2002), p. 656

[Kouznetsov et al., 2006](#) V.V. Kouznetsov, C.O. Puentes, A.R.R. Bohorques, S.A. Zacchino, M. Sortino, M. Gupta, Y. Vazquez, A. Bahsas, A.J.

Luis

Lett. Org. Chem., 3 (2006), p. 300

[View in Scopus ↗](#)

[Kouznetsov et al., 2012](#) V.V. Kouznetsov, R.F.A. Rojas, V.L.Y. Méndez, M.P. Gupta

Lett. Drug. Desi. Disc., 9 (2012), p. 680

[View in Scopus ↗](#)

[Kuan et al., 2003](#) C.Y. Kuan, A.J. Whitmarsh, D.D. Yang, G. Liao, A.J. Schloemer, R.J. Davis, P. Rakic

Proc. Natl. Acad. Sci. U.S.A., 100 (2003), p. 15184

[View in Scopus ↗](#)

[Kubicek et al., 2007](#) S. Kubicek, O.R.J. Sullivan, E.M. August, E.R. Hickey, Q. Zhang, M.L. Teodoro, S. Rea, K. Mechtler, J.A. Kowalski, C.A.

Homon, T.A. Kelly, T. Jenuwein

Mol. Cell., 25 (2007), p. 473



[View PDF](#)

[View article](#)

[View in Scopus ↗](#)

[Lee et al., 2004](#) B.D. Lee, Z. Li, K.J. French, Y. Zhuang, Z. Xia, C.D. Smith

J. Med. Chem., 47 (2004), p. 1413

[CrossRef ↗](#) [View in Scopus ↗](#)

[Li et al., 2007](#) Q. Li, J. Min, Y.H. Ahn, J. Namm, E.M. Kim, R. Lui, H.Y. Kim, Y. Ji, H. Wu, T. Wisniewski, Y.T. Chang

Chem. Bio. Chem., 8 (2007), p. 1679

[CrossRef ↗](#) [View in Scopus ↗](#)

[Long et al., 2005](#) Y.C. Long, C. Li, H.H. Chein, C.T. Cherng

Euro. J. Med. Chem., 40 (2005), p. 928

[Lown and Sim, 1976](#) J.W. Lown, S.K. Sim

Can. J. Chem., 54 (1976), p. 2563

[CrossRef ↗](#) [View in Scopus ↗](#)

[Lu et al., 2008](#) J.J. Lu, L.H. Meng, Y.J. Cai, Q. Chen, L.J. Tong, L.P. Lin, J. Ding

Cancer Biol. Ther., 7 (2008), p. 1017

[CrossRef ↗](#)

[Martirosyan et al., 2004](#) A. Martirosyan, R. Rahim-Bata, A. Freeman, C. Clarke, R. Howard

J. Biochem. Pharmacol., 68 (2004), p. 1729

 [View PDF](#) [View article](#) [View in Scopus ↗](#)

[Matson et al., 1993](#) J.A. Matson, K.L. Colson, D.N. Belofsky, B.B.J. Bleiberg

Antibiotics, 46 (1993), p. 162

[CrossRef ↗](#)

[Mcchesney et al., 1962](#) E.W. Mcchesney, W.F. Banks, J.P. Mc Auliff

Antibiot. Chemother., 12 (1962), p. 583

[Meshram et al., 2012](#) H.M. Meshram, B.C. Reddy, D.A. Kumar, M. Kalyan, P. Ramesh, P. Kavitha, J.V. Rao

Ind. J. Chem., 51 (2012), p. 1411

[View in Scopus ↗](#)

[Moyer et al., 1997](#) J.D. Moyer, E.G. Barbacci, K.K. Iwata, L. Arnold, B. Boman, A. Cunningham, C. Diorio, J. Doty, M.J. Morin, M.P. Moyer, M.

Neveu, V.A. Pollack, L.R. Pustilink, M.M. Reynolds, D. Salon, A. Theleman

Cancer. Res., 57 (1997), p. 4838

[View in Scopus ↗](#)

[Mphahlele et al., 2014](#) M.J. Mphahlele, M.M. Maluleka, T.J. Makhafola, P. Mabeta

Molecule, 19 (2014), p. 18527

[CrossRef ↗](#) [View in Scopus ↗](#)

Mulchin et al., 2010 B.J. Mulchin, C.G. Newton, J.W. Baty, C.H. Grasso, W.J. Martin, M.C. Walton, E.M. Dangerfield, C.H. Plunkett, M.V. Berridge, J.L. Harper, M.S.M. Timmer, B.L. Stocker
Bioorg. Med. Chem., 18 (2010), p. 3238

 [View PDF](#) [View article](#) [View in Scopus ↗](#)

Nasveschuk et al., 2014 C.G. Nasveschuk, A. Gagnon, S. Garapaty-Rao, S. Balasubramanian, R. Campbell, C. Lee, F. Zhao, L. Bergeron, R. Cummings, P. Trojer, J.E. Audia, B.K. Albrecht, J.C.P. Harmange
ACS Med. Chem., 5 (2014), p. 378

[CrossRef ↗](#) [View in Scopus ↗](#)

Okten et al., 2013 S. Okten, O. Cakmak, R. Erenler, O. Yuce, S. Tekin
Turk. J. Chem., 37 (2013), p. 896

[CrossRef ↗](#) [View in Scopus ↗](#)

Ortiz et al., 2014 L.M.G. Ortiz, M. Tillhon, M. Parks, I. Dutto, E. Prospero, M. Savio, A.G. Arcamone, F. Buzzetti, P. Lombardi, A.I. Scovassi
BioMed. Res. Int., 2014 (2014), p. 1

[View in Scopus ↗](#)

Pezzoni et al., 1991 G. Pezzoni, M. Grandi, G. Biasoli, L. Capolongo, D. Ballinari, F.C. Giuliani, B. Barbieri, B. Pastori, E. Pesenti, N. Mongelli, F. Spreafico
Br. J. Cancer, 75 (1991), p. 1047

[CrossRef ↗](#)

Pierre et al., 2011 F. Pierre, P.C. Chua, S.E. Brien, A. Siddiqui-Jain, P. Bourbon, M. Haddach, J. Michaux, J. Nagasawa, M.K. Schwaebe, E. Stefan, A. Vialettes, J.P. Whitten, T.K. Chen, L. Darjanian, R. Stansfield, K. Anderes, J. Bliesath, D. Drygin, C. Ho, M. Omori, C. Proffitt, N. Streiner, K. Trent, W.G. Rice, D.M. Ryckman
J. Med. Chem., 54 (2011), p. 635

[CrossRef ↗](#) [View in Scopus ↗](#)

[Rao, 1974](#) K.V. Rao

Cancer. Chemother. Rep., 24 (1974), p. 11

[View in Scopus ↗](#)

[Rao et al., 1963](#) K.V. Rao, K. Biemann, R.B.J. Woodward

Am. Chem. Soc., 85 (1963), p. 2532

[CrossRef ↗](#) [View in Scopus ↗](#)

[Reyes et al., 2010](#) M.A.V. Reyes, A. Zentella, M.A.M. Urbina, A. Guzman, O. Vargas, M.T.R. Apan, J.L.V. Gallegos, E. Diaz

Eur. J. Med. Chem., 45 (2010), p. 379

[CrossRef ↗](#)

[Ryckebusch et al., 2003](#) A. Ryckebusch, R. Derprez-Poulain, L. Maes, D.M.A. Fontaine, E. Mouray, P. Grellier, C. Sergheraert

J. Med. Chem., 46 (2003), p. 542

[View in Scopus ↗](#)

[Ryckebusch et al., 2008](#) A. Ryckebusch, D. Garcin, A. Lansiaux, J.F. Goossens, B. Baldeyrou, R. Houssin, C. Bailly, J.P. Hénichart

J. Med. Chem., 51 (2008), p. 3617

[CrossRef ↗](#) [View in Scopus ↗](#)

[Sagheer et al., 2013](#) O.M. Sagheer, K.Y. Saqur, M.M. Ghareeb

Int. J. Pharm. Pharm. Sci., 5 (2013), p. 464

[View in Scopus ↗](#)

[Schmidt et al., 2008](#) F. Schmidt, C.B. Knobbe, B. Frank, H. Wolburg, M. Weller

Onco. Repo., 19 (2008), p. 1061

[View in Scopus ↗](#)

[Serda et al., 2010](#) M. Serda, R. Musiol, J. Polanski

14th International conference on Synthetic Organic Chemistry. C013 (2010)

[Google Scholar ↗](#)

[Shaikh et al., 1986](#) I.A. Shaikh, F. Johnson, A.P.J. Grollman

Med. Chem., 29 (1986), p. 1329

[CrossRef ↗](#) [View in Scopus ↗](#)

[Sheetal et al., 2012](#) B.M. Sheetal, R.K. Ravindra, T. Tasneem, Y.K. Mahadevappa

Med. Chem. Res., 21 (2012), p. 185

[Sidoryk et al., 2015](#) K. Sidoryk, M. Switalska, A. Jaromin, P. Cmoch, I. Bujak, M. Kaczmarek, J. Wietrzyk, E.G. Dominguez, R. Zarnowski,

D.R. Andes, K. Bankowski, M. Cybulski, Ł. Kaczmarek

Eur. J. Med. Chem., 105 (2015), p. 208

 [View PDF](#) [View article](#) [View in Scopus ↗](#)

[Solin et al., 1982](#) T. Solin, K. Matsumoto, K. Fuwa

Inorg. Chim. Acta., 65 (1982), p. 172

[Spaczyńska et al., 2014](#) E. Spaczyńska, D. Tabak, K. Malarz, R. Musiol

Der. Pharma. Chemica, 6 (2014), p. 233

[View in Scopus ↗](#)

[Srivastava et al., 2005](#) Srivastava, S.K., Khan, M. Khanuja, S.P.K., 2005. US 6,893,668 B2.

[Google Scholar ↗](#)

[Su et al., 1995](#) T.L. Su, T.C. Chou, J.Y. Kim, J.T. Huang, G. Ciszewska, W.Y. Ren

J. Med. Chem., 38 (1995), p. 3226

[CrossRef ↗](#) [View in Scopus ↗](#)

[Tan et al., 1991](#) G.T. Tan, J.M. Pezzuto, A.D. Kinghorn, S.H. Hughes

J. Nat. Prod., 54 (1991), p. 143

[CrossRef ↗](#) [View in Scopus ↗](#)

[Thanh et al., 2014](#) N.T.C. Thanh, N.N. Bich, V.L. Meervelt
Acta. Cryst., 70 (2014), p. 297

[Tseng et al., 2008](#) C.H. Tseng, Y.L. Chen, P.J. Lu, C.N. Yang, C.C. Tzeng
Bioorg. Med. Chem., 16 (2008), p. 3153

 [View PDF](#) [View article](#) [View in Scopus ↗](#)

[Wakelin and Denny, 1990](#) L.P.G. Wakelin, W.A. Denny
Molcu. Basis. Specifi. Nucleic. Acid. Drug. Int. (1990), p. 191

[CrossRef ↗](#) [Google Scholar ↗](#)

[Wakeling et al., 2002](#) A.E. Wakeling, S.P. Guy, J.R. Woodburn, S.E. Ashton, B.J. Curry, A.J. Barker, K.H.Z.D. Gibson
Cancer. Res., 62 (2002), p. 5749

[View in Scopus ↗](#)

[Wall et al., 1966](#) M.E. Wall, M.C. Wani, C.E. Cook, K.H. Palmer, A.T. McPhail, G.A. Sim
J. Am. Chem. Soc., 88 (1966), p. 3888

[CrossRef ↗](#) [View in Scopus ↗](#)

[Weber et al., 2000](#) C.K. Weber, J.R. Slupsky, C. Herrmann, M. Schuler
U.R. Rapp. C. Block. Oncogene., 19 (2000), p. 169

[CrossRef ↗](#) [View in Scopus ↗](#)

[Wellbrock et al., 2004](#) C. Wellbrock, M. Karasarides, R. Marais
Nat. Rev. Mol. Cell. Biol., 5 (2004), p. 875

[View in Scopus ↗](#)

[Xiang et al., 2015](#) P.J.H. Xiang, Y. Zhou, B. Yang, H.J. Wang, J. Hu, J. Hu, S.Y. Yang, Y.L. Zhao
Molecule, 20 (2015), p. 7620

[CrossRef ↗](#) [View in Scopus ↗](#)

[Yamato et al., 1988](#) Yamato, Mastoshi, Tsutaka, Okayama-shi Okayama-ken 1988. EP0264124A1.

[Google Scholar ↗](#)

[Zhang and Zhang, 2005](#) G.Y. Zhang, Q.G. Zhang

Exp. Opin. Invest. Drugs., 14 (2005), p. 1373

[CrossRef ↗](#) [View in Scopus ↗](#)

[Zhihu et al., 2002](#) D. Zhihu, C.T. Shou, W. Priya, Y. Xiaolong, P. Alan, L. Andrejs

Biochem. Pharmacol., 63 (2002), p. 1415

Cited by (278)

[Design, synthesis, and evaluation of anti-breast cancer activity of colchicine - combretastatin A-4 analogues containing quinoline as microtubule-targeting agents](#)

2024, Journal of Molecular Structure

[Show abstract](#) ✓

[Investigation on the pharmacological profile for new synthesized bis heterocyclic analogs containing nitrogen atom as anti-cancer therapy target](#)

2024, Journal of Molecular Structure

[Show abstract](#) ✓

[Design, 3D-QSAR, molecular docking, ADMET, molecular dynamics and MM-PBSA simulations for new anti-breast cancer agents](#)

2024, Chemical Physics Impact

[Show abstract](#) 

[Design, synthesis, biological evaluation and molecular docking studies of quinoline-anthranilic acid hybrids as potent anti-inflammatory drugs](#)

2024, Organic and Biomolecular Chemistry

[Show abstract](#) 

[One-Pot Synthesis of 2-\(Alkylsulfanyl\)quinolines from Aryl Isothiocyanates and Allenes or Alkynes](#)

2024, European Journal of Organic Chemistry

[Show abstract](#) 

[Inhibition of cancer cells by Quinoline-Based compounds: A review with mechanistic insights](#)

2024, Bioorganic and Medicinal Chemistry

[Show abstract](#) 



[View all citing articles on Scopus](#) 

Peer review under responsibility of King Saud University.

© 2016 The Authors. Production and hosting by Elsevier B.V. on behalf of King Saud University.



All content on this site: Copyright © 2024 Elsevier B.V., its licensors, and contributors. All rights are reserved, including those for text and data mining, AI training, and similar technologies. For all open access content, the Creative Commons licensing terms apply.





Gastrointestinal Protective Effect of *Zizyphus xylopyrus* (Retz) Willd Leaf Extract Against Indomethacin and HCl-EtOH Induced Ulcers

Buy Article:

\$68.00 + tax

(Refund Policy)

ADD TO CART

BUY NOW

Authors: Jain, Shweta; Jain, Sourabh; Chauhan, Nagendra S.; Vaidya, Ankur

Source: Current Traditional Medicine, Volume 5, Number 2, 2019, pp. 152-158(7)

Publisher: Bentham Science Publishers

DOI: <https://doi.org/10.2174/2215083804666181012124047>



Abstract



References



Citations



Supplementary Data

Background: *Zizyphus xylopyrus* (Retz.) Willd. (Rhamnaceae) is a straggling shrub or a small tree, armed with spines, found throughout north-

western India, Pakistan and China.

Methods: The aerial and root barks, leaves and fruits of Zizyphus species are used in medicine for the treatment of various diseases such as weakness, liver complaints, obesity, diabetes, skin infections, fever, diarrhea, insomnia and digestive disorders. Ethanolic extract of leaves of Zizyphus xylopyrus (Retz) Willd was prepared by solvent extraction and subjected to study the protective effect against Indomethacin and HCl-EtOH induced ulcer using Ranitidine (100 mg/kg) and Omeprazole (8 mg/kg) as standard respectively.

Results: Histopathological lesions with marked disorientation of the gastric epithelium was observed in negative control, while extract treated rats showed a better protected mucosa with intact epithelium in comparison to standard treated rats. Ulcer index and percentage ulcer protection also represent protecting effects of the extract.

Conclusion: Ethanolic extract of Z. xylopyrus (Retz) Willd leaves extract was found to be significantly protective against gastric ulcers.

Keywords: Gastric ulcer; HCl-EtOH; Zizyphus xylopyrus (Retz); diabetes; indomethacin; willd leaf

Document Type: Research Article

Publication date: June 1, 2019

[More about this publication?](#)

Enhancement of Permeability and Dissolution Profile of Poorly Permeable Drug by Using Controlled Crystallization Bottom Up Technique

Anju GAUNIYA ¹*, Rupa MAZUMDER ¹ & Kamla PATHAK ²

¹ Noida Institute of Engineering and Technology (Pharmacy Institute), Greater Noida, 201306, India

² Pharmacy College Saifai, U.P. University of Medical Sciences Saifai, Etawah, 206130, India

SUMMARY. The aim of the present study was to increase the permeability and dissolution profile of a low permeable drug (atenolol) by converting the drug into nanocrystals formulation which ranges in nano size. The method of preparation of nanocrystals used was bottom-up technique (high speed homogenization) using SLS and HPMC. 3² factorial designs was applied and the effect of variation in concentration of SLS and HPMC on particle size, % yield, permeability and dissolution was evaluated. The prepared nanocrystals were further aimed to characterize in solid state by particle size, % yield, SEM, zeta potential, X-Ray Diffraction (XRD) patterns, permeability, *in vitro* dissolution and stability studies. Result showed size of particles were found in nano-size and SEM and XRD revealed the crystalline nature of the nanocrystals. Nanocrystals were having good dissolution profile and good permeability. The stability result showed the prepared nanocrystals were stable. Permeability and dissolution profile of atenolol can be increase by nanocrystallization technology.

RESUMEN. El objetivo del presente estudio fue aumentar el perfil de permeabilidad y disolución de un fármaco de baja permeabilidad (atenolol) convirtiendo el fármaco en una formulación de nanocristales que varía en tamaño nano. El método de preparación de nanocristales utilizado fue la técnica de abajo hacia arriba (homogeneización de alta velocidad) utilizando SLS y HPMC. Se aplicaron 32 diseños factoriales y se evaluó el efecto de la variación en la concentración de SLS y HPMC sobre el tamaño de partícula, el porcentaje de rendimiento, la permeabilidad y la disolución. Los nanocristales preparados tenían el objetivo adicional de caracterizarse en estado sólido por tamaño de partícula, % de rendimiento, SEM, potencial zeta, patrones de difracción de rayos X (XRD), permeabilidad, disolución *in vitro* y estudios de estabilidad. El resultado mostró que el tamaño de las partículas se encontró en nano-tamaño y SEM y XRD revelaron la naturaleza cristalina de los nanocristales. Los nanocristales tenían buen perfil de disolución y buena permeabilidad. El resultado de estabilidad mostró que los nanocristales preparados eran estables. El perfil de permeabilidad y disolución de atenolol puede aumentarse mediante la tecnología de nanocristalización.

KEY WORDS: bioavailability, dissolution studies, nanocrystals, permeability, solubility.

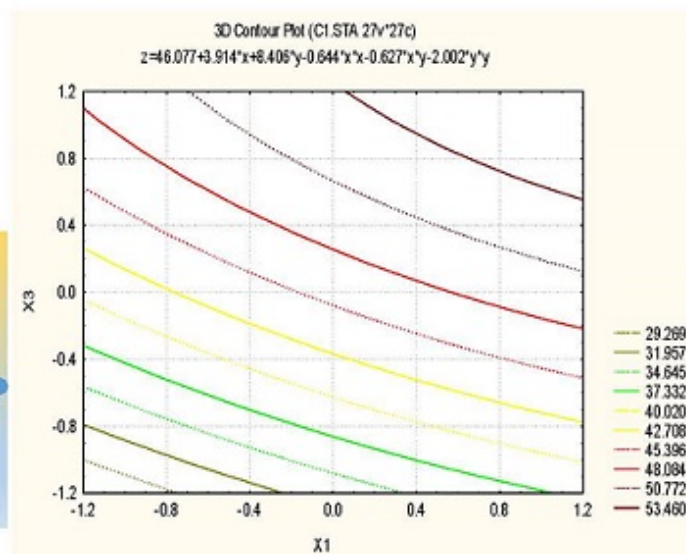
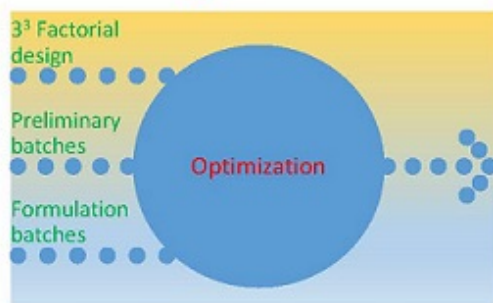
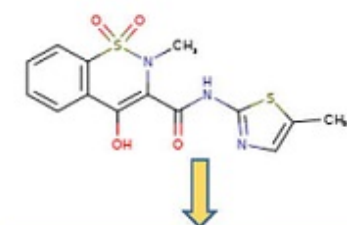
* Author to whom correspondence should be addressed. *E-mail:* anju.gauniya@gmail.com

This is archived platform of the CBL journal, Readers/Authors should navigate to new site at <https://pubs.thesciencein.org/journal/index.php/cbl>

Chemical Biology LETTERS

ISSN 2347-9825

 All
Browse By: [Author](#) [Issue](#) [Title](#) [Other Journals](#)
[Home](#) [About](#) [Login](#) [Register](#) [Search](#) [Current](#) [Archives](#) [Editorial Board](#) [Submission](#)
Home > Vol 6, No 1 (2019) > **Dahiya**



Formulation optimization of multicomponent aqueous coground mixtures of Meloxicam for dissolution enhancement

Sunita Dahiya, Atul Kaushik, Kamla Pathak

SCOPUS CiteScore 2020

4.4

The CBL Journal has started using Article ID from 2022 volume (in place of page number) for unique identification of published articles.

2022 Vol 9 [Issue 1](#) [Issue 2](#)

2021 Vol 8

[Iss 1 pg 1-44](#) [Iss 2 pg 45-87](#)

[Iss 3 pg 88-130](#) [Iss 4 pg 141-264](#)

2020 Vol 7

[Iss 1 pg 1-72](#) [Iss 2 pg 73-165](#)

[Iss 3 pg 166-196](#) [Iss 4 pg 197-250](#)

2019 Vol 6

[Iss 1 pg 1-22](#) [Iss 2 pg 23-61](#)

2018 Vol 5

[Iss 1 pg 1-40](#) [Iss 2 pg 41-99](#)

2017 Vol 4

[Iss 1 pg 1-62](#) [Iss 2 pg 63-90](#)

2016 Vol 3

[Iss 1 Pg 1-31](#) [Iss 2 Pg 32-63](#)

2015 Vol 2

Abstract

In present work, the role of various formulation excipients for dissolution enhancement of a BCS Class II drug, meloxicam was studied by formulating multicomponent aqueous coground mixtures using lactose, microcrystalline cellulose and three solubilizers; polyethylene glycol 400, propylene glycol and polyvinyl pyrrolidone. A 3³ full factorial design was employed using solubilizers' concentrations as independent variables whereas angle of repose and *in vitro* drug dissolution as dependent variables in order to optimize the amounts of solubilizers. The results revealed more than fivefold increase in drug dissolution in some experimental batches compared to that of pure drug powder. Full and reduced models were evolved for the dependent variables and the reduced models were further validated using extra design check points. The studies suggested that the incorporation of optimized amounts of solubilizers could be successfully employed for achieving desired flow properties and enhanced drug dissolution of poorly water soluble meloxicam. The method emerged as a simple, cost-effective, and organic solvent-free green approach toward formulation development of meloxicam and may also be applied to other limited water-soluble drugs.

Keywords

meloxicam; poorly water soluble drug; optimization; factorial design; solvent free approach; dissolution enhancement



ISSN 2347-9825

Authors/visitors are advised to use Firefox browser for better experience of journal site.

Open Access: Researcher from developing/low economy countries can access the journal contents through WHO-HINARI .

The ScienceIn

[Iss 1 Pg 1-21](#) [Iss 2 Pg 22-44](#)

2014 Vol 1

[Iss 1 Pg 1-39](#) [Iss 2 Pg 40-103](#)

Article Tools

[Indexing metadata](#)

[How to cite item](#)

[Finding References](#)

[Email this article \(Login required\)](#)

[Email the author \(Login required\)](#)

[Submit Manuscript](#)

[Author Guidelines](#)

[Focus and Scope](#)

[Peer Review Process](#)

[Publication Ethics](#)

[Editorial Board](#)

[Instructions to Authors](#)

[Email Alerts](#)

[Subscription](#)

[Open Access Policy](#)

USER

Username

Password

Remember me

JOURNAL CONTENT

Search

Search Scope

All ▾

Search

Browse

By Issue

By Author

By Title

Other Journals

SUBSCRIPTION

Login to verify subscription

INFORMATION

For Readers

For Authors

For Librarians

ABOUT THE AUTHORS

Sunita Dahiya
University of Puerto Rico
Puerto Rico

Atul Kaushik
IPS College of Pharmacy
India

Kamla Pathak
Uttar Pradesh University of Medical
Sciences
India






KEYWORDS

[Antibacterial](#) [Antimalarial activity](#)
[Antimicrobial](#) [Inflammation](#) [Molecular](#)

[docking](#), [Nanoparticles](#), [Oxidative stress](#),
[SPECT](#), [cancer](#), [cytokines](#), [energy](#),
[homeostasis](#), **[inflammation](#)**,
[leukocytes](#), [lipid peroxidation](#), **[male](#)**
[infertility](#), [molecular docking](#),
[obesity](#), **[oxidative stress](#)**,
[photodynamic therapy](#), [reactive oxygen](#),
[species](#), **[semen quality](#)**

[Journal Help](#)

FONT SIZE

 IN 38,955	 BR 1,326
 US 11,006	 GB 1,176
 SG 9,922	 PK 1,120
 CN 4,644	 KR 1,108
 IR 1,812	 TR 1,079
 ID 1,424	 MY 984



CURRENT ISSUE

ATOM	1.0
RSS	2.0
RSS	1.0

Investigating Gastroprotective Potential of Liquisolid Curcumin against the Role of Endogenous Aggressive Factors and Oxidative Stress Markers

Vijay Sharma,¹ Kamla Pathak^{2*}

¹Department of Pharmaceutics, SGT College of Pharmacy, Shree Guru Gobind Singh Tricentenary University-Gurugram, Badli Road, Gurugram, Haryana, INDIA.

²College of Pharmacy Saifai, Uttar Pradesh University of Medical Sciences, Saifai, Etawah, Uttar Pradesh, INDIA.

ABSTRACT

Background: The study investigated the efficacy of Liquisolid Curcumin (LSC) over curcumin for gastroprotective action against ethanol induced acute gastric ulcers and the modulation of endogenous oxidative stress markers, in Wistar rats (*p.o*). **Materials and Methods:** The experimental design comprised of six groups namely control (Treated with 0.1% w/v CMC), disease control (Treated with absolute ethanol), positive control (Treated with omeprazole; 40 mg/Kg), Test-1 (Treated with curcumin; 50 mg/Kg); and Test- 2 and 3 groups treated with LSC equivalent to 25 and 50 mg/Kg, respectively. Gastroprotection was assessed by ulcer index, total acid and gastric mucus. The oxidative stress markers estimated were malondialdehyde (MDA), tissue Glutathione (GSH), Catalase (CAT) and Superoxide Dismustase (SOD). **Results:** Oral administration of LSC caused significant ($P < 0.01$) reduction in gastric lesions in dose dependent manner. The total acidity lowering effect and protective effect on mucus layer was more than curcumin and comparable to omeprazole under the test conditions. Additionally, the LSC significantly increased the activity/levels of GSH, CAT and SOD and suppressed the MDA level in gastric mucosa ($P < 0.05$). Histological studies demonstrated superior morphological integrity of gastric mucosa via LSC. **Conclusion:** LSC demonstrated superior gastroprotection via suppression of gastric acid, restoration of free radical scavenging enzymes and reduction in the lipid peroxidase production in comparison to curcumin.

Key words: Curcumin, Liquisolid curcumin, Liquisolid compacts, Gastroprotection, Oxidative stress markers.

INTRODUCTION

Gastric ulcer is the result of an imbalance between aggressive factors and safeguarding of mucosal integrity through the endogenous protective mechanism.¹ The severity of disease may lead to upper gastrointestinal hemorrhage and perforation leading to high mortality and morbidity rates.² Several endogenous factors including high acid secretion and imperfect mucosal barrier contribute towards initiation and progression of the underlined disease.³ The etiology of gastric ulcers is also associated with *H. pylori* infection that imbalances pepsin secretion, reflux of bile component, formation of free radicals, mucus-bicarbonate barrier,

surface active phospholipids, mucosal blood flow, cell renewal and migration, enzymatic and non-enzymatic antioxidants and some growth factors.^{4,5} Other factors include induction of proinflammatory TNF- α expression, Reactive Oxygen Species (ROS), neutrophil infiltration, increased lipid peroxidation and decreased glutathione activity.⁶

The treatment is primarily focused on limiting the hazardous effects of acid secretion, generation of ROS, as well as to regulate various oxidative stress markers and enzymatic activities. The

Submission Date: 19-07-2018;

Revision Date: 19-12-2018;

Accepted Date: 29-03-2019

DOI: 10.5530/ijper.53.3.85

Correspondence:

Dr. Kamla Pathak,

Professor, College of

Pharmacy, Uttar Pradesh

University of Medical Sci-

ences Saifai, Etawah, Uttar

Pradesh- 206130, INDIA.

Phone: +91-05688-276023

E-mail: kamlapathak5@

gmail.com



www.ijper.org

long-term therapeutics based on proton pump inhibitors, prostaglandins, cytoprotective agents and histamine antagonists cause adverse drug reactions and the long-term use may result in changes in the biochemical architecture. Thus, the gastroprotective research has shifted its paradigm to molecules of natural origin, curcumin being one of them.⁷ Curcumin a phytoconstituent of *Curcuma longa* is a potent polyphenolic antioxidant recommended for the effective protection of gastric lesions and treatment of gastric ulcers.⁸ Presence of both phenolic OH and CH₂ group of β-diketone moiety remarkably contribute to its antioxidant property. Curcumin inhibits generation of H₂O₂, in macrophages and directly lowers *OH.⁹⁻¹⁰ Despite the fact that curcumin is therapeutically acclaimed it suffers from poor solubility (0.6 µg/mL) and dissolution¹¹ and hence limited clinical efficacy. Pharmaceutical research has adopted various techniques to optimize the solubility of curcumin in order to improve its therapeutic efficacy.¹²⁻¹⁵

Liquisolid technique is a promising method that has been utilized to enhance the dissolution rate and bioavailability of various poorly water-soluble drugs. Our research on curcumin reported improved dissolution and bioavailability of curcumin using the potentials of liquisolid technology. The optimized liquisolid tablets exhibited higher cumulative drug release than the directly compressed tablets of curcumin. Furthermore, *ex vivo* permeation of curcumin through goat gastrointestinal mucosa was recorded to be significantly ($P < 0.05$) enhanced and its oral bioavailability was increased by 18.6-fold in New Zealand rabbits. *In vitro* cytotoxicity against NCL 87 cancer cells substantiated its anticancer efficacy.¹⁶ In continuation with the encouraging results, the present study was undertaken to comparatively investigate the antiulcer effect of optimized Liquisolid Curcumin (LSC) formulation against curcumin in ethanol induced gastric damage model. Additionally, the ulceroprotective activity was also assessed biochemically by monitoring various oxidative stress markers in Wistar rats.

MATERIALS AND METHODS

Drugs and Chemicals

Curcumin (Lot # PC/CL/10LOT/09) was kindly supplied by Natural Remedies Private Limited (Bengaluru, India). Omeprazole was purchased from Biological E Ltd., India. Trichloroacetic acid and carboxy methyl cellulose were purchased from S. D. Fine Chemical Ltd. (Mumbai, India). Tris buffer solution was procured from Mivon Chemicals, Mumbai. Ethanol, Masson's

Trichrome Stain and 5, 5-dithiobis-2-nitro benzoic acid (DTNB) were purchased from Sigma Aldrich Ltd., U.S.A.

Formulation of Liquisolid Curcumin

A total of 12 liquisolid compositions using one non-volatile solvent per group [Group –I (PEG 200); Group –II (PEG 400) and Group III (tween 80)] using MCC PH102 as a carrier material and Aerosil® as a coating material were formulated. The Ratio (R) of carrier and coating material used was 20:1, for all the systems. The Φ values calculated for carrier and coating material were utilized to determine the liquid Load Factor (L_f) and with the help of liquid load factor and amount of liquid medication (W), the appropriate amount of carrier and coating material was calculated as reported in Table 1.

For preparation, MCC PH102 was mixed with the drug liquid solution (Liquid medication). Blending was carried out for 2 min in a glass pestle mortar for even distribution of liquid medication in MCC PH102, during primary stage. In the secondary stage liquid-powder admixture was evenly spread as a uniform layer on the surface of the mortar and left for 5 min to allow sufficient adsorption of drug solution on to the surface of carrier particles. The damp, liquid-powder mixture was converted into the dry and freely flowing powder by the gradual addition of Aerosil® (coating material) with the continuous blending. Obtained product was termed as Liquisolid Curcumin (LSC). All the LSC were subjected to pre and post compression studies¹⁶ and the optimized liquisolid formulation was selected to be screened for its gastroprotective potential.

Experimental Protocol

The experimental protocol was approved by Institutional Animal Ethical committee vide letter no: IAEC/RAP/03966. All the animal experiments were conducted in full compliance with the institutional ethical and regulatory principles and as per the spirit of Association for Assessment and Accreditation of Laboratory Animal Care and International's expectations for animal care and use/ethics committees. Wistar rats were randomly divided into six experimental groups (Group I, II, III, IV, V and VI), each containing six animals. Group I was designated as control, Group II (disease control), while Group III termed as positive control (Standard). Other groups were Group IV (Test-1), while Group V and VI were Test-2 and 3, respectively. All the rats were fasted for 24 h and deprived of water for 2 h before starting the treatment protocol. Initially, rats in each group were administered with 0.1% w/v CMC (10 mL/Kg, *p.o.*). After 1 hr Group II was treated with absolute ethanol

(5mL/Kg BW, *p.a.*) and sacrificed by cervical dislocation under deep ether anesthesia, after 1 h of ethanol administration. Post one hour the rats of Group III were administered omeprazole (40mg/Kg, *p.a.*), Group IV was treated with curcumin (50mg/Kg, *p.a.*), while Group V and VI was administered LSC equivalent to 25 and 50 mg of curcumin/Kg *p.a.*, respectively to observe dose dependency. After 4 h of each treatment, the animals of Group III, IV, V and VI were administered absolute ethanol (5mL/Kg, *p.a.*) followed by euthanization by deep anesthesia using diethyl ether and sacrificed by cervical dislocation method. The stomach was immediately removed and the complete gastric content was collected by gently pressing the stomach. The stomach was opened along with greater curvature and rinsed with normal saline to wash out blood clots and adhered material to assess the extent of gastric damage.

Ulcer Index

The extent of gastric mucosal damage was observed and rated according to the ulcer score scale described by Dekanski *et al.*¹⁷ Ulcer Index (UI) was measured by following equation.

$$UI = U_N + U_S + U_P \times 10^{-1} \dots \dots \dots (1)$$

where, U_N = Average number of ulcers/animal; U_S = Average number of severity score; U_P = Percentage of animals with ulcers. The Ulcer inhibition was calculated using eq. 2.

$$\% \text{ Ulcer Inhibition} = [(U.I._{\text{Non treated}} - U.I._{\text{Treated}}) / U.I._{\text{Non treated}}] \times 100 \dots \dots \dots (2)$$

Gastric Content

The collected gastric content was centrifuged at 3000 rpm for 10 min, the supernatant was collected and the volume of supernatant was measured. The supernatant samples were titrated (back titration) against 0.01 mol/L sodium hydroxide (NaOH) using phenolphthalein as indicator.¹⁸ The total acidity was expressed as milliequivalents using Eq. 3.

$$\text{Total acidity} \left(\frac{mEq}{L} \right) = \frac{mL \text{ of NaOH}}{\text{liter juice}} \times 50 \dots \dots \dots (3)$$

Gastric Mucus

The stomach tissues were soaked for 2 h in 0.1% alcian blue. Uncomplexed dye was removed by two successive washes of 0.25 M sucrose at 15- and 45-min. Dye complexed with mucus was diluted by immersion in 10 ml aliquots of 0.5 M magnesium chloride for 2 h. The resulting blue solution was stirred with diethyl ether and the absorbance of the aqueous phase was measured at 580 nm. The quantity of mucus was calculated by standard curves of alcian blue and the result expressed in mg of alcian blue/g tissue.¹⁹

Assessment of Oxidative Stress in Tissues

The levels of MDA (Malondialdehyde), GSH (Tissue glutathione), CAT (Catalase) and SOD (Super Oxide Dismutase) were measured to estimate the potential difference between LSC over curcumin on oxidative stress in ethanol induced gastric ulcer model.²⁰ The stomach was weighed and homogenized in potassium phosphate buffer, pH 7.4 and centrifuged (845.32 x g) for 15 min. The supernatant was used for MDA and enzymatic assays.

Estimation of Lipid Peroxide

Lipid peroxide content in gastric mucosal tissue was determined by thiobarbituric acid reaction.²¹ The absorbance of the supernatant was read at 540 nm at room temperature against blank. The amount of MDA (nmol MDA/mg protein) sample was calculated according to the eq. 4.

$$nmol \text{ of MDA} = \frac{\text{Absorbance at 540nm} \times \text{final volume of test solution}}{0.156} \dots \dots \dots (4)$$

Estimation of tissue glutathione

Five hundred milligrams of tissue was homogenized in 10 ml of 200 mM potassium phosphate buffer, pH 6.5 and 50% v/v trichloroacetic acid was added to the aliquot. Homogenized, vortex for 10 min and then centrifuged (3381.3 x g). 0.4 M Tris buffer and 0.01M, DTNB was added to supernatant²² and absorbance was measured at 415 nm. The amount of GSH ($\mu\text{g}/\text{mg}$ of protein) was calculated by the following equation 5,

$$GSH = \frac{\text{Absorbance at 412 nm} \times 50 \times 3.5 \times 2.25 \times 1}{0.337 \times 2 \times \text{mg of protein}} \dots \dots \dots (5)$$

Blank determination was carried out without tissue homogenate.

Estimation of catalase activity

Fifty milliliters of the supernatant was added to the cuvette containing 2.95 ml of 19 mM/L solution of H_2O_2 prepared in potassium phosphate buffer, pH6.4. The change in absorbance was monitored at 240 nm at 1 min interval for 3 min.²³ Catalase activity (nmol of H_2O_2 consumed/ min/ mg protein) was calculated by equation 6.

$$\text{Catalase activity} = \frac{\text{Decrease in absorbance per min} \times \text{volume of assay}}{0.081 \times \text{volume of homogenate} \times \text{mg of protein}} \dots \dots \dots (6)$$

Estimation of superoxide dismutase activity

Supernatant was assayed for SOD activity by following the inhibition of pyrogallol autoxidation.²⁴ SOD activity (SOD units per mg of protein) was calculated according $SOD \text{ unit per ml of sample} = \frac{(A \times B) \times 100}{A \times 50} \dots \dots \dots (7)$

where, A is the absorbance difference in control in 1 min and B is the absorbance difference in test sample.

Histology

The specimens of tissues were collected from the preserved stomachs of rats. Tissue fragments were stained with hematoxylin and eosin and Masson's trichome. The studies were carried out by light microscopy (40 X) for the assessment of histological changes.

Statistical Analysis

The obtained data was subjected to one-way Analysis of Variance (ANOVA) followed by Dunnett's Test using the GraphPad Prism V5.0 (GraphPad Software, Inc., San Diego, California, USA). The *P* values of < 0.01 were considered as highly significant, while *P* values < 0.05 were considered as statistically significant.

RESULTS

Effect of LSC on Gastric Lesions

Macroscopic analysis revealed absence of lesions in control group I (Figure 1A). The animals of Group II showed macroscopic damage that was evidenced by the presence of ulcerative hemorrhage (Figure 1B) with the clear appearance of erosive and ulcerative linear gastric lesions. Disruption of the surface epithelium with bleeding, deep necrotic lesions into the mucosa and edema of the sub-mucosal layer with redness was clearly observed. On the other hand the gastric mucosa of the rats treated with standard drug omeprazole (Group III) was apparently normal in appearance (Figure 1C). The animals of Group IV (Test Group-1) were able to reverse the damage, up to some extent as assessed by the change in colour of stomach from red to dark pink with less hemorrhagic streaks and substantial damage of mucosa (Figure 1D). On the other hand, Group V (Test-2), did not evidence macroscopic toxicity as the morphological integrity of the gastric mucosa with retained and the necrosis of the mucosal surface was absent (Figure 1E). On comparing the results of Group IV and V, treated with two different forms of curcumin i.e. curcumin (50 mg/Kg) and LSC (25 mg/Kg) respectively, better gastric protection was evidenced in Group V. Furthermore, Group VI (Test-3) treated with double dose of LSC (50 mg/Kg) completely reversed the lesions with the score of 1.5 (Figure 1 F), a perfect pink to red colored stomach and no sign of damage was recorded as with standard control group (Figure 1C), indicating dose dependent effect of LSC on gastroprotection.

Additionally, the gastric lesions were judged by measuring the ulcer index and the data is given in Table 2. The ulcer control group displayed highest value of ulcer index 27.4 ± 4.6 that was followed by Group IV (treated with curcumin). The ulcer index of curcumin treated

group was almost 1.5 times lower than ulcer control group suggesting effective gastroprotection by curcumin. However, it was not as effective as omeprazole. On the other hand Group V and VI, treated with LSC showed a significant decrease ($P < 0.01$)[#], in ulcer index as compared to Ulcer control group. Correspondingly, oral administration of omeprazole, LSC at 25 and 50 mg/Kg showed 88.32, 84.67 and 86.86% ulcer inhibition, respectively that was ≈ 2.5 times more than curcumin (32.84%).

Gastric Content

In the ulcer control group, administration of ethanol caused a significant increase ($P < 0.01$)^{*} in the gastric secretion volume to the tune of 2.84 ± 0.10 mL as compared to Group I (1.68 ± 0.08 mL). However, administration of omeprazole significantly reduced ($P < 0.01$)[#] the gastric secretions (Table 2), which was not observed in Group IV treated with curcumin. Paradoxically the gastric secretion volume (2.16 ± 0.12 mL) was almost comparable to that of group II. In contrast, LSC showed remarkable reduction in the gastric secretion volume with significant reduction ($P < 0.01$) in both the doses of 25 mg/Kg (1.64 ± 0.04 mL) and 50mg/Kg (1.42 ± 0.08 mL). Remarkably the volumes were similar for both the doses.

Another parameter that was evaluated was gastric acidity that was approximately two-fold higher (8.84 ± 0.64 mEq/L) in Group II (Ulcer control), in comparison to the control Group I (4.82 ± 0.11 mEq/L). On omeprazole treatment the value got significantly decreased ($P < 0.01$)[#] to 4.23 ± 0.12 mEq/L. Treatment with curcumin reduction in the acidity level up to some extent ($P > 0.05$)^{ns} (Table 2), while administration of LSC (25 and 50 mg/Kg) showed significant ($P < 0.01$) reduction in gastric acidity (4.85 ± 0.13 and 3.96 ± 0.09 mEq/L, respectively).

On comparative analysis of mucus content, oral administration of ethanol had a detrimental effect on gastric mucus wall and caused a significant depletion ($P < 0.01$) in the mucus content (118.9 ± 14.92 mg/g) as compared to control (209.5 ± 12.62 mg/g) and Group III (omeprazole treated; 198.0 ± 15.07 mg/g). While LSC showed protective effect on mucus layer especially in Group VI, with the total mucus content of 196.4 ± 15.03 mg/g of stomach, similar to omeprazole treatment. However, curcumin treatment (Group IV) did not offer protect to the extent LSC could do.

Oxidative Stress Markers

In reference to the control, administration of ethanol significantly increased the levels of MDA ($P < 0.01$), by

Table 1: Formulation Details of Liquisolid Curcumin (LSC1 – LSC12).

GROUP No.	Formulation Code	Drug (%w/w)	R = Q/q	Nonvolatile solvent (W) (mg)	Liquid load factor (Lf)	Carrier material (Q)	Coating material (q)
Group – I	LSC-1	40	20:1	150.00	0.27	538.50	26.92
	LSC-2	50	20:1	100.00	0.27	359.06	17.95
	LSC-3	60	20:1	67.75	0.27	239.49	11.97
	LSC-4	70	20:1	42.85	0.27	153.86	7.69
Group – II	LSC-5	40	20:1	150.00	0.28	535.71	26.78
	LSC-6	50	20:1	100.00	0.28	357.14	17.85
	LSC-7	60	20:1	67.75	0.28	238.21	11.91
	LSC-8	70	20:1	42.85	0.28	153.03	7.65
Group – III	LSC-9	40	20:1	150.00	0.35	425.53	26.78
	LSC-10	50	20:1	100.00	0.35	283.68	17.85
	LSC-11	60	20:1	67.75	0.35	189.21	11.91
	LSC-12	70	20:1	42.85	0.35	121.56	7.65

Non-volatile solvent used: PEG 200 (Group – I; LSC1 – LSC4); PEG 400 (Group –II; LSC5 – LSC8); Tween 80 (Group –III; LSC9 – LSC12).

Table 2: Comparative Data for the Gastroprotective Effect of Liquisolid Curcumin over Curcumin, Administered Orally in Wistar rats.

Group (n=6)	Treatment	Ulcer index score	Ulcer Inhibition (%)	Gastric juice volume (mL)	Total gastric acidity (mEq/L)	Mucus (mg/g stomach)
Group I (Control)	0.1%w/v CMC (10 mL/Kg)	0.00	----	1.68±0.08	4.82±0.11	209.5±12.62
Group II (Ulcer control)	Absolute ethanol (5mL/ Kg)	27.4 ± 4.6*	----	2.84±0.10*	8.84±0.64*	118.9±14.92*
Group III (Standard Control)	Omeprazole (40 mg/Kg)	2.8 ± 0.8#	88.32	1.12±0.06#	4.23±0.12#	198.0±15.07#
Group IV (Test Group-1)	Curcumin (50 mg/Kg)	18.4 ± 2.4**	32.84	2.16±0.12*	6.98±0.19 ^{ns}	146.7±12.64*
Group V (Test Group -2)	LSC equivalent to 25 mg/ Kg of curcumin	4.2 ± 0.6#	84.67	1.64±0.04#	4.85±0.13#	179.3±16.23#
Group VI (Test Group-3)	LSC equivalent to 50 mg/ Kg of curcumin	2.9 ± 0.4#	86.86	1.42±0.08#	3.96±0.09#	196.4±15.03#

All the values are expressed as mean ± SD. Levels of statistical significance were determined by One – Way ANOVA followed by Dunnett's significant difference. * indicates Significant in comparison to Group I, # indicates Significant, as compared to Group II, ns indicates Non-significant.

almost three-fold (Table 3). Treatment with omeprazole showed a reduction in MDA level (0.614 ± 0.036 nmol/mg protein) to approximately half of the value, exhibited by ethanol treatment II (1.232 ± 0.312 nmol/mg protein). Curcumin treatment demonstrated a decrease in MDA levels but to a lesser extent than omeprazole treatment. In contrast the levels of MDA in test Group V and VI treated with LSC, were significantly attenuated

($P < 0.01$) as compared to ulcer control Group II. The attenuation was dose dependent.

In reference to control, the level of GSH and markers of free radical scavenging enzymes CAT and SOD decreased significantly ($P < 0.01$) in group II. Treatment with Omeprazole elicited reversal of the markers comparable to the levels of control group. Furthermore, treatment with curcumin (Group IV) displayed resto-

Table 3: Comparative Data Showing Effect of Liquisolid Curcumin on Oxidative Stress Factors in Ethanol Induced Gastric Ulcer in Wistar Rats.

Treatment group (n=6)	MDA (nmol MDA/mg protein)	GSH ($\mu\text{g}/\text{mg}$ of protein)	CAT (nmol of H_2O_2 consumed/min/mg protein)	SOD (SOD units per mg of protein)
Group I (Control)	0.427 \pm 0.024	18.76 \pm 1.042	0.163 \pm 0.008	0.582 \pm 0.023
Group II (Ulcer Control)	1.232 \pm 0.312*	4.864 \pm 1.446*	0.050 \pm 0.014*	0.262 \pm 0.036*
Group III (Standard Control)	0.614 \pm 0.036#	15.96 \pm 1.622#	0.145 \pm 0.043#	0.514 \pm 0.060#
Group IV (Test Group – 1)	0.997 \pm 0.012*	9.04 \pm 1.893*	0.084 \pm 0.048*	0.386 \pm 0.089*
Group V (Test Group – 2)	0.698 \pm 0.028#	12.961 \pm 1.022#	0.138 \pm 0.054#	0.491 \pm 0.047#
Group VI (Test Group – 3)	0.592 \pm 0.022#	15.48 \pm 1.226#	0.151 \pm 0.062#	0.522 \pm 0.026#

All the values are expressed as mean \pm SD. * indicates Statistically significant difference in comparison to Group I, # indicates Statistically significant difference, as compared to Group II.

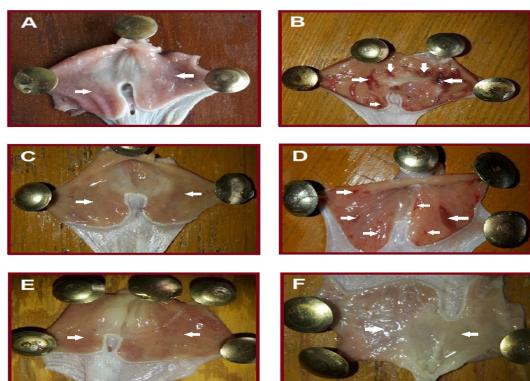


Figure 1: Gross Macroscopic Evaluation of Gastric Lesions: (A) Group I (Normal Control); (B) Group II (Ulcer Control) administered with ethanol (5mL/Kg BW *p.o.*); (C) Group III (Standard Control) administered with omeprazole (40mg/Kg BW *p.o.*); (D) Group IV (Test Group 1) administered with pure curcumin (50 mg/Kg BW *p.o.*); (E) Group V (Test Group 2) administered with LSC (equivalent to 25mg of curcumin/Kg BW *p.o.*); (F) Group VI (Test Group 3) administered with LSC (equivalent to 50mg of curcumin /Kg BW *p.o.*).

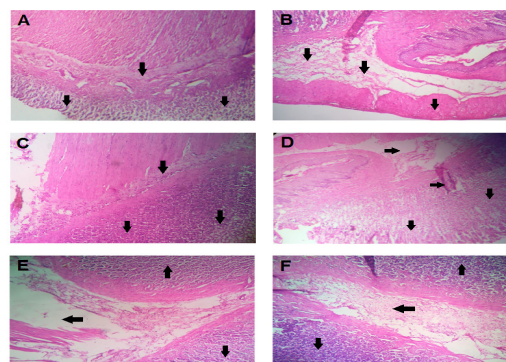


Figure 2: Histological Evaluation of Gastric Lesions Under Microscope at 40X: (A) Group I (Normal Control); (B) Group II (Ulcer Control) administered with ethanol (5mL/Kg BW *p.o.*); (C) Group III (Standard Control) administered with omeprazole (40mg/Kg BW *p.o.*); (D) Group IV (Test Group 1) administered with pure curcumin (50 mg/Kg BW *p.o.*); (E) Group V (Test Group 2) administered with LSC (equivalent to 25mg of curcumin/Kg BW *p.o.*); (F) Group VI (Test Group 3) administered with LSC (equivalent to 50mg of curcumin/Kg BW *p.o.*).

ration of the depleted level of GSH, CAT and SOD (Table 3) when compared to Group II, but less significantly ($P < 0.05$) in comparison to Group V and VI. The restoration particularly for CAT and SOD levels in Group V and VI was less as compared to standard treatment of omeprazole in Group III. As recorded, Group III significantly ($P < 0.01$) restored the levels of GSH and SOD, but the restoration in the depleted level of CAT was less significant ($P < 0.05$) as compared to Group V and VI.

Histology

The control Group I showed the presence of normal gastric mucosa that contained crypts of overlying gas-

tric glands lined by mucus secreting cells with rounded nuclei. The lamina propria was intact, infiltrated by scattered lymphocytes, blood vessels and fibrous tissue (Figure 2A). Group II exhibited severe injuries on mucosal layer and produced the characteristic zone of necrotizing mucosal lesions with severe microscopic gastric mucosal damage. Necrosis hemorrhage and focal ulceration in superficial mucosal epithelium with inflammatory cell infiltration and congestion of blood vessels in sub-mucosa is apparent in Group II (Figure 2B). In comparison to Group II, Group III recovered the ulcer base with restored surface epithelium (Figure 2C), validated by decreased ulcer score (Table 2). In Group IV, the surface mucus cells more or less restored (Fig-

ure 2D), while Group V and VI successfully reverted the mucosal damage, endorsed by absence of chronic inflammatory cells and recovery of surface mucosal cells (Figure 2E and F).

DISCUSSION

The gastroprotective effectiveness of LSC over curcumin was evaluated in ethanol induced inflammatory model in Wistar rats. The model selection was based on the fact that ethanol promotes oxidative stress, both by increasing the formation of ROS and depleting the oxidative defense mechanism in the cell.²⁵ Additionally, it also induces TNF- α expression for neutrophil mediated ROS generation as well as for apoptosis. ROS mediated induction of lipid peroxidation and protein oxidation are primarily involved in the pathogenesis of ethanol induced ulcers in the gastric mucosa and free radical scavenging is one of the mechanism implicated in the healing of gastric ulcers.²⁶ Preventive antioxidants such as SOD and GSH act as the first line of defense that prevents the destructive action of oxidative damage. The superoxide radical reacts with the cellular lipids, leading to the formation of lipid peroxide which gets metabolized to MDA.²⁷ Ethanol induced damage to gastric mucosa is coupled with significant depletion in the levels of sulphhydryl compounds, especially GSH.²⁸ This decrease in the level of GSH results in enhanced lipid peroxidation which causes increased GSH consumption. In contrast, an increase in gastric non-protein sulphhydryl content limits the production of oxygen derived free radicals and could be related to gastric protection in ethanol induced ulcer model. Malondialdehyde being a degradation product of unsaturated fatty acids and a biomarker of oxidative stress, measurement of gastric MDA level can be utilized for indirect estimation of lipid peroxidation.²⁹

Curcumin, a highly potent polyphenolic antioxidant decreases ethanol induced increased gastric acid levels, which is beneficial to prevent acid-induced aggravation of ulcers.³⁰ As shown in Table 2, significant reduction in ulcer index, gastric juice volume as well as total gastric acidity and enhancement in ulcer inhibition along with increased mucus secretion by the mucosal cells of the stomach was observed in the groups treated with omeprazole/LSC (Group III, V and VI), in reference Group II (Ulcer control). Curcumin, on the other hand demonstrated lesser activity which may be attributed to its poor solubility. LSC with higher solubility than curcumin affected higher dissolution of the active and hence superior therapeutic efficacy.¹⁶

The mucoprotective potential of LSC over is an indicative of amelioration. Curcumin also accelerates the ulcer healing phenomenon by inhibiting gastric acid secretion and anti-inflammatory activity preventing inducible TNF- α production at post-transcriptional level and affecting oxidative stress along with total antioxidant capacity, as well as by inhibiting IL-6 secretion and preventing apoptosis.³¹ LSC exhibited significant ($P < 0.01$) protective and ulcer inhibition efficacy in a dose dependent manner (25 and 50 mg/Kg), which was non-significant ($P > 0.05$) in case of pure curcumin even at similar highest concentration (50 mg/Kg), which could be due to its poor solubility/absorption that resulted as failure in strengthening of defensive mechanism.

In particular, generation of oxygen free radicals and lipid peroxidation plays a key role in ethanol induced development of gastric lesions. The oxidative stress in gastric tissue causes damage to key biomolecules (Lipids) which is apparent from the stimulated lipid oxidation leading to increased accumulation of MDA (Table 3) and these increased levels of MDA are thought to reflect free radical mediated cell membrane damage.³² Glutathione is tripeptide and important non-enzymatic cytosolic antioxidant, acts as a reductant and cofactor for some antioxidant enzymes.³³ GSH and other antioxidants plays crucial role in free radical degradation, which would otherwise outcome of lipid peroxidation.³⁴ The endogenous antioxidant enzymes, CAT and SOD in the gastric mucus are the key component of cellular defense system against ROS. However, SOD destroys the highly reactive radical superoxide by converting it into the less reactive peroxide, H_2O_2 which can be destroyed by CAT reaction.³⁵ CAT is a highly reactive enzyme that reacts with H_2O_2 to form water and molecular oxygen. Decreased activity of GST, CAT and SOD (Table 3) after ethanol administration may be due to enhancement of MDA, which inhibit protein synthesis and activities of certain enzymes. Vice-versa decreased intrinsic oxidative stress in gastric mucosa by increased GSH availability results in lowering of peroxide production and hence reduces the level of MDA.³⁶ This decrease might be due to elevated level of TNF- α in gastric tissue of ethanol treated rats.³⁷

Administration of LSC significantly enhanced the activity of GSH, CAT and SOD in a dose dependent manner, probably due to prevention of accumulation of excessive free radicals thereby protecting stomach from damage, suggesting superior gastro-protective activity in comparison to curcumin that exhibited poorly significant enhancement ($P > 0.05$) in enzyme levels. The marked effect of LSC could be attributed to its high radical scavenging activity³⁸ which is probably due to

contribution of large number of molecules available in the system (Gastric media), due to enhanced dissolution. Curcumin attenuated the increased lipid peroxidase damage and prevented the depletion of GSH, CAT and SOD made by ethanol up to an extent with a highly significant difference ($P < 0.01$), when compared to omeprazole. In contrast, LSC increased the levels of these circulating factors close to control (Group I) and Group III non-significantly ($P > 0.05$), supporting the hypothesis of improved solubility of curcumin via LSC. Being a poly phenolic aromatic compound, curcumin bears ability of scavenging the reactive free radicals either from phenolic -OH group or -CH₂ group of the β -diketone moiety.³⁹ Since, reactive free radicals can undergo electron transfer or abstract H-atom from either of these two sites. Some studies reported that antioxidant activity of curcumin is due to phenolic -OH group.⁴⁰ However, some studies suggest that hydrogen abstraction from the -CH₂ group is responsible for its antioxidant activity.⁴¹ The said mechanism can be proposed for LSC, whereby high concentration of curcumin molecules from LSC afforded higher antioxidant activity than pure curcumin as evident in Table 3. Another research claims effective blockage of ethanol induced overproduction of ^{*}OH to prevent ROS mediated gastric lesions. In addition to H₂O₂, ^{*}OH is also formed from peroxy nitrite generated from O₂⁻ and NO. LSC thus offers further defense against oxidative damage by scavenging ^{*}OH generated from other sources. ^{*}OH, being most reactive can interact with almost any compound in the cell including lipid, protein, DNA, carbohydrate, thiols and other low molecular weight antioxidants.⁴² This is how ^{*}OH is scavenged with ultimate oxidation of macromolecules and antioxidants, lead to pathogenesis. The chemical structure of curcumin is suitable for interaction with free radicals and its ^{*}OH-scavenging effect has been demonstrated.⁴³ However, direct scavenging of ^{*}OH can be considered an important pleiotropic effect of curcumin for gastroprotection, which enhances its potential for possible use as an antiulcer compound.

Histological evidences further substantiate the superiority of LSC for gastroprotection over curcumin. Upon ethanol administration, the back-diffusion of gastric acid into the mucosal wall could directly lead to vascular leakage and aggressive damaging effect in the basement membrane of both epithelial and mucosal cells in the gastric wall.⁴⁴ Furthermore, brief cessation of mucosal blood flow results in increased acidity, which in turn, results in the formation of hemorrhagic erosions after ethanol treatment.⁴⁵ Omeprazole treatment recovered the ulcer base with restored surface epithelium that was

validated by decreased ulcer score (Table 2). Curcumin treatment was also effective in restoration however, LSC treatment successfully reverted the mucosal damage, endorsed by absence of chronic inflammatory cells and recovery of surface mucosal cells. This confirms superior therapeutic efficacy of LSC over curcumin.

CONCLUSION

Liquisolid curcumin demonstrated significant gastroprotection in comparison to pure curcumin. The improved gastroprotective action may be due to high solubility of the former that resulted in strengthening of gastric mucosa, restoring the free radical scavenging enzymes and reducing the lipid peroxide production, efficiently. The results revealed that treatment with liquisolid curcumin resulted in maintaining the integrity of gastric mucosa by attenuating the histological changes comparable to the effects exhibited by omeprazole. The present research proves that liquisolid technology is a simple, cost effective and commercially viable technique which may be attractive to industrialists due to its promising outcomes.

ACKNOWLEDGEMENT

Authors are thankful to Natural Remedies Private Limited, Bengaluru, India for providing free sample of curcumin, to carry out the present research work.

CONFLICT OF INTEREST

The authors report no conflicts of interest.

ABBREVIATIONS

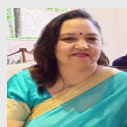
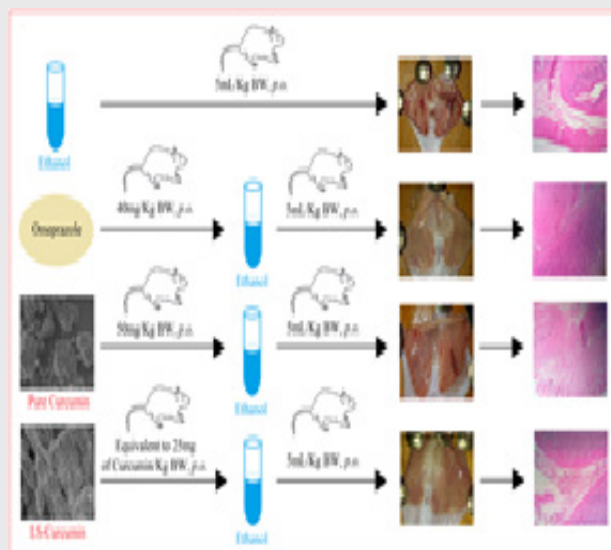
LSC: Liquisolid curcumin; **ROS:** Reactive oxygen species; **MDA:** Malondialdehyde; **GSH:** Tissue glutathione; **CAT:** Catalase; **SOD:** Super oxide dismutase.

REFERENCES

1. Golbabapour S, Hajrezaie H, Hassandarvish P, Majid NA, Hadi AHA, Nordin N, *et al.* Acute toxicity and gastroprotective role of *M. pruriens* in ethanol induced gastric mucosal injuries in rats. *BioMed Res Int.* 2013;4:1-13.
2. Thamocharan G, Sekar G, Ganesh T, Sen S, Chakraborty R, Kumar NS. Antiulcerogenic effect of *Lanatacamara Linn* leaves on *in vivo* test models in rats. *Asian J Pharm Clin Res.* 2010;3(3):57-60.
3. Khushtar M, Kumar V, Javed K, Bhandari U. Protective effect of ginger oil on aspirin and pylorus ligation-induced gastric ulcer model in rats. *Ind J Pharm Sci.* 2009;71(5):563-7.
4. Dhiyaaldeen SM, Amin ZA, Darvish PH, Mustafa IF, Jamil MM, Rouhollahi E, *et al.* Protective effects of (1-(4-hydroxy-phenyl)-3-methylpropenone chalcone in indomethacin induced gastric erosive damage in rats. *BMC Vet Res.* 2014;10(1):1-14.
5. Allen A, Flemstrom G. Gastrointestinal mucus bicarbonate barrier: Protection against acid and pepsin. *AJP Cell Physiology.* 2005;288(1):C1-19.

6. Halliwell B, Gutteridge JMC. Role of free radicals and catalytic metal ions in human disease: An overview. *Methods Enzymol.* 1990;186:1-85.
7. Shoaib A, Tarique M, Khushtar M, Siddiqui HH. Anti-ulcerogenic activity of hydromethanolic extract of *Andrographis paniculata* in indomethacin and indomethacin plus pylorus ligation induced gastric ulcer in rats. *Asian J Biomed Pharm Sci.* 2014;4(39):8-15.
8. Yadav SK, Sak AK, Jha RK, Sah P, Shah DK. Turmeric (curcumin) remedies gastroprotective action. *Pharmacogn Rev.* 2013;7(13):42-6. doi: 10.4103/0973-7847.112843
9. Chattopadhyay I, Bandyopadhyay U, Biswas K, Maity P, Banerjee RK. Indomethacin inactivates gastric peroxidase to induce reactive-oxygen mediated gastric mucosal injury and curcumin protects it by preventing peroxidase inactivation and scavenging reactive oxygen free radical. *Biol Med.* 2006;40(8):1397-408.
10. Tuorkey M, Karolin K. Anti-ulcer activity of curcumin on experimental gastric ulcer in rats and its effect on oxidative stress/antioxidant, IL-6 and enzyme activities. *Biomed Environ Sci.* 2009;22(6):488-95.
11. Kurien BT, Singh A, Matsumoto H, Scofield RH. Improving the solubility and pharmacological efficacy of curcumin by heat treatment. *Assay Drug Dev Technol.* 2007;5(4):567-76.
12. Akbar MU, Zia KM, Nazir A, Iqbal J, Ejaz SA, Akas MSH. Pluronic-based mixed polymeric micelles enhance the therapeutic potential of curcumin. *AAPS Pharm Sci Tech.* 2018;19(6):2719-39. <https://doi.org/10.1208/s12249-018-1098-9>.
13. Rachmawati H, Edityaningrum CA, Mauludin R. Molecular inclusion complex of curcumin- β -cyclodextrin nanoparticle to enhance curcumin skin permeability from hydrophilic matrix gel. *AAPS Pharm Sci Tech.* 2013;14(4):1303-12. <https://doi.org/10.1208/s12249-013-0023-5>.
14. Jaisamut P, Wiwattanawongsa K, Graidist P, Sangsen Y, Wiwattanapatapee R. Enhanced oral bioavailability of curcumin using a supersaturatable self-micro emulsifying system incorporating a hydrophilic polymer; *in vitro* and *in vivo* investigations. *AAPS Pharm Sci Tech.* 2018;19(2):730-40. <https://doi.org/10.1208/s12249-017-0857-3>.
15. Nadaf SJ, Killedar SG. Curcumin nanocochleates: Use of design of experiments, solid state characterization, *in vitro* apoptosis and cytotoxicity against breast cancer MCF-7 cells. *J Drug Deliv Sci Tech.* 2018;47:337-50.
16. Sharma V, Pathak K. Effect of hydrogen bond formation/replacement on solubility characteristics, gastric permeation and pharmacokinetics of curcumin by application of powder solution technology. *Acta Pharm Sin B.* 2016;6(6):600-13.
17. Dekanski JB, MacDonald A, Sacra P. Effects of fasting, stress and drugs on gastric glycoprotein synthesis in the rat. *Br J Pharmacol.* 1975;55(3):387-92.
18. Sohair RS, Mahmoud AA, Mohammad HA. Ameliorative effect of the sea cucumber *Holothuria arenicola* extract against gastric ulcer in rats. *J Basic Appl Zool.* 2015;72:16-25.
19. Corne SJ, Morrissey SM, Woods RJ. A method for the quantitative estimation of gastric barrier mucus. *Proc Physiol Soc.* 1974;242:116-7.
20. Mahmoud YI, El-Ghffar EA. Spirulina ameliorates aspirin-induced gastric ulcer in albino mice by alleviating oxidative stress and inflammation. *Biomed Pharmacotherap.* 2019;109:314-21.
21. Ohkawa H, Ohishi N, Yagi K. Assay for lipid peroxides in animal tissues by thiobarbituric acid reaction. *Anal Biochem.* 1979;95(2):359-64.
22. Sedlack J, Lindsay RH. Estimation of total protein-bound and non-protein sulfhydryl groups in tissue with Ellman's reagent. *Anal Biochem.* 1968;25:192-205.
23. Clairbone A. Assay of catalase, in: R.A. Greenwald (Ed.), *Hand Book of Method of Oxygen Free Radical Research.* Boca Raton. 1985.
24. Marklund S, Marklund G. Involvement of super oxide anion radical in the auto oxidation of pyrogallol and a convenient assay for super oxide dismutase. *Eur J Biochem.* 1974;47:469-74.
25. Hoek JB, Pastorino JG. Ethanol, oxidative stress and cytokine-induced liver cell injury. *Alcohol.* 2002;27(1):63-8.
26. Dockmeci D, Akpolat M, Aydogdu N, Doganay L, Turan FN. L-Cartinine inhibits ethanol induced gastric mucosa injury in rats. *Pharmacol Rep.* 2005;57:481-8.
27. Babbs CF, Steiner NG. Detection and quantitation of hydroxyl radical using dimethyl sulfoxide as molecular probe. *Methods Enzymol.* 1990;186:137-47.
28. Singer TP, Kearney EB. Determination of succinic dehydrogenase activity. *Methods Biochem Anal.* 1957;4:307-33.
29. Hamdan D, El-Readi MZ, Tahrani A, Herrman F, Kaufman D, Farrag N, *et al.* Chemical composition and biological activity of *Citrus jambhiri* Lush. *Food Chem.* 2011;127(2):394-403.
30. Farzaei MH, Abdollahi M, Rahimi R. Role of dietary polyphenols in the management of peptic ulcer. *World J Gastroenterol.* 2015;21(21):6499-17. doi: 10.3748/wjg.v21.i21.6499.
31. Xueting M, Donghui X, Sika X, Yanping Z, Shibo X. Novel role of Zn (II)-curcumin in enhancing cell proliferation and adjusting proinflammatory cytokine-mediated oxidative damage of ethanol-induced acute gastric ulcers. *Chem Biol Interact.* 2012;197(1):31-9.
32. Ajeigbe K, Oladejo E, Emikpe B, Asuk A, Olaleye S. The dual modulatory effect of folic acid supplementation on indomethacin induced gastropathy in the rat. *Turk J Gastroenterol.* 2012;23(6):639-45.
33. Hiraishi H, Terano A, Ota S, Mutoh H, Sugimoto T, Harada T, *et al.* Protection of cultured rat gastric cells against oxidant-induced damage by exogenous glutathione. *Gastroenterol.* 1994;106(5):1199-1207.
34. Sohair RF, Mahmoud AA, Mohannad H, Al-killidar N. Ameliorative effect of the sea cucumber *Holothuria arenicola* extract against gastric ulcer in rats. *J Basic Appl Zool.* 2015;72:16-25.
35. Ighodaro OM, Akinloye OA. First line defence antioxidants-SuperOxide Dismutase (SOD), Catalase (CAT) and Glutathione Peroxidase (GPX): Their fundamental role in the entire antioxidant defence grid. *Alexandria J Med.* 2018;54(4):287-93. Available online: <https://doi.org/10.1016/j.ajme.2017.09.001>.
36. Nakajima A, Yamada K, Zou LB, Mizuno M, Nabeshima T. Interleukin-6 protects PC12 cells from hydroxyoneal induced cytotoxicity by increasing intracellular glutathione levels. *Free Rad Bio Med.* 2002;32(12):1324-32.
37. Pitrowski J, Pitrowski E, Skrodzka D, Slomiany A, Slomiany BL. Gastric mucosal apoptosis induced by ethanol: Effect of antiulcer agents. *Biochem Mol Bio Int.* 1997;42(2):247-54.
38. Assimopoulou AN, Sinakos Z, Papageorgiou VP. Radical scavenging activity of *Crocus sativus* L. extract and its bioactive constituents. *Phytother Res.* 2005;19(11):997-1000.
39. Badria FA, Ibrahim AS, Badria AF, Elmarakby AA. Curcumin Attenuates Iron Accumulation and Oxidative Stress in the Liver and Spleen of Chronic Iron-Overloaded Rats. *PLoS One.* 2015;10(7):e0134156. <https://doi.org/10.1371/journal.pone.0134156>.
40. Kapoor S, Priyadarsini KI. Protection of radiation induced protein damage by curcumin. *Biophys Chem.* 2001;92(1-2):19-126.
41. Jovanovic SV, Boone CW, Steenken S, Trinoga M, Kaskey RB. How curcumin works preferentially with water soluble antioxidants. *J Am Chem Soc.* 2001;123(13):3064-8.
42. Birben E, Sahiner UM, Sackesen C, Erzurum S, Kalayci O. Oxidative stress and antioxidant defense. *World Allergy Organ J.* 2012;5(1):9-19. doi: 10.1097/WOX.0b013e3182439613.
43. Ruby AJ, Kuttan G, Babu KD, Rajasekharan KN, Kuttan R. Antitumour and antioxidant activity of natural curcuminoids. *Cancer Lett.* 1995;94(1):79-83.
44. Tuorkey M, Karolin K. Anti-ulcer activity of curcumin on experimental gastric ulcer in rats and its effect on oxidative stress/antioxidant, IL-6 and enzyme activities. *Biomed Environ Sci.* 2009;22(6):488-95.
45. Puurunen J. Gastric mucosal blood flow in ethanol-induced mucosal damage in the rat. *Eur J Pharmacol.* 1980;63(4):275-80.

PICTORIAL ABSTRACT



Professor Kamla Pathak, with a teaching and research experience of more than 28 years, is currently working as Professor, Pharmacy College Saifai, Uttar Pradesh University of Medical Sciences, Saifai, Etawah, India. She is actively engaged in research on oral/topical modulated/targeted drug delivery systems. She has authored over 240 research /review articles in journals of international and national repute; 7 book chapters, one book and three patents. She has a h-index of 28 (Scopus) and has guided 7 Ph.Ds and 120+ postgraduate theses. Has served as consultant to pharmaceutical industry.

SUMMARY

- Lquisolid curcumin demonstrated superior gastroprotection via suppression of gastric acid, restoration of free radical scavenging enzymes and reduction in the lipid peroxidase production in comparison to curcumin in Wistar rats.

ABOUT AUTHORS



Dr. Vijay Sharma is working as Professor & Head, Department of Pharmaceutics, SGT University, Gurugram (Haryana). He has 14 years of teaching experience in pharmaceutical courses at UG and PG level, with good understanding of educational compliance and regulatory standards. His research proficiency in pre-formulation studies, dosage form development and targeted delivery of bio-macromolecules for cellular therapies, contributed numerous national and international publications to his credit.

Cite this article: Sharma V, Pathak K. Investigating Gastroprotective Potential of Lquisolid Curcumin against the Role of Endogenous Aggressive Factors and Oxidative Stress Markers. Indian J of Pharmaceutical Education and Research. 2019;53(3):527-36.



International Journal of Biological Macromolecules

Volume 137, 15 September 2019, Pages 20-31

Liquisolid system of paclitaxel using modified polysaccharides: *In vitro* cytotoxicity, apoptosis study, cell cycle analysis, *in vitro* mitochondrial membrane potential assessment, and pharmacokinetics

Vijay Sharma^a, Kamla Pathak^b  

Show more 

 Share  Cite

<https://doi.org/10.1016/j.ijbiomac.2019.06.188> 

[Get rights and content](#) 

Abstract

The research was aimed to develop a liquisolid formulation of paclitaxel using novel, highly porous liquisolid carriers (modified polysaccharides) to enhance bioavailability of orally administered paclitaxel. Modified polysaccharides namely co-grinded treated guar gum (C-TGG), co-grinded treated tamarind kernel powder (C-TTKP) and co-grinded treated locust bean

gum (C-TLBG) were developed by sequentially subjecting the corresponding polysaccharides to wetting, drying and co-grinding with mannitol (1:1). A total of 12 liquisolid systems of paclitaxel (LSP-1 to LSP-12) were formulated using non-volatile solvent (polysorbate 80/Solutol HS 15®), carrier material (C-TGG/C-TTKP/C-TLBG), and Aerosil® 200 as coating material, and evaluated for pre-compression parameters. The liquisolid systems were directly compressed to produce liquisolid tablets (LTP-1 to LTP-12) and assessed for post compression parameters, cytotoxic/cellular analysis and pharmacokinetics. The modified polysaccharides exhibited narrow symmetrical particle size distribution, high liquid absorption potential, diminutive swelling index, favorable *in vitro* biodegradability and compression amenability. Among the directly compressed liquisolid tabs, LTP-10 exhibited highest CDR of $98.70 \pm 2.68\%$ and permeability of 61.59%. The IC_{50} of <20 mmol/L indicated remarkable cytotoxic potential on human gastro-enteric tumor cancerous cell lines (NCI-N87). Additionally, LTP-10 exhibited significantly high values for cell death 37.92 and 54.17% ($P < 0.01$) in early and late apoptosis and mitochondrial membrane potential regain (33%) in comparison to paclitaxel ($P < 0.05$) and 5-fluorouracil ($P < 0.01$). Pharmacokinetics revealed C_{max} of 536.48 ± 4.63 $\mu\text{g/L}$ at 1.64 ± 0.44 h for LTP-10 indicating enhancement in bioavailability (5.43 fold) of paclitaxel on oral administration.

Introduction

Low drug solubility often manifests itself as poor performance characteristics of the dosage form and disappointing *in vivo* consequences like incomplete drug release, reduced bioavailability and higher inter-patient variability. Traditional solubility enhancement approaches are based either on chemical or mechanical modification of the environment surrounding the drug particle/molecule, or physically altering the macromolecular characteristics of aggregated drug particles [1,2]. The popular formulation tools employed for solubility/dissolution enhancement are salt formation, cosolvency, complexation, micronization, melt sonocrystallization [3], lyophilization, steam-aided granulation [4], solubilization by surfactants, solid solution, and inclusion of drug solution in soft gelatin capsule [5]. Other approaches to improve the bioavailability of drugs include, use of adjuvants [6]; formulation of liposomes, nanoparticles, use of drug phospholipid complex [7], and fabrication of structural analogues of the drug [8].

Liquisolid technology utilizes the concept of converting the liquid medication/poorly water soluble solid drug dissolved in a suitable non-volatile solvent, into a dry looking, non-adherent, free flowing and compactable powder by its simple

admixture with selected carrier and coating material. The literature extensively cites findings on the effect of water soluble carriers on dissolution and bioavailability of poorly water soluble drugs using liquisolid technique. The principle of liquisolid technology is based on adsorption/absorption of liquid medication by carrier system, which requires excipients with high porosity, large specific surface area and sufficiently high liquid absorption capacity [9].

Paclitaxel (PCT), a poorly water soluble anticancer drug is commercialized as intravenous infusion (Taxol®) wherein the drug is solubilized using cremophore. The latter is reported to cause hypersensitivity reactions [10]. The drug presents poor oral bioavailability (7%) and enhancement of its solubility using cremophore is reported to cause gastric irritation [6,11]. Although continual research to produce cremophore free formulation is underway, a non-invasive delivery system of PCT with improved bioavailability is still elusive. Natural polysaccharides are relatively complex carbohydrates and provide adequate mechanical properties for pharmaceutical applications as fibers, films, adhesives, rheology modifiers, hydrogels, emulsifiers, and drug delivery agents [12]. For instance, natural polysaccharides have proven to enhance the contact between drug and human mucosa due to their high mucoadhesive properties [13]. Natural polysaccharides, such as gaur gum [14], tamarind kernel powder [15] and locust bean gum [16], have been evaluated in various drug delivery systems due to high viscosity, broad pH tolerance and adhesivity [17]. This has led to their application as stabilizer, thickener, gelling agent, and binder in food and pharmaceutical industries. Other important properties of polysaccharides that justify their use as pharmaceutical excipients include non-carcinogenicity [18], biocompatibility [19], high drug holding capacity [20] and high thermal stability [21].

Guar gum (GG) a polysaccharide obtained from the endosperm of the seed of the guar plant, *Cyanaposis tetragonolobus*, family *Leguminosae*. Chemically, it consists of a high-molecular-weight polysaccharide, namely galactomannan, which is based on a mannan (M) backbone with galactose (G) side groups [22]. The molecular structure reveals that guar gum is a straight chain galactomannan with galactose on every other mannose unit. β 1-4 glycosidic linkages couple the mannose units and the galactose side chains are linked through α 1-6. The mannose to galactose ratio has been estimated at 1.8:1 to 2:1 [23,24]. GG is considered safe for administration as there are no evidences of mutagenicity, teratogenicity, sensitization, negative reproductive effects and non-carcinogenic [25]. Tamarind kernel powder (TKP), a product obtained from the plant *Tamarindus indica*, family *Fabaceae* and is chemically composed of natural branched polysaccharide (65%) with a molecular weight of 700–880 kDa [26], gum, protein (15.4 to 22.7%), oil (3.0 to 7.4%), crude fiber (7 to 8.2%), non-fiber carbohydrates (61 to 72.2%), ash (2.45 to 3.3%) [27]. TKP also contains various phenolic antioxidants and is composed of a (1N4) β -D-glucan

backbone substituted with side chains of α -D-xylopyranose and β -D-galactopyranosyl linked (1N2)- α -D-xylo-pyranose linked (1N6) to glucose residues [28]. The major carbohydrates present in TKP are glucose, xylose and galactose in a ratio of 2.80:2.25:1.00 [29]. TKP meets the criteria for a polymer to be considered low risk under 40 CFR 723.250 [30] and no mammalian toxicity is anticipated from dietary, inhalation, or dermal even at high dose exposure to TKP [31]. Locust bean gum (LBG), a polysaccharide, is obtained from the seeds of fruit pod from carob tree (*Ceratonia siliqua*) family *Leguminosae* [32]. LBG a non-ionic galactomannan is based on D-mannose units joined by 1, 4-linkages to form long straight chains. Galactose units are attached to mannose units by 1, 6-glycosidic linkages. LBG has an average ratio of 1:4 galactose to mannose units, with the galactose units attached in blocks known as substituted regions [33]. The segments of the chain is composed of unsubstituted b-D-mannopyranosyl units, alternating with other chain segments in which a-D-galactopyranosyl side branches are linked to each of the main chain units [34]. LBG is not associated with any adverse toxic or nutritional effects even at the highest doses, there is no concern with respect to the genotoxicity and no carcinogenic effects are reported [35].

Therefore, the aim of the present research was to develop liquisolid formulation of PCT using a carrier system prepared by modifying the physicochemical properties of natural polysaccharides (GG, TKP and LBG). To the best of our knowledge the use of the listed polysaccharides in their modified form has not been reported as carrier for liquisolid system. Likewise use of Solutol HS15® as non-volatile solvent for developing liquisolid compacts is a novel approach. Thus the objective is to optimize liquisolid system of PCT using modified polysaccharides and to assess the formulation *in vitro* cytotoxicity, apoptosis, cell cycle analysis, *in vitro* mitochondrial membrane potential and pharmacokinetic parameters. The research undertaken may offer a commercially viable option for non-invasive drug delivery system of PCT with enhanced bioavailability.

Section snippets

Materials and methods

Paclitaxel was kind gift from Fresenius Kabi, Kolkata, India. Propylene glycol, Solutol HS 15®, acetonitrile HPLC grade, Masson's trichrome stain, PEG200 and 400 were purchased from Sigma Aldrich Ltd., St. Louis, MO, USA; Aerosil® 200,

mannitol, methanol and ethanol from S. D. Fine Chem. Limited, Mumbai, India. Guar gum, locust bean gum and tamarind kernel powder were procured from Altrafine Gums, Ahmedabad, Gujarat, India, Water HPLC grade was purchased from Qualigens Fine Chemicals, GSK,...

Equilibrium solubility

PCT is practically insoluble in water and the experimental solubility values of 0.003 ± 0.002 and 0.007 ± 0.001 mg/mL in hydrochloric acid buffer, pH 1.2 and double distilled water respectively were quite close to those reported in literature [45]. The present research proposes enhancement in drug solubility through liquisolid technique, using non-volatile solvent(s). Correspondingly, PEG 200, PEG 400, polysorbate 80 and Solutol HS 15® were selected to estimate the saturation solubility of PCT. ...

Conclusion

Modified polysaccharides were developed as novel liquisolid tablet excipient that exhibited large specific surface area, high liquid load factor, remarkably good powder properties, compression amenability and favorable *in vitro* biodegradability. The LiquiSol Tabs of paclitaxel developed using modified polysaccharides enhanced the dissolution and hence the oral bioavailability of the drug. *In vitro* cytotoxicity, apoptosis and cell cycle analysis proved the cytotoxic potential of the dosage form...

[Recommended articles](#)

References (80)

L.P. Ruan *et al.*

[Improving the solubility of ampelopsin by solid dispersions and inclusion complexes](#)

J. Pharm. Biomed. Anal. (2005)

C. Cavallari *et al.*

Improved dissolution behaviour of steam granulated piroxicam

Eur. J. Pharm. Biopharm. (2002)

R.P. Gullapalli

Soft gelatin capsules (softgels)

J. Pharm. Sci. (2010)

H. Gelderblom *et al.*

Cremophor EL

The drawbacks and advantages of vehicle selection for drug formulation, Eur. J. Cancer (2001)

M. Lu *et al.*

Liquisolid technique and its application in pharmaceuticals

Asian J Pharm Sci. (2017)

A.K. Singla *et al.*

Paclitaxel and its formulations

Int. J. Pharm. (2002)

V. Gupta *et al.*

Tamarind kernel gum: an upcoming natural polysaccharide

Sys. Rev. Pharm. (2010)

J. Sujja-areevath *et al.*

Release characteristics of diclofenac sodium from encapsulated natural gum mini-matrix formulations

Int. J. Pharm. (1996)

M. Sano *et al.*

Lack of carcinogenicity of tamarind seed polysaccharide in B6C3F mice

Food Chem. Toxicol. (1996)

S. Burgalassi *et al.*

Development and in vitro/in vivo testing of mucoadhesive buccal patches releasing benzydamine and lidocaine

Int. J. Pharm. (1996)



View more references

Cited by (11)

Starch-based carriers of paclitaxel: A systematic review of carriers, interactions, and mechanisms

2022, Carbohydrate Polymers

Citation Excerpt :

...Paclitaxel in tablets is mostly amorphous, with very small particle size and larger surface area, which is beneficial for dissolution kinetics improvement compared with the crystalline form. In addition, the hydrophilic carrier provided apparent water solubility, which increased the bioavailability of oral paclitaxel by ~5.43 fold (Sharma & Pathak, 2019). In practice, excipients in the tablet defend the activity of paclitaxel and guide its release at the designated site....

Show abstract 

The importance of the coating material type and amount in the preparation of liquisolid systems based on magnesium aluminometasilicate carrier

2021, European Journal of Pharmaceutical Sciences

Citation Excerpt :

...Even though a lot of advantages of this material including its long-term utilization in the pharmaceutical industry, low price and good stability, the surface area, and hence absorption capacity of microcrystalline cellulose are significantly lower (1.18 m²/g) in comparison to rather novel excipients. For example, Sharma and Pathak (2019) introduced a novel highly porous carriers prepared by subjecting polysaccharides (guar gum, tamarind kernel, locust bean gum) to wetting, drying, and co-grinding with mannitol. From the commercially available materials, especially mesoporous silica (e.g., Neusilin® US2, Syloid® XDP 3050, Syloid® XDP 3150, Parateck® SLC 500) have been lately gaining increasing attention due to their high specific surface area (more than 300 m²/g) and excellent absorption/adsorption capacity....

[Show abstract](#) ✓

Effective formulation strategies for poorly water soluble drugs

2021, Advances and Challenges in Pharmaceutical Technology: Materials, Process Development and Drug Delivery Strategies

[Show abstract](#) ✓

Construction and anti-tumor activities of disulfide-linked docetaxel-dihydroartemisinin nanoconjugates

2020, Colloids and Surfaces B: Biointerfaces

Citation Excerpt :

...20,000 cells were analyzed by flow cytometer (BD, FACS-Calibur, USA) [45]. The mechanism on the inhibition of tumor cell growth was evaluated by cell cycle study [46–49]. In brief, 4T1 cells (1 * 10⁶ cells/well) were incubated with media....

[Show abstract](#) ✓

Mechanistic aspects of drug loading in liquisolid systems with hydrophilic lipid-based mixtures

2020, International Journal of Pharmaceutics

Citation Excerpt :

...Moreover, it was confirmed for all LSS that drug dissolution was much faster in both media in comparison to the physical mixture. Similar results were reported in several studies dealing with the preparation and evaluation of LSS containing different model drugs, e.g. paclitaxel

(Sharma and Pathak, 2019), eplerenone (Khames, 2019) and ketoconazole (Molaei et al., 2018). These results support the claim that LSS are very promising systems for the enhancement of the in vitro dissolution profiles of problematic poorly soluble drugs....

[Show abstract](#) ✓

[Liquisolid Technique: A Novel Technique with Remarkable Applications in Pharmaceutics](#) ↗

2024, Current Drug Discovery Technologies



[View all citing articles on Scopus](#) ↗

[View full text](#)

© 2019 Elsevier B.V. All rights reserved.



All content on this site: Copyright © 2024 Elsevier B.V., its licensors, and contributors. All rights are reserved, including those for text and data mining, AI training, and similar technologies. For all open access content, the Creative Commons licensing terms apply.

